Best practices for automation and control of mine dewatering systems

PJ Oberholzer

21696683

Dissertation submitted in fulfilment of the requirements for the degree *Magister* in Mechanical Engineering at the Potchefstroom Campus of the North-West University

Supervisor: Dr JF van Rensburg

May 2015

Abstract

Title: Best practices for automation and control of mine dewatering systems

Author: Mr PJ Oberholzer

Supervisor: Dr J van Rensburg

Keywords: Best practice, automation, cavitation, overheating, efficiency, failure, multistage centrifugal pump, control, schedule

Typical deep level mines use up to 27 ML water per day for mining operations. Multistage centrifugal pumps up to 2500 MW are used in an upward cascading manor to dewater the shaft. The dewatering systems at some mines are automated to enable surface control. Automation of the pumps is typically based on the best practice procedure known when implemented. Best practice procedures are used to ensure safe pumping operations. It was found that pump failures could still occur even with the best practice implemented.

Unexpected failures of pumps are of major concern because they can result in the flooding of a mine. Flooding increases the risk of environmental damage and injury to the mining personnel. An additional concern is the maintenance cost of multistage centrifugal pumps. Overhaul cost of a seized multistage centrifugal pump is almost R1-million.

The aim of this study was to improve established best practice procedures for pump automation. This could be achieved by investigating the general root cause of failures of automated pumps. Additional instrumentation and protection devices to prevent similar incidents were examined. Revised system control parameters were developed to ensure that the pumps operated within the design specifications.

The improved best practices proved to prevent failures as a result of overheating and cavitation. Increasing the pump reliability and availability enabled surface control. The control of the automated dewatering system realised an electricity cost saving of R6-million. The automated system also made it possible to calculate the real-time pump efficiency within 5%.

Previous best practice procedure was found to be inadequate to prevent all possibilities of failure. Additional precaution measurements were added to prevent pump failure.

Acknowledgements

The research reported in this dissertation is my own work. Recognition was given to the external sources used in the document. Any errors or omissions brought to the attention of the author will be corrected.

I would like to thank our Lord, our Saviour for creating the earth and giving mankind the responsibility to care for it.

Thank you to TEMM International (Pty) Ltd and HVAC International (Pty) Ltd for the opportunity, financial assistance and support to complete this study.

I would like to thank Prof Eddie Mathews for giving me the opportunity to complete this study.

I would like to thank Prof Marius Kleingeld for trusting me to manage the pump automation project.

I would like to thank Dr Johan van Rensburg for his guidance and insight during the completion of this dissertation.

Thank you to Mr Rudi Joubert and Mr Willem Schoeman for sharing your experience on project management and technical knowledge.

Lastly I would like to thank my wife, Elizabeth Oberholzer, for supporting me in completing this dissertation. Thank you for your understanding during the time the document was completed.

Table of contents

List of figures

List of tables

Nomenclature

Symbol		Description	Unit
A	-	Area of the valve	m^2
a	-	Acceleration	m/s^2
$BO(n_{pa}-1)_t$	-	n^{th} top offset calculated daily profile	%
C_p	-	Specific heat constant	J/kg.K
CO_t	-	Control offset defined daily profile	%
CR_t	-	Control range calculated daily profile	%
D	-	Inside diameter of pipe	m
ΔP	-	Differential pressure across pump	Pa
ΔP_V	-	Differential pressure across valve	Pa
ΔT	-	Differential temperature across pump	°C
DL_{end}	-	Dam level at the end of period	%
DL_{Max}	-	Maximum dam level available	%
DL_{Start}	-	Dam level at the start of period	%
η	-	Efficiency	%
η_{ans}	-	Pump station efficiency	%
f	-	Friction coefficient of pipe	-
F_{Eq}	-	Equivalent force	N
F_N	-	Normal force	N
F_{sf}	-	Static friction force	N
g	-	Gravitational constant	m/s^2
H	-	Head	m
h_{dn}	-	Discharge nozzle friction head	m
h_{elb}	-	Pipe elbow friction head	m
h_f	-	Pipe friction head	m
h_{fdp}	-	Discharge pipe friction head	m
h_{fsp}	-	Suction pipe friction head	m
h_L	-	Component friction head	m
h_{NRV}	-	NRV friction head	m
H_s	-	Static head	m
h_s	-	Suction head	M
h_{sn}	-	Suction nozzle friction head	m
H_{Ssi}	-	Static head of suction pipe	m
H_{Tot}	-	Total head of the pump station	m
h_V	-	Valve friction head	m
I	-	Motor current	a
K_L	-	Loss coefficient	-
l	-	Length of pipe	m
M	-	Torque	Nm
m	-	Mass	kg
MDL_t	-	Minimum defined daily profile	%

μ	-	Joule-Thompson coefficient	K/Pa
n	-	Amount of substance	Mol
n_{p_in}	-	Number of pumps feeding dam	-
n_{p_out}	-	Number of pumps draining dam	-
n_{pa}	-	Number of pumps available	-
n_{pr}	-	Number of pumps running	-
$NPSHa$	-	Net positive suction head available	m
ω	-	Rotational speed	Rad/s
P	-	Pressure	Pa
P_H	-	Pressure of head	Pa
P_i	-	Inlet pressure	Pa
P_m	-	Motor input power	W
P_o	-	Outlet pressure	Pa
P_P	-	Stored potential pressure	Pa
P_s	-	Absolute suction pressure	Pa
P_{Tot}	-	Total power of pump station	W
P_v	-	Vaporisation pressure	m
PP_i	-	Power per pump	W
Q	-	Volume flow	m^3/s
$\dot{Q}_{p\_out}$	-	Flow per pump draining dam	l/s
$\dot{Q}_{settler}$	-	Flow of settler feeding dam	l/s
$\dot{Q}_{Tot}$	-	Total flow of pump station per column	m^3/s
$\dot{Q}_{p\_in}$	-	Flow per pump feeding dam	l/s
R	-	Universal gas constant	J/mol.K
ρ	-	Fluid density	kg/m^3
T	-	Temperature	K
t	-	Time	s
$TO(n_{pa}-1)_t$	-	n^{th} top offset calculated daily profile	%
U_S	-	Friction coefficient	-
v	-	Specific volume	m^3/kg
$\dot{V}$	-	Fluid velocity	m/s
$\dot{V}_i$	-	Inlet velocity	m/s
$\dot{V}_o$	-	Outlet velocity	m/s
Vol	-	Volume	m^3
Z_i	-	Inlet height	m
Z_o	-	Outlet height	M

Abbreviations

Abbreviation		Description
3-CPFS	-	Three Chamber Pump Feeder System
AMD	-	Acid Mine Drainage
BAC	-	Bulk Air Coolers
BO	-	Bottom Offset
CO	-	Control Offset
CR	-	Control Range
DE	-	Drive-End
DSM	-	Demand Side Management
EE	-	Energy Efficiency
IPCM	-	Intermediate Pumping Chamber Main shaft
IPCS	-	Intermediate Pumping Chamber Sub shaft
LS	-	Load Shifting
MDL	-	Minimum Dam Level
NDE	-	Non-Drive End
NPSHa	-	Net Positive Suction Head available
NPSHr	-	Net Positive Suction Head required
NRV	-	Non-Return Valve
PC	-	Peak Clipping
low pH	-	power of Hydrogen
PLC	-	Programmable Logic Controller
RP	-	Refrigeration Plants
SCADA	-	Supervisory Control And Data Acquisition
TO	-	Top Offset
ToU	-	Time of Use
VSD	-	Variable Speed Drive

Chapter 1: Introduction

This chapter explains deep level mine water consumption. An overview of a mine reticulation system is given. It focuses on the different methods to dewater a deep level mine. This chapter also lists the advantages of automating the dewatering system.

1.1. Water usage in mining

Water is a critical natural resource required for most living organisms. Humans are required for the underground operations in deep level mines. Underground operation is known to be challenging due to the robust environment [1]. Mines use water to serve various needs providing a safe environment for its underground employees.

Figure 1 displays the different sectors of water consumers in South Africa [2]. The mining, industrial and power generation sector only consumes 8% of the water from the water suppliers.

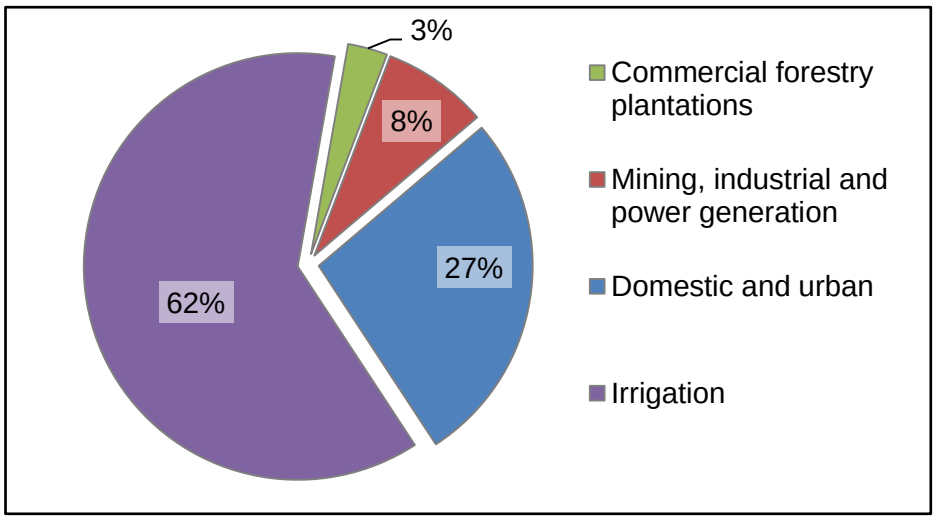

Figure 1: South African water consumption per industry

Deep level mines are designed to operate with a specific amount of water in the water reticulation system. The amount of water required depends on the size of the mine, production rate, demand and storage capacity. Managing the water balance of a mine correctly will improve efficiency of water consumption. Water must be bought and added to the reticulation system from the local water supplier if the water level is low [3], [4].

As with all natural resources, only a limited amount of water is freely available. Water found in a mine has a high acidity (low pH) and high concentration of sulphate and heavy metals [5]. The water mines dispose, is often referred as Acid Mine Drainage (AMD). AMD can contaminate water surrounding a mine with heavy metals. Heavy metals in the water have a harmful effect on humans and the biota [6].

The water in a deep level mine typically consists of a closed loop system. Mines are required to optimise water management to ensure minimum water is bought from the local water supplier. One strategy is to ensure excess water from rainfall or fissure water is stored to supplement the system when it is depleted [3].

1.1.1. Cooling

The typical depth of a deep level gold mine in South Africa is 3500 m. Virgin rock face temperature of up to 65°C was measured underground [7]. Heat is directly transferred into the ambient underground temperature from the surrounding rock. This makes cooling equipment essential in maintaining a safe working environment below 28°C wet-bulb temperature [8].

Typically Bulk Air Coolers (BAC) are the primary cooling method of underground ambient temperature at a mine. A BAC cools the air that the ventilation system forces down the shaft [9]. Air is cooled through a BAC with horizontal cooling water spray chambers, vertical pack towers or circuit cooling coils [10], [11].

Secondary coolers are installed underground to re-cool the air. This is similar to the surface BAC but takes place underground [12]. This is usually required when a mine exceeds a depth of 2000 m.

Tertiary cooling is usually required when the cooled air exceeds 1300 m in depth from the last BAC [13]. Spot coolers and cooling cars are utilised to cool the ambient temperatures in the haulages and stopes [14]. The cooled air is directed into the desired direction which requires cooling [2]. This tertiary equipment usually has a high mobility in order to move with mine development.

The cooling capacity of water is limited to the relative high freezing point of 0°C at sea-level. Ice is often used for underground cooling. The size of the ice particles has an influence on the cooling efficiency. Smaller ice particles have a larger area in contact to allow heat exchange. The large areas increase the rate of cooling as well as the melting rate. The improved cooling capacity of the ice reduces the amount of water entering the shaft [8].

1.1.2. Mining operations

Mines use several types of drilling equipment to drill holes for explosives or support for suspended equipment. Hydro drills use the pressure of the water developed due to the head as an energy source. Other drill types use water to cool the drill and minimise dust through suppression [14], [15]. The pressure of the water can also be utilised to drive hydropower loaders or winches [8].

Explosives are used to blast ore from the rock faces or to develop new working areas. Underground blasting results in a sudden temperature increase. Spraying water on the rock face is an effective method to neutralise the temperature rise [13]. The ambient temperature

must be maintained within mining regulations before the next shift can enter. The water spray also acts as dust suppression for the dust released by the blasting [3].

The water pressure of the service water is used for cleaning and sweeping [8], [16]. A flexible hose is installed to the service water column to improve manoeuvrability. Water-jet nozzles installed on the flexible hoses increase the water velocity and concentrate the direction of flow. This water has enough force to move the fine broken ore and dust [7].

Mines often utilise the used hot water to hoist ore. Crushers are installed underground to obtain the desired ore particle size. The particles are dispensed in the used hot water to form slurry. Positive displacement pumping systems are utilised to transfer the slurry. A positive displacement pumping system can be in direct contact or isolated with a feeder or pressure exchange system from the slurry [17].

1.2. Background to mine water reticulation systems

Mines use dewatering systems to remove the used service water, fissure and groundwater from the shaft [14]. The used hot water is gravity fed to the settlers near shaft bottom through the trenches from each level [18]. Settlers remove debris contaminating the water as a result of mining activities. The clear hot water and mud water are then transferred to the respective reservoirs [9], [19].

Lime flocculent is added to the contaminated water before it enters the settler. The flocculent binds with the debris in the water to increase their density. The bonded debris then settles at the bottom to allow separation from the clear hot water. The water must have a low pH of 8.5 for optimal performance of the process [9].

Mines often install a filter plant on the surface to remove the smaller particles from the water. The settlers only remove larger particles to allow minimum damage to the dewatering system. The most commonly found cooling system has small cavities through which the water is transferred. The smallest particles will cause blockage, reducing the flow and efficiency of the system.

The temperature of the hot water from underground is between 30 and 35°C [2]. Water with a temperature of 3°C is required for effective cooling through the cooling equipment. A water cooling system is installed to achieve the desired temperature.

The cleaned water is then transferred to pre-cool towers [7]. Pre-cool towers spray the water to allow heat exchange with the atmosphere. Some pre-cool towers have fans to increase

the velocity of the air the water spray is in contact with to improve heat exchange efficiency. The pre-cool towers lower the temperature of the water to approximately 8°C.

The pre-cool towers do not have enough cooling capacity to reduce the water temperature to 3°C in the summer. Refrigeration Plants (RP) proved to be the most efficient method to cool the water [9]. RP operate on the vapour compressor refrigeration cycle. Refrigerant gas, such as Freon or R-134a is compressed, condensed, expanded and evaporated. The service water is cooled in a high pressure heat exchange vessel in the evaporator stage. A closed water cycle is used for the condenser stage with cooling towers [2].

RP are usually located on the surface of a mine [4]. Some mines have installed secondary underground RP. This reduces the load of the dewatering system, because not all the water is pumped to the surface.

It is recommended, when optimising the pump schedule of the dewatering system, to monitor the entire water reticulation system. This is especially important when the pressure of the service water is harvested with a turbine or 3-CPFS. It ensures that all the dam levels are controlled within acceptable limits for safe and sustainable mining [12].

Figure 2 displays a typical water reticulation system of a mine. The water cycles in a clockwise manner. The pre-cool towers, refrigeration plants, refrigeration plant cooling towers, settlers, hot water dams, mud reservoirs, slurry pumps and electrical pump chamber often exist of multiple units. Only one unit is displayed in the figure.

1.3. Mine dewatering systems

Mines require water for multiple applications to enable safe and sustainable mining. This water must also be removed from the shaft to prevent flooding. A dewatering system is installed to remove water from underground. Dewatering systems were already utilised in ancient Rome for underground operations [1].

Shaft dewatering is done in an upward cascading method to overcome the static head. The water is pumped from the reservoir of the pump chamber near shaft bottom to a reservoir of a higher pump chamber. This is repeated until the used hot water reaches the reservoir on surface. The distance between two pump chambers can be up to 1380 m.

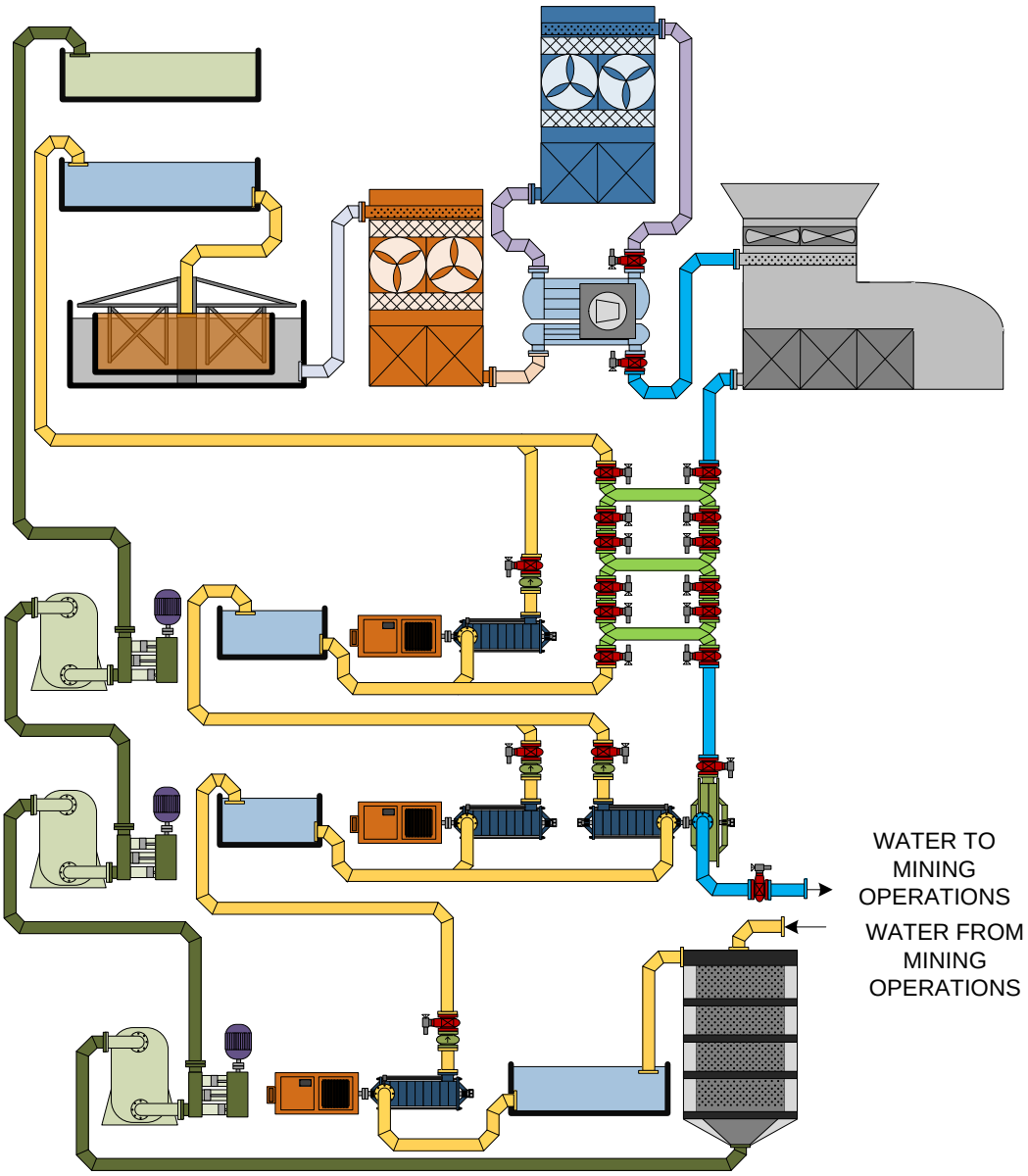

	HOT WATER DAM		HOT WATER PIPE		FILTER PLANT		FILTERED HOT WATER PIPE
	PRECOOLING TOWER		COLD WATER PIPE		REFIGITATION PLANTS		CHILL WATER PIPE
	BULK AIR COOLER		3-CPFS		TURBINE POWERED PUMP CHAMBER		ACTUATOR CONTROLLED VALVE
	SETTLER		ELECTRIC PUMP CHAMBER		SLURRY WATER PIPE		MUD RESERVOIR
	SLURRY PUMP CHAMBER		SLURRY DAM		REFRIGIRATION PLANT COOLING TOWER		REFRIGIRATION PLANT COOLING WATER PIPE

Figure 2: Typical water reticulation system of a mine

1.3.1. Pumps

Multistage centrifugal pumps are the preferred pumps to transfer fluid in many different applications in the industrial and other sectors [1], [20], [21]. Multistage centrifugal pumps are designed to tolerate more robust environments due to their flexibility and durability [22]. Newly developed multistage centrifugal pumps are designed for improved wear resistance, increased availability and reduced maintenance cost. The designs also make maintenance easier to decrease the period the pump is unavailable [1].

A single-stage centrifugal pump creates a discharge pressure by increasing the fluid velocity through a rotating impeller [20]. A multistage centrifugal pump consists of multiple successive single stages. The outlet of the first stage is guided directly to the inlet of the second stage. Only the last stage has an outlet for the discharge flow.

The pumps are generally powered with electrical motors ranging from 1500 to 4000 MW. One of the major disadvantages of pumps is the high electricity consumption [23]. Figure 3 illustrates the electricity consumption per mining process of a mine. Typically pumps used for dewatering is the third highest electricity consumer on a mine. The figure was adapted from A. Botha [14].

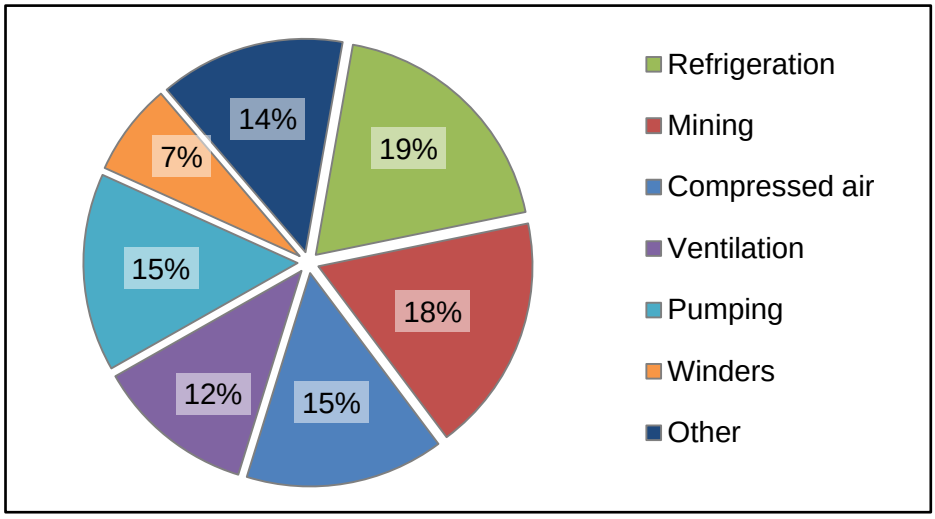

Figure 3: Electricity consumption per mining process

It is often found that energy consumption of a pump or pump chamber starts to increase over time in operation. Effective pump monitoring can determine the source of the increased energy consumption. The energy consumption can be reduced through the following [23]:

- Replacing a pump with a low efficiency,
- Replacing the internal parts and components of a deteriorated pump, and
- Reducing the internal energy loss of a pump station.

Mines started to use alternative methods to dewater the shafts due to the high electricity consumption of the pumps. The potential energy of the service water entering the shaft is harvested through a hydropower turbine or a Three Chamber Pump Feeder System (3-CPFS) [16]. Energy harvesting systems usually have a high initial infrastructure cost [24]. Both the systems must have a pump station and dissipater installed in parallel in case of failure. The dissipater will also be used to meet the water demand if the system flow is insufficient [25], [26].

1.3.2. Three chamber pump feeder system

A 3-CPFS harvests the potential energy of the service water entering the shaft to pump the clear hot water [27]. The surface water has a high pressure due to the head of the water in the columns. Installing a 3-CPFS can result in an electricity reduction of up to 80% [13].

The basic principle of a U-tube is applied on a 3-CPFS via a series of valves. One or multiple booster pumps are installed to overcome the friction head in the columns. A PLC controls the valves and pumps in sequence to ensure the potential energy if fully harvested [26]. Figure 4 is a basic diagram of a 3-CPFS.

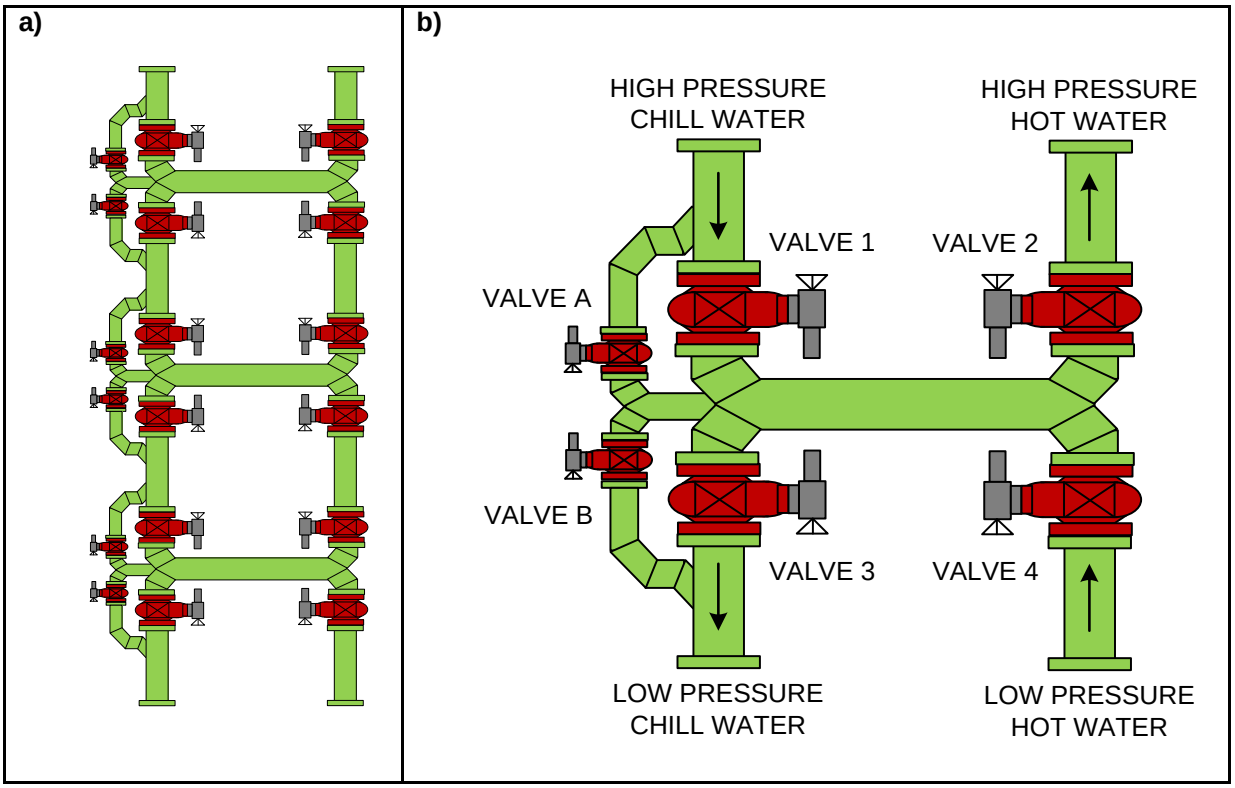

Figure 4: Three chamber pump feeder system a) three stages and b) single stage

Table 1 explains the operation of one stage of a 3-CPFS [27]. The single stage in Figure 4 b must be used with the explanation.

Table 1: Operation of a 3-CPFS

Step	Action	Result
1	Valves closed	Chamber is filled with hot water with low pressure and no flow.
2	Valve A opens	Pressure inside the chamber equalises to the pressure of the chill water.
3	Valves 1 and 2 open	The higher pressure of the chill water forces the hot water out of the chamber.
4	Valves A,1 and 2 close	The chamber is filled with chill water with high pressure and no flow.
5	Valve B opens	Pressure inside the chamber decreases to less than the pressure of the hot water at the inlet. This forms a vacuum relative to the inlet hot water pressure.
6	Valves 3 and 4 open	The hot water fills the chamber due to the relative vacuum formed. Chill water is sent down the shaft.
7	Valves B, 3 and 4 close	Low pressure inside the chamber with no flow similar to the initial step. Step 2 to 7 is repeated during operation.

1.3.3. Hydropower turbines

Multiple shafts have installed turbines to harvest the potential energy of the service water. The turbines are usually installed near a pumping chamber. Some shafts have multiple turbines installed. The output shaft can either be coupled to a generator or a multistage pump. The output power of a turbine can vary from 1 to 5 MW [7].

Pelton wheel turbines are the most efficient type of turbine. The typical efficiency of a turbine installed in a mine ranges from 55 to 60%. Experimental Francis turbines installed were found inadequate for this application [13].

A Pelton wheel turbine consists of a shaft, wheel, multiple buckets and water jet nozzles. The buckets are installed on the periphery of the wheel. The buckets are shaped in the form of spoons held together. The water jet nozzles increase the velocity of the water. The water is directed at a tangent angle to the wheel onto the centre of the buckets where the two spoons join. This causes a moment on the wheel which results in rotation of the shaft [28]. Figure 5 graphically shows the operation principle of a Pelton wheel turbine.

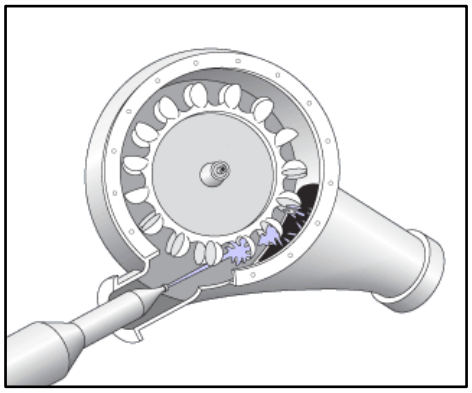

Figure 5: Operation of a Pelton wheel **[1]

Turbines are primarily used to harvest the potential energy of the service water entering the shaft. The power generated from the turbines is often secondary applied to dewater the shaft. The scheduling of the turbines should be included in the dewatering system.

1.4. Advantages of automation and control

The South African electricity supplier introduced a Time-of-Use (ToU) tariff structure for industrial power consumers. The daily profile is divided into peak, standard and off-peak periods. The periods are determined according to the electricity demand. The tariff is directly influenced by the ToU. Other factors such as the distribution distance, voltage and season also influence the cost. The 2014/2015 weekday winter cost tariff can be seen in Figure 6 [29].

Demand Side Management (DSM) projects were implemented according the ToU tariff structure. The aim of DSM projects is to assist high electricity consumers to incentivise electricity use in the lowest cost periods. This also reduces the electricity load on the grid of South Africa. Typical DSM projects on high electricity consumers include the following [2]:

- Load Shifting (LS) – Low to zero electricity load is consumed in the peak periods through spreading the load into the other periods,
- Peak Clipping (PC) – Reducing electricity load in the peak periods, and
- Energy Efficiency (EE) – Daily electricity load is decreased.

** Some of the figures are for illustration purposes only and are not intended to represent state of the art technology. The reference for these figures will be footnoted.

[1] Learn Easy. [Online]. Available: www.learneasy.info. [Accessed 30 July 2014].

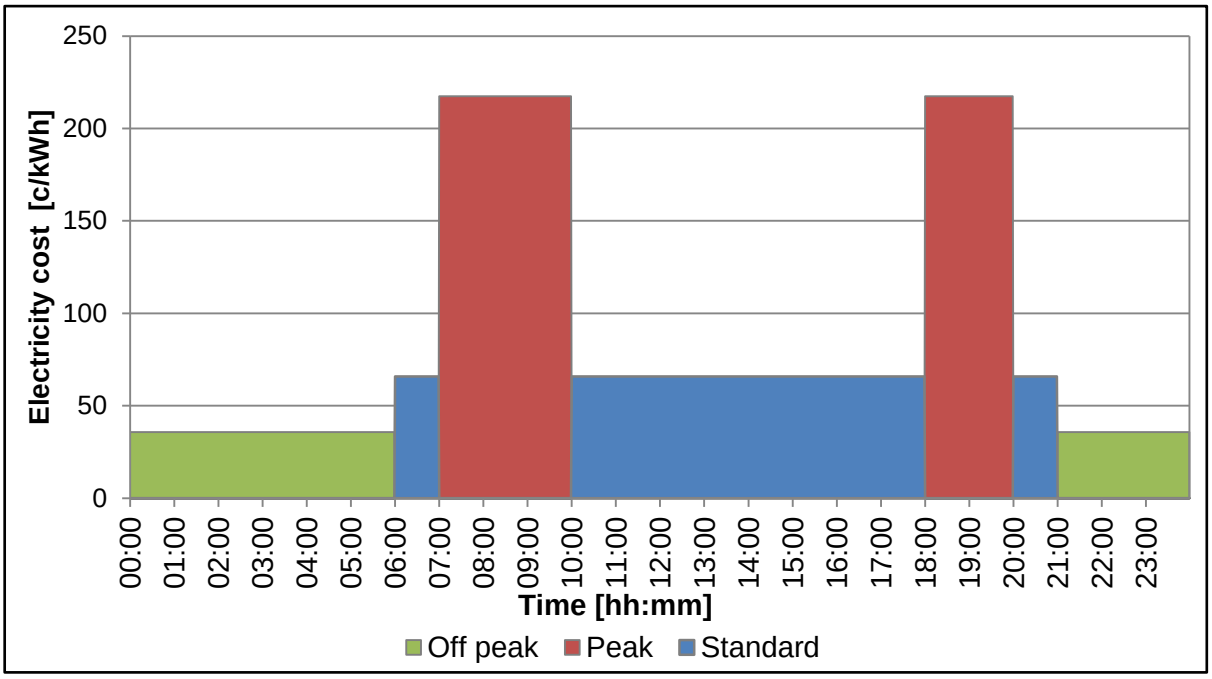

Figure 6: Weekday Time-of-Use winter electricity tariff (2014/2015)

Dewatering systems have the potential to realise electricity cost saving through optimising the control schedule according to the ToU tariff structure [30], [31]. This is achieved by preparing dam levels to allow spare capacity to switch off pumps during the Eskom peak periods [32]. Real-time monitoring to update the control schedule is required for LS [33].

The potential electricity savings of a dewatering system is determined through calculations, measurement and verification and simulation [32]. A comparison of potential savings achieved between manual and automated pump stations was done. It was determined that manual pump control could achieve only 60% of the potential savings, whereas an automated pump system could achieve up to 96%. Human intervention limits the savings achieved [34].

It was proved that additional savings could be achieved if the pump load was minimised in the standard periods. The pump load is shifted to the least expensive off-peak periods. The correct starting and stopping time is crucial to realise additional savings. Pump automation is recommended for real-time control [19].

The number of switches per pump has a direct impact on the maintenance frequency of a pump. A pump experiences additional axial thrust until the impeller is balanced. The number of stops and starts must be considered when optimising the control schedule [35], [32]. Automation of pumps allows for monitoring the number of switches and to prevent unnecessary cycling.

Additional savings can be achieved by including the installed alternative dewatering systems such as the turbines and 3-CPFS into the pump schedule. A mine shaft will achieve maximum savings when the entire water reticulation system is automated. This includes the BACs, FP, pre-cool towers, alternative dewatering systems, distribution of service water and dewatering pumps. The systems can be interlocked to ensure safe and sustainable mining when automated [36].

Workforce is often limited during the festive seasons or industrial action (also known as legal strikes). Safe dewatering can be sustained during these periods if the pump system is automated. Automation has the potential of labour cost savings. Less pump operators will be required if a pump system is automated [1].

Pump monitoring is another advantage of pump automation. Instrumentation is required to ensure safe remote operation. The performance and condition of each pump can be determined from the data logged from the instrumentation [36]. Maintenance cost savings can be achieved through correctly analysing the data.

1.5. Objectives and problem statement

Dewatering systems are crucial for sustainability in deep level mines. These systems are being automated to reduce the amount of human intervention. Automation is achieved through monitoring certain operating conditions. These conditions are then interlocked to initiate an alarm or a stop sequence when it exceeds normal operating conditions.

The purpose of this study is to improve the current best practice of pump automation. This will be achieved through investigating automated pump failure and detect the conditions leading to failure. Reviewing the purpose of the installed instruments will make it possible to identify the need for additional instrumentation or control alterations.

Remote control of the automated pumps can be achieved if they are connected to a data network. The automated pump system makes it possible to control it from a centralised system. This enables real-time control of the entire system. This is achieved through status feedback over the network of all the individual control parameters.

This study will also verify the feasibility of controlling an automated mine dewatering system from a surface control room. The control will focus on maintaining save operating dam levels and electricity cost savings through minimising pumping in the peak periods.

Data from the conditions monitored of the automated pumps will be collected in real-time. This is to limit the time the pump is operated at out of normal conditions. Access to the data

will make it possible to determine the most feasible method to calculate the real-time pump efficiency.

The study will lastly use the installed instrumentation for automation and determine a method to calculate the real-time efficiency. The method must exclude the pump flow. An accurate flow meter is expensive and multiple pumps often use one column for dewatering.

1.6. Overview of dissertation

Chapter 1

This chapter explains deep level mine water consumption. An overview of a mine reticulation system is given. It focuses on the different methods to dewater a deep level mine. This chapter also lists the advantages of automating the dewatering system.

Chapter 2

The basic operating principle of a multi-stage centrifugal pump is explained. Understanding the operating principle makes the investigation on the current best practice of automation possible. Identifying and motivating the parameters to monitor with pump automation, including auxiliaries. The characteristic and results of pump cavitation are discussed.

Chapter 3

A case study is presented of a pump that failed after it had been automated. The pump failure was examined to determine the root cause of failure. Additional precautions and safety measures are considered to prevent a similar incident. The control philosophies for a dewatering system are discussed. An alternative method to determine pump efficiency in real-time is implemented.

Chapter 4

The results of the installed instrumentation of a pump are shown. The additional precautions and safety measures are verified to determine if it will prevent a similar incident. Pump running statuses are discussed with the implemented control philosophies. The real-time efficiencies of the pumps calculated are shown.

Chapter 5

A conclusion based on the results obtained is made. The results also make it possible to suggest alterations to the project. From this study several opportunities for further studies were identified. These opportunities are also discussed in this chapter.

Chapter 2: Pump automation overview

Understanding the operating principle of a multi-stage centrifugal pump is necessary to improve the automation of the system. The current best practice to automate a multi-stage centrifugal pump is investigated. This assists in motivating the conditions that should be monitored when automating pump system.

2.1. Introduction

Automation of a pump or pump station has multiple potential advantages. Several parameters should be investigated when automating a pump. This ensures the best possible solution is installed. The parameters that must be investigated will be discussed in this chapter.

Included in pump automation is pump monitoring. This allows for safe remote start or stop without direct human intervention. The differences between condition and performance monitoring will be compared. Critical conditions and deliverables that should be included in the pump automation to ensure optimal pump operation will be investigated.

All the necessary auxiliaries of a pump should be considered and automated when a pump is automated. The discharge valve is one of the key auxiliaries to automate within the pump system. The different types of valves often used as discharge valves are discussed. Several methods to automate the discharge valve are also included in this chapter.

Pump cavitation is known as a destructive condition that results in pump failure. The origin of cavitation is discussed and methods included in pump automation specified by manufacturers are investigated. The effect of cavitation on the hydrodynamic performance of a pump is also determined.

2.2. Multi-stage centrifugal pumps

The expected lifetime of a multistage centrifugal pump is 15 years. The regular life of a pump can be increased with up to 15% if the correct maintenance is done. This can reduce the energy consumed with up to 7% [1]. The lifetime reduces when the pump operates outside the design conditions. Maintenance frequency should be increased if the fluid transferred has corrosive properties [22].

Refurbishing a pump is not feasible if the cost exceeds 40% of the price of a new pump. Refurbishing or upgrading a pump typically involves internal renovation, modernization of the seal system and a revamp of the lubrication oil system. Pump system upgrades include increasing the rating of the pump power source, pump re-wheeling, control valve modification and various piping changes [37].

A pump should be investigated for refurbishment if the power consumption increases with a constant discharge flow. The increased power consumption is an indication of a decreasing efficiency. A decreased efficiency implies that the pump must pump for a longer period to

transfer the same amount of fluid. Condition monitoring and performance monitoring of the pump can assist with the decision on when to refurbish the pump [38].

Upgrading the motor or the impeller can result in an energy saving of up to 3.5%. When a pump is upgraded as a unit, including electrical equipment and motor pump, the saving can improve with up to 10%. If the pump system is examined as a system, including pumps, piping, control and operating strategies, a saving of up to 60% is achievable [33].

A breakdown of the total cost of a typical multistage centrifugal pump during its operation cycle is illustrated in Figure 7 [33], [22]. At 40%, power consumption is the largest expense of a pump during its operation cycle. Maintenance contributes to 25% of the total cost of a pump. Installing effective pump monitoring equipment to improve pump reliability can result in power consumption and maintenance cost saving [39].

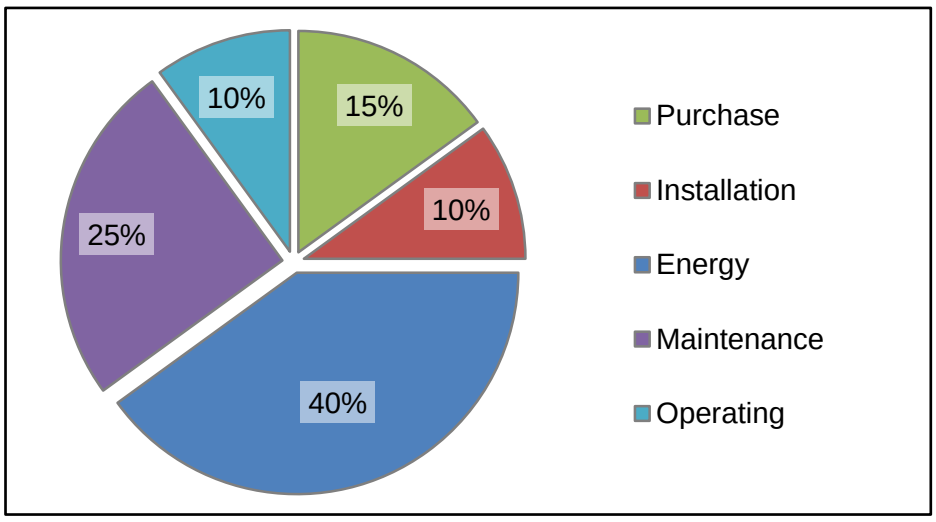

Figure 7: Breakdown of total cost of a pump during its lifetime

2.2.1. Failures

Failure of pumps is a concern for any pumping station. It can result in the pump system not meeting the demand when no spare capacity is available. This increases the risk of flooding a mine. The following list is the main reasons for pump failure [40]:

- Design, fabrication and assembly faults,
- Incorrect installation or commissioning,
- Change in operating conditions, and
- Mechanical wear from operation.

Pumps are designed with little clearance tolerances to achieve the highest efficiency possible. This reduces the out of design operation margin [41]. Fabrication and assembly of

a pump are of utmost importance due to small tolerances. A pump will experience additional internal stresses and vibration, which can result in failure [42], [43].

Correct installation and commissioning of a pump are important to ensure all safeties and trips are operational [41]. A condition monitoring or safety circuit is only as effective as the least trustworthy data collected from the pump. If the data is unreliable or corrupt, the condition monitoring will not be as effective [33], [43].

A change in operating condition can result in transient flow. During transient flow, the equipment is subject to rapid temperature, pressure and speed changes. In most cases of transient flow the conditions exceeds the design condition [40], [42].

The most common incorrect operations of centrifugal pumps that lead to failure are [44]:

- Insufficient suction pressure leading to cavitation,
- Excessively high flow rate for the Net Positive Suction Head available (NPSHa),
- Prolonged operation at lower than acceptable flow rates,
- Operation of the pump at zero or near zero flow rate,
- Improper operation of pumps in parallel,
- Failure to maintain adequate bearing lubrication, and
- Failure to maintain satisfactory flushing of mechanical seals.

Knowledge and experience obtained can assist on determination of failure through visual inspection. It is recommended for confirmation of failure to be revealed from metallurgical laboratory tests [45].

2.2.2. Head required

The head required in a pumping system is the static head plus the friction head. The static height is the difference in height between the fluid surface the reservoir pumping from, to the highest point of travel of the fluid [46]. The friction head is the differential pressure of the fluid through the component used to transport the fluid [47].

Experimental results define loss coefficients for each component. The friction head is due to velocity change, direction changes or flow restriction. Friction head is calculated with Equation 2.1 from the loss coefficient [48].

$$h_L = K_L \frac{\dot{V}^2}{2g} \tag{2.1.}$$

h_L	-	Component friction head	m
K_L	-	Loss coefficient	-
$\dot{V}$	-	Fluid velocity	m/s
g	-	Gravitational Constant	m/s^2

Valves are used to control flow in a pumping system. A valve that is fully closed will have an infinite loss coefficient to produce zero head at the outlet. The total friction head of a system containing more than one component is the sum of the losses. The loss coefficients of the following components are usually considered within a pumping system:

- Suction and discharge nozzles,
- Inline pipe diameter variations,
- Valves and flow restrictions, and
- Elbows, bends and tees.

The flow of fluid through a pipe causes friction that results in an additional friction head. The friction is a function of the type of flow and internal smoothness of the pipe. The friction head due to the friction is calculated with Equation 2.2 [49].

$$h_f = f \frac{l}{D} \frac{\dot{V}^2}{2g} \tag{2.2.}$$

h_f	-	Pipe friction head	m
f	-	Friction coefficient of pipe	-
l	-	Length of pipe	m
$\dot{V}$	-	Fluid velocity	m/s
D	-	Inside diameter of pipe	m
g	-	Gravitational Constant	m/s^2

The total head required by a pump is illustrated with Figure 8. The water is pumped from reservoir A to reservoir B. The differential height difference between the water surface A and the highest point of travel is defined as H_s.

More pumps are often specified and installed than required when designing a pumping station. This allows one or more pumps to be on standby in case of an emergency. It is frequently found that design parameters are neglected and all the pumps are operated simultaneously [50].

The efficiency of the pumping system decreases if the number of pumps operated simultaneously increases and discharges into one column. The increased flow through pipes and pipeline components increases friction losses. The total energy to transfer the same amount of water increases due to deteriorated efficiency. Controlling according the design will reduce the energy consumed and maintenance cost [50].

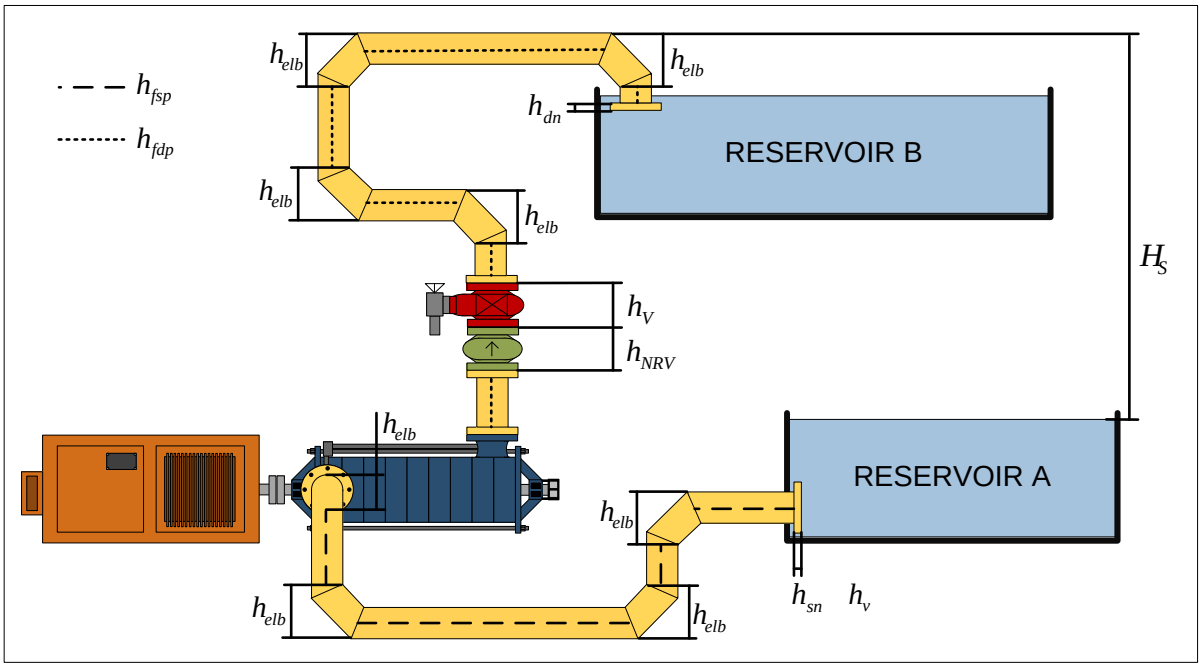

Figure 8: Pumping system total head required

The friction head due to the suction and discharge nozzle is defined as h_{sn} and h_{dn} respectively. The friction caused by the pipe from the suction to pump inlet is defined as h_{fsp}. The valve and NRV on the pump outlet causes a friction head defined respectively as h_V and h_{NRV}. The friction head from the valve to the discharge is defined as h_{fdp}. There is a total of eight identical elbows in the system that individually causes a friction head defined as h_{elb}. The total head required by the pump is calculated with Equation 2.3 [46].

$$H = H_s + h_{sn} + h_{fsp} + h_V + h_{NRV} + h_{fdp} + h_{dn} + 8h_{elb} \quad 2.3.$$

H	-	Head	m
H_s	-	Static head	m
h_{sn}	-	Suction nozzle friction head	m
h_{fsp}	-	Suction pipe friction head	m
h_V	-	Valve friction head	m
h_{NRV}	-	NRV friction head	m
h_{fdp}	-	Discharge pipe friction head	m
h_{dn}	-	Discharge nozzle friction head	m
h_{elb}	-	Pipe elbow friction head	m

The total head developed is the sum of differential energy across the pump. The differential energy consists of the potential and kinetic energy from the pump inlet to the pump outlet. Equation 2.4 illustrates how to calculate the head that a pump develops [51].

$$H = \frac{(P_o - P_i)}{\rho g} + (Z_o - Z_i) + \frac{\left(\dot{V_o}^2 - \dot{V_i}^2\right)}{2g} \quad 2.4.$$

H	-	Head	m
P_o	-	Outlet pressure	Pa
P_i	-	Inlet pressure	Pa
Z_o	-	Outlet height	M
Z_i	-	Inlet height	m
$\dot{V}_o$	-	Outlet velocity	m/s
$\dot{V}_i$	-	Inlet velocity	m/s
ρ	-	Fluid density	kg/m^3
g	-	Gravitational Constant	m/s^2

The velocity of the fluid has a direct impact on the friction head of a system. Pumps in a pump system are often installed in parallel. The velocity of the fluid is increased if more than one pump transfers fluid in a single discharge column. The increased velocity increases the friction head of the system [23]. The increased pressure also adds risk of column failure.

2.3. Current best practices to automate a pump

It is desired to operate pumps at their maximum efficiency, reliability, capacity and minimum operating and maintenance cost. This will reduce the total running cost of the pumping station [40]. Pump monitoring is included in the current best practice when automating a pump. Pump monitoring promotes preventative maintenance to predictive maintenance. This results in only necessary components being replaced, instead of changing certain components after a set time period [40], [52].

Effective pump monitoring can improve pump reliability through root-cause failure analysis. It can identify a condition at an early stage that could lead to pump damage. This reduces the risk of unpredictable failure and down time [40], [42]. Replacing or repairing the weakening component before failure can also enhance the performance of the pump [42], [52].

Multiple instruments are installed on a pump to monitor several conditions and deliverables. Proven reliable instrumentation should be installed for pump monitoring. The feedback received from instrumentation should be interlocked in a control program. The functionality and failure probability of a component should be taken into consideration when designing a pump monitoring system [53].

The normal condition and deliverables of a new pump should be logged before wear or damage occurs as a reference point. Operating ranges of the pump of healthy operation should be defined and logged [40], [52]. An alarm must be activated if the defined limit is reached, determined from the healthy operation data. If the condition continues to exceed healthy conditions, an emergency shutdown must be initiated [40], [42].

Modern pump systems must be seen as an integrated operation including the hardware, software, operating procedures, control philosophies and process condition. Pump monitoring is included in the system to increase the availability of a pump [53]. All components of an individual pump, including the motor, transmission, pump, auxiliaries, valves, lubrication and seal system must be monitored continuously [42].

Pump monitoring can be divided into two groups, namely performance monitoring and condition monitoring. Performance monitoring determines the efficiency of a pump with the deliverable. Condition monitoring reduces the risk of failure. Performance monitoring does not replace condition monitoring. It assists with the analysis of the condition monitoring data. [54]. Figure 9 shows the different parameters and benefits [54].

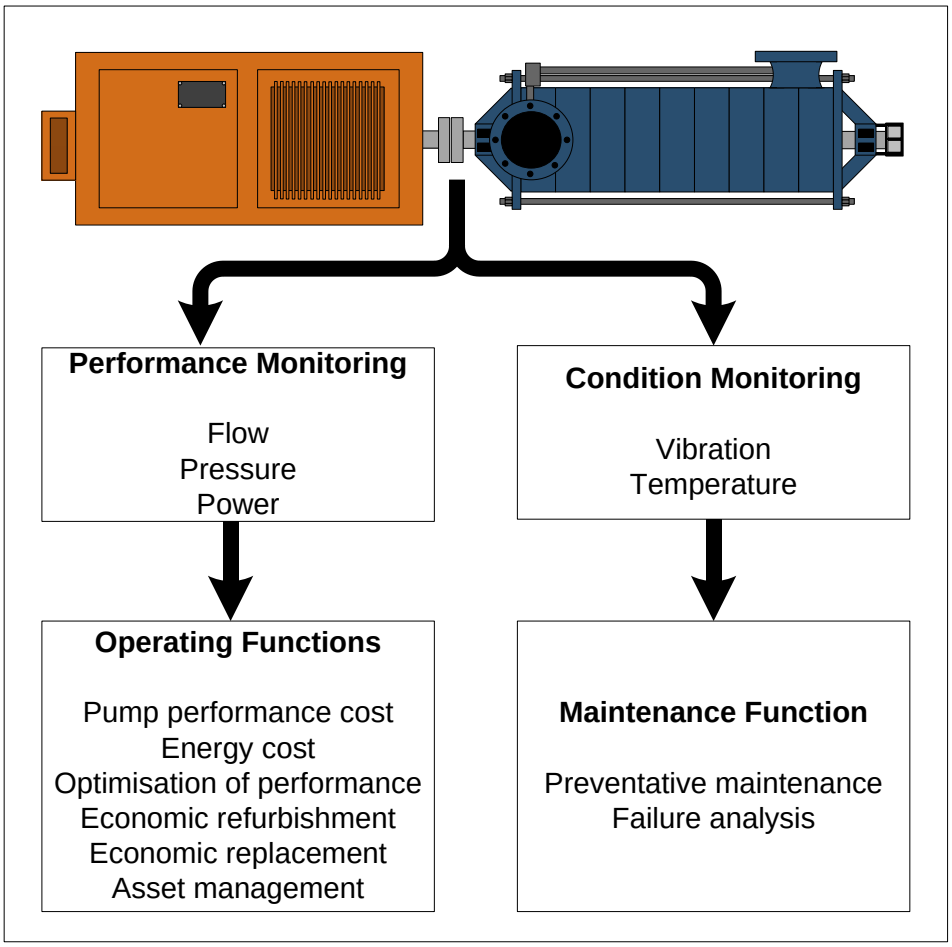

Figure 9: Pump condition and performance monitoring

The data obtained from pump monitoring has to be analysed correctly. Technical training and experience of pump operators and technicians will assist in interpreting the data correctly [54]. Understanding the characteristics of a pump will allow early identification of a failing part or component [53]. Several parameters should be monitored for pump monitoring. The parameters monitored forming part of the current best practices of centrifugal pump are shown in Figure 10 [36], [55]. These parameters are according to the literature and the mine standards where the project was implemented.

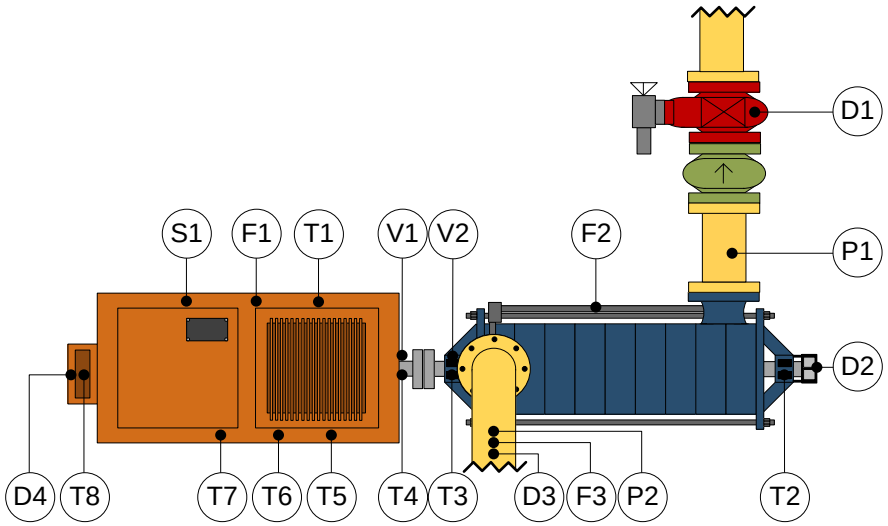

T = TEMPERATURE S = SWITCHGEAR F = FLOW
V = VIBRATION D = DISPLACEMENT POSITIO P = PRESSURE

NR.	DESCRIPTION	NR.	DESCRIPTION
S1	SWITCHGEAR HEALTHY	P2	SUCTION PRESSURE
F1	MOTOR COOLING WATER	F3	SUCTION FLOW
T1	MOTOR AIR	D3	SUCTION VALVE POSITION
V1	MOTOR DE BEARING	T3	PUMP DE BEARING
V2	PUMP DE BEARING	T4	MOTOR DE BEARING
F2	BALANCE DISC	T5	MOTOR WINDING U
D1	ACTUATED DISCHARGE VALVE	T5	MOTOR WINDING V
P1	DISCHARGE PRESSURE	T6	MOTOR WINDING W
D2	PUMP IMPELLER DISPLACEMENT	T8	MOTOR NDE BEARING
T2	PUMP NDE BEARING	D4	MOTOR SHAFT DISPLACEMENT

Figure 10: Instrumentation required for pump automation

Flow

The flow of a pump must be included in pump monitoring. Worn internal parts can be detected if the rated design flow from the manufacturer is not delivered at a specific speed [42], [56]. A pump can be damaged if the flow through a pump is less than the design minimum. Installing flow sensors will prevent the pump against minimum flow [38].

Pumps should be started at the nearly closed discharge valve position. The pump generates head as the discharge valve opens to overcome the pressure in the discharge column. For minimum flow restriction the suction and discharge valves should be opened fully when the start-up sequence has been completed [57].

It is often found that the discharge valve of a pump is throttled to regulate the flow of the pump [52]. Additional wear occurs on the internal components if the discharge valve is throttled. This increases the maintenance cost and frequency of a pump [47].

Balance disc flow monitoring is recommended [38]. The balance disc flow acts as a thrust bearing for the pump to counteract the axial force of the impeller. The water is pumped between the balance disc and the balancing chamber, creating a thin film layer water bearing [52].

Pressure

The pump columns are often undersized, both in design and due to inconsistent maintenance frequencies [23]. When a pump starts with low flow against a barely open discharge valve, the pressure will be greater than normal operating pressures. The discharge column from the pump outlet to the discharge valve should be designed to endure the higher pressures during start-up [57].

The water level inside the discharge column is determined with pressure sensors. A pump must always be started with a full discharge column. If the column is drained, the column must be filled before the pump can be started. The safety trip circuit of the pump during start-up should include the water pressure of the discharge column.

Power

It is recommended to install a Variable Speed Drive (VSD) to control the flow of a pump. A VSD alters the current frequency and voltage frequency of the motor to adjust the rotational speed accordingly [20]. Reducing the motor frequencies of a pump via a VSD also has an energy-saving potential [23].

Using a VSD ensures the rotational velocity is gradually increased to operating speed when starting and gradually decreased when stopped, resulting in less mechanical strain induced on the pump from the moment of inertia. This reduces the maintenance frequency of a pump and motor [47].

An increase in power consumption on a pump that is controlled on the discharge pressure or flow via a VSD can be an indication of a worn impeller. The rotational velocity of the pump has to be increased to meet the demand of the system. A high power alarm will alert the pump operators of the additional power consumption [56]. A pump dewatering system requires a constant head at full load power. VSD's are not installed on the pump dewatering systems.

During pump start-up, for a brief period, the power consumed is higher than the operating power. This is a result of system friction and moment of inertia. The additional system friction during start-up includes the discharge head, barely open discharge valve, non-return valve not opening or transient flow through the pump [6]. The real-time motor power can indicate whether the pump is operated incorrectly.

The torque required for four different starting speeds are displayed in Figure 4. It can be seen that the basic profiles of the graphs are similar. The period of fluctuation during start-up is directly proportional to the start-up speed. The fluctuation is a result of system friction and moment of inertia.

The fluctuation for all four speeds settles at approximately 2300 Nm. The torque increases to a maximum of 3600 Nm from where the torque decreases to operating torque. The operating torque is required to account for the pump and motor friction forces. The graph is a combination of the graphs found in S Elaoud and E Hadj-Taïeb [58]. The original graphs are shown in Appendix A.

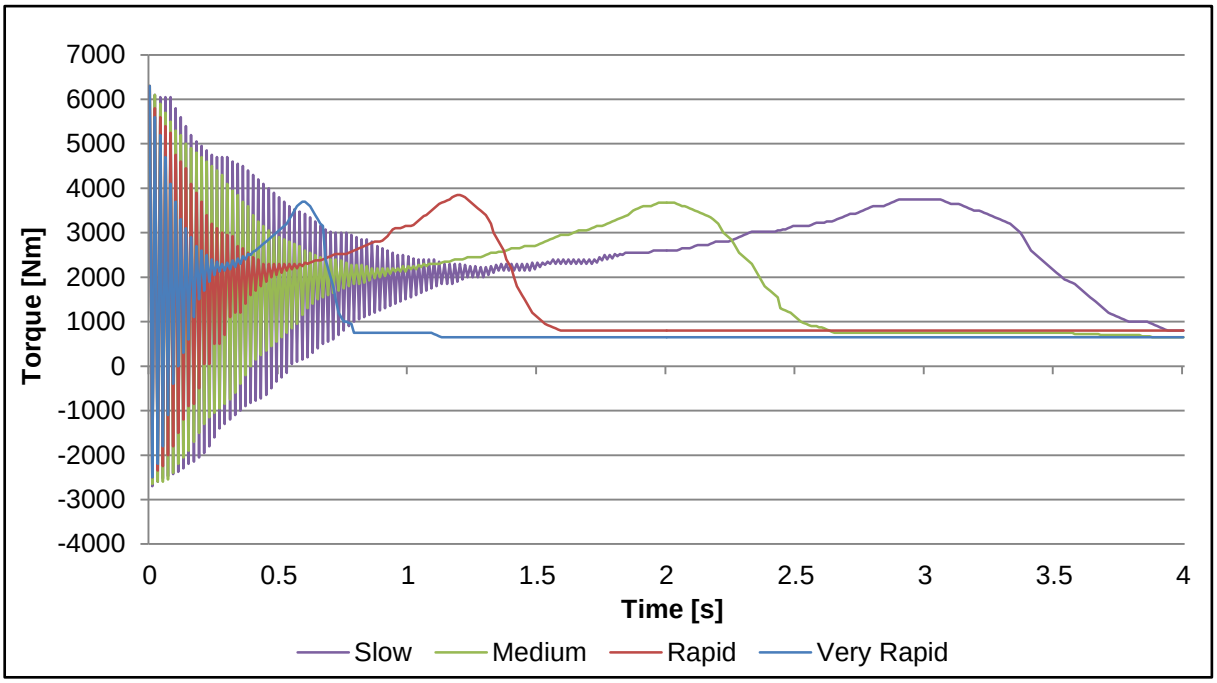

Figure 11: Pump motor torque for four start-up sequences

Vibration

Vibration monitoring is a good indication of the condition of a machine. Proper vibration analyses can extend the lifetime of a pump. Excessive vibrations can be an indication of a failing component inadvertently destroying itself [59]. Defects that are construction-related, caused by improperly installed equipment or incorrect operating conditions can be also detected with vibration sensors [60]. The following list contains key purposes of vibration monitoring [61]:

1. The overall magnitude can indicate the presence of a failed or failing component.
2. Frequencies can indicate the root cause of damage.
3. Time-base waveforms and orbital paths of rotor lateral motion.
4. Amplitude and phase angles of dynamic motion component of the rotor.

The largest vibration forces are noticeable at the rotor. Vibrations transferred from the rotor to stationary parts can result in catastrophic failure. The pedestal, pump casing and foundation also experience the vibration forces transferred from the rotor. Measurement of the vibration should be as close to the origin as possible for accurate readings [61].

The current best practice is to install two non-contact vibration sensors at the pump and motor bearings. It measures axial vibration forces and static centreline position of the rotor relative to the mounting. Pumps are monitored to ensure the operation thrust forces are within design specifications [61]. Vibration measurements assist with the detection of rotor

vibration. The natural frequency for most pumps in the tangent direction is higher than in the axial direction [62].

A vibration sensor installed on the casing, inlet or outlet column of a pump, measures the vibration of the fluid. Fluid vibrations are an indication of the fluid energy. Transient flow and cavitation can be detected from measuring fluid vibration [59]. It must be noted that casing vibration measurement does not measure shaft vibration.

Plotting the results of a vibration sensor can indicate multiple defects and operating errors of a pump. Figure 12 illustrates the difference between the graphs of a pump with various defects or operating errors. The graphs are simplified from N R Sakthivel et el. [63]. The original graphs can be found in Appendix A.

It can be seen that a pump with a bearing defect will have the maximum amplitude of vibration of the primary sine wave. A pump with only a seal defect reduces the amplitude of vibration of the primary sine wave. The other defects only change the frequency of the secondary sinus wave. Experience in the field of vibration analysis will enable a person to identify the different defects from vibration graphs.

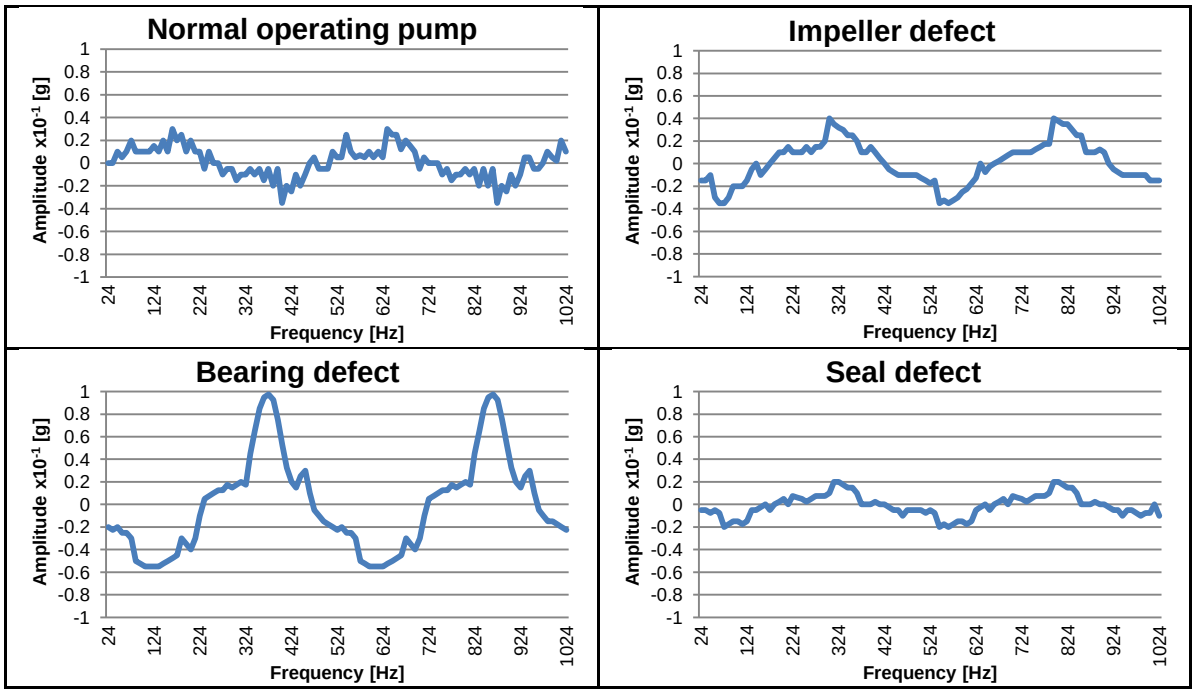

Figure 12: Graphs of defects detected with vibration sensors

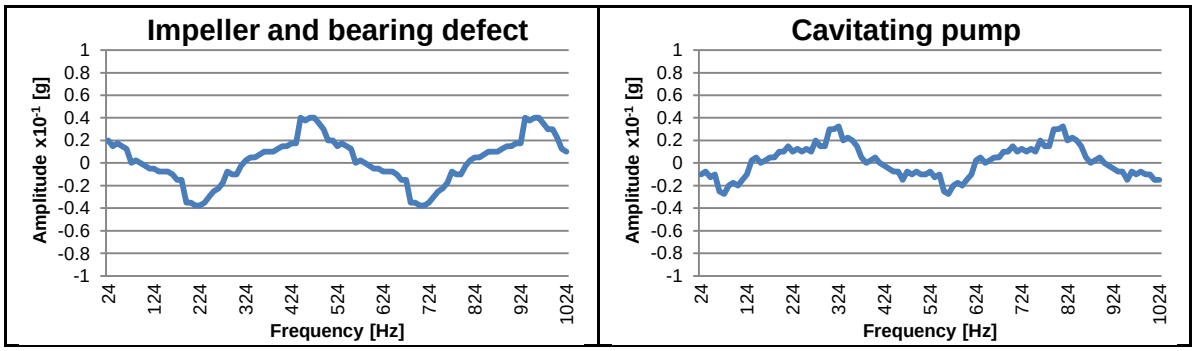

Figure 12 (continue): Graphs of defect detected with vibration sensors

Each of these vibration defects has a direct impact on the hydrodynamic performance of a pump. Interpretation of the origin of the vibration can be determined through the correct interpretation of the vibration results. Replacing or repairing the defective component will improve the performance of the pump [64].

A handheld vibration sensor can be used if the automation budget does not allow for permanent installed vibration sensors. Measuring vibration should be schedule based or if additional vibration is suspected. The following guidelines should be considered with handheld vibration sensors [60]:

- Measure as close to the bearing as possible,
- Take readings at precisely the same spot,
- Measurement should take place perpendicular to surface ±10°,
- Hand pressure should be even and consistent, and
- Magnetic mounts can assist with pressure and consistency.

Temperature

An increase in temperature is an indication of energy loss as a result of friction. A failing component or a pump operating outside its design specification induces additional friction. Monitoring the temperature can reduce failure of a pump or a component. Temperature probes and infrared thermometers are often installed to monitor crucial part of a pump [42].

Zero or low flow through a pump will lead to failure. If the discharge flow of a pump is restricted through blockage, discharge valve or non-return valve not opening, it can result in periods of zero flow. The energy transferred into the fluid will cause the temperature of the fluid to increase. If the temperature exceeds the saturation temperature of the fluid, the fluid will form vapour. This is known as a vapour-lock. The pump will not be able to develop a head with internal gas-fluid mixture. The pump must be stopped before damage occurs, allowing the vapour to condense [44].

Heat transfer between the pumped liquid and the internal part of a pump causes the material of internal components to expand. The expansion will result in contact between the rotating and stationary parts [57]. This can lead to damage reducing the efficiency and reliability, increasing the maintenance frequency and total failure [65].

Bearings are a crucial part of a centrifugal pump. Friction between the static and rotating parts of a pump is reduced with the use of bearings [34]. The temperature of the bearings should be constantly monitored to prevent failure. Wear on the bearings will increase due to incorrect installation, misalignment, improper lubrication levels, looseness or high rotor unbalance [66].

Temperature probes are installed to monitor a specific component or condition of a pump. If the monitored temperature increases, it must be inspected for a defect or incorrect operation [22]. If no defect is found, other factors that can cause a rise in temperature must be investigated. A combination of the data obtained from all the instrumentation can be a guide for the investigation.

Most modern motors have internal temperature sensors on each motor winding. The temperature of the motor windings should be included in the safety circuit of the pump [53]. It is also recommended to monitor the temperature of the cooling auxiliaries of the motor, such as cooling water or air, to prevent failure.

2.4. Valves and automation

Shut-off devices are used to regulate the direction of motion of hydraulic fluids. It is important to choose the appropriate valve for the application. When specifying a valve the shut-off conditions, operational conditions and fluid properties should be considered [67]. When control valves are operated incorrectly, it can result in cavitation, noise and failure [68].

The flow varying restricting component of a valve is connected to a stem. The stem exits the body of the valve to enable control from the outside. A spindle is connected directly or through a gearbox to the stem for manual control. For automation of a pump station remote control functionality is required. The spindle is thus replaced with an actuator to enable remote control [69].

Actuated valves are hydraulic, pneumatic or electrical powered. The hydraulic actuator requires a highly reliable pressure source, for example a pump. A pneumatic actuator requires a compressed air source and an electric actuator requires the designed electric supply. The friction force of the valve determines the rated size of the actuator [67], [70].

The positions of the valve at the inlet and outlet of a pump should be monitored to ensure that the required flow is possible. The mechanical limits of the actuators must be set correctly if the valve is controlled via an actuator. This allows maximum flow with the least restriction when the pump is operated. The closed valve prevents fluid to enter the outlet of the pump from the discharge head or pumps in parallel [71].

Cavitation can occur in throttled valves due to the increased velocity through a valve. This increases the dynamic pressure and reduces the static pressure of the fluid in that area. If the static pressure drops below the saturated vapour pressure for the specific condition, the fluid will flash and form bubbles. When the fluid exits the valve, the pressure will force the formed bubbles to implode [68], [72].

Figure 13 illustrates the four distinct types of isolating valves used at pump outlets. Several operating parameters should be considered when selecting a valve. The parameters are temperature rating, pressure rating, material compatibility, shutoff sealing ability and pressure losses [73]. The less obvious parameters are the leakage through the gland packing and the physical size or shape of the flow passage.

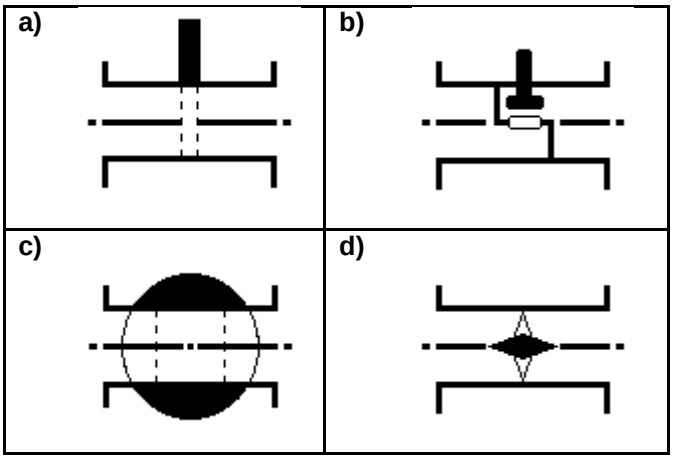

Figure 13: Schematic isolating valves: a) gate, b) globe, c) ball and d) butterfly

The passage of flow for most valves is straight, with the same dimensions of the column. A few valves do not have a straight passage flow. The bore of some valve can also be smaller than the pipeline the valve is installed in. Both these factors cause additional pressure losses and increases maintenance cost [73].

Each valve type has its own advantages and disadvantages. It is thus important to specify the correct valve for the application. Table 2 is a comparison of the advantages, disadvantages and the recommended application of each valve type [74].

Table 2: Valve type comparison

Valve	Gate	Ball	Globe	Butterfly
Type	**Open/Close**	**Open/Close**	**Throttling**	**Throttling**
Advantages	Minimal pressure loss across valve Low flow restriction induced with debris	Minimal pressure loss across valve Low flow restriction induced with debris Compact design High capacity Good shut-off	Good shut-off High opening and closing frequency Inline replacement of trim High capacity Noise reduction cage available Smooth control	Compact design Minimal pressure loss across valve Low cost High throughput capacity Smaller shaft and actuator
Disadvantages	Poor sealing characteristic Valve must be removed for maintenance	Temperature range limited due to seats High flow restriction Cavitation Valve must be removed for maintenance	High pressure loss due to tortuous flow path Noise reduction cage reduces capacity	Poor sealing characteristics Efficient control limited to 60° open Specialized lining, oversized shaft and actuator are required for tight shut-off
Recommended applications	Not for frequent opening or closing Throttled control is not recommended	Not for service with highly corrosive fluids Most suitable for handling slurries	Flow regulation Tight shut-off applications	Low-pressure applications

Valves that use a spindle to control the position of the flow restriction body have glands to seal the valve. The type of gland is dependent upon the fluid properties. The seals may require a liquid quench, a piped vent, or a gas blanket. Incorrectly specified glands will cause early leakages which can increase the maintenance intervals [73].

It is often found that maintenance on valves is based on a time schedule. Installing condition monitoring equipment on these valves can detect if a valve is not operating correctly. This can reduce the maintenance frequency on the valves [68].

Valves often deteriorate more rapidly if used in a corrosive medium and significant temperature gradients. Wear to the internal components, connections and welds is often found on shut-off devices [75]. It is often difficult to open a valve if a large differential pressure is present across the valve [57], [73]. The differential pressure induces additional friction in a valve.

The discharge valve of a pump can induce water hammer during start up or shut down of a pump. The control of an actuated valve should be programmed correctly to prevent water hammer [76]. The response of the discharge valve actuator is not directly proportional to the control signal [20].

2.4.1. Gate valves

A gate valve has a straight flow passage through the valve. The valve has a disc, known as the gate or knife, to restrict the flow. The gate moves perpendicularly to the flow to open or close the valve [69]. The valve has a bonnet area to house the gate when fully open. The gate is attached to a stem with square screw thread to control the position of the gate. Figure 14 displays a sectional view of a gate valve.

A gate valve is often used as shut-off devices for large diameter pipes with high pressure. A gate valve is highly reliable, especially when operating in a medium containing abrasive particles [56], [67].

Figure 14: Sectional view of a gate valve [2]

[2] Trade India. [Online]. Available: www.tradeindia.com. [Accessed 04 June 2014].

2.4.2. Globe valves

A globe valve consists of a plug-type disc seated against a port. The port is perpendicular to the inlet and outlet flanges to enable the plug to restrict the flow. This flow path is known as a tortuous flow path [77]. The flow is forced upward through the port to the outlet [69]. Figure 15 displays a sectional view of a globe valve.

Figure 15: Sectional view of a globe valve[3]

Globe valves are commonly used in pipelines that transfer fluid which contains pulverised solids. In this regard it was found that the current globe valve design had multiple disadvantages. The pulverised solid in the fluid damages the internal components of the valve. This results in wear of the airproof components and dramatically shortens the lifetime of the valve [78].

Cage-style trims were designed to prevent cavitation in globe valves. The cages are designed to regulate the flow evenly through the valves. Prior to the trim a downstream orifice was installed inline to protect the valve against cavitation. This results in only moving the cavitation to the orifice instead of inside the valve [39].

2.4.3. Ball valves

A ball valve has a ball in line with the flow passage. The ball has a straight bore hole to allow flow through the valve. The ball rotates from parallel to perpendicular with reference to the inlet and outlet. When the ball is rotated to its maximum position, the flow is shut-off [79].

[3] Weir. [Online]. Available: www.weirpowerindustrial.com. [Accessed 04 June 2014].

Figure 16: Sectional view of a ball valve[4]

2.4.4. Butterfly valves

The flow follows a straight passage through a butterfly valve. The valve consists of an in-line disc that rotates from parallel to perpendicular with reference to the inlet and outlet [69]. A pressure loss is present even when the butterfly valve is fully open due to presence of the disc in the flow path [80]. Figure 17 is an isometric view of a butterfly valve.

Figure 17: Isometric view of a butterfly valve[5]

A butterfly valve is often used to control the flow of gas, oil, water or air in large transport systems. The typical operating range of a butterfly valve is between 30% and 70% open. If the opening exceeds 70%, the pressure loss is almost constant [81]. Butterfly valves require more torque to operate than the other valves due to the torque induced by the liquid on the disc [70].

[4] Global valve & Controls. [Online]. Available: www.globalvalveandcontrols.com. [Accessed 21 June 2014].
[5] Weir. [Online]. Available: www.weirpowerindustrial.com. [Accessed 04 June 2014].

2.4.5. Non-return valve

Pumps that operate against a high head or in parallel should have a Non-Return Valve (NRV) installed in-line on the discharge column. This acts as a mechanical safety if the controlled discharge valve fails. The NRV will prevent the pressure in the discharge column to rotate the pump backward [57], [58].

Figure 18 displays two types of NRV. Valve a in Figure 18 is known as a piston type NRV. It operates on the same principle as a globe valve. The main difference is the plug is spring-loaded instead of attached to a stem. Adjusting the stiffness of the spring will determine the pressure at which the valve will allow flow through.

Valve b in Figure 18 is known as a swing type NRV. It has a disc that pivots on a hinge. As soon as the inlet pressure is higher than the outlet, the disc will open. The outlet pressure and gravitational force ensure that the valve closes. The body of the valve prevents the disc to pivot past the closed position.

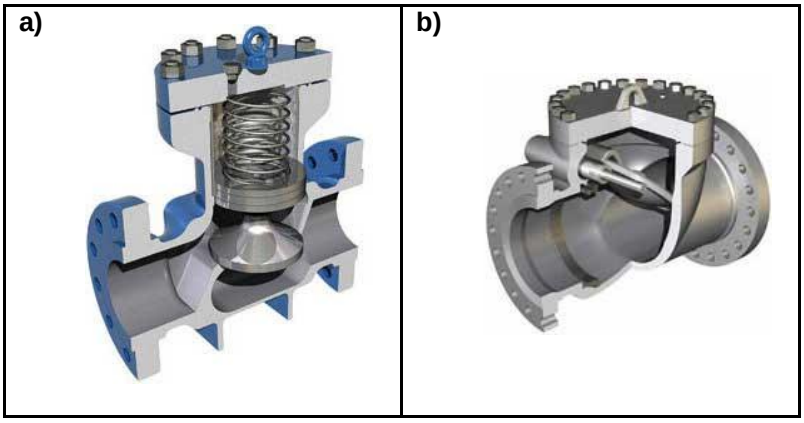

Figure 18: Sectional view of NRV: a) piston type; and b) swing type[6]

2.5. Characteristics of pump cavitation

Pump cavitation occurs when the static pressure within the pump drops below the saturated vapour pressure of the specific fluid. The saturated vapour pressure depends on the properties of the fluid. When the static pressure drops below saturation vapour pressure, the fluid flashes and vaporisation occurs. The bubbles formed flow to the higher discharge pressure where the bubbles collapse and condense [82].

The collapsing bubbles release a sudden energy force inside the pump. This energy damages the internal components of a pump [59]. Damaged caused by these collapsing

[6] Explore the World of Piping. [Online]. Available: www.wermac.org. [Accessed 04 June 2014].

bubbles is known as cavitation pitting. Pitting is often mistaken as corrosion as the appearance on an impeller is very similar. Figure 19 illustrates pitting caused by cavitation on an impeller.

Figure 19: Cavitation pitting on an impeller[7]

The sudden energy force released inside the pump also has an effect on the rest of the pump and the structure. The energy often causes the pump to vibrate. Excessive or constant vibration of a pump can result in a catastrophic failure [63], [83].

Some of the input energy is lost in the form of heat during cavitation. Cavitation can thus be detected in the temperature of the discharge fluid. The temperature fluctuation during cavitation can result in structural stress in the pump [65].

Cavitation can be detected when observing the torque of a pump operating at full load. Figure 20 illustrates the same pump operated normally and with cavitation present. The torque of the pump under normal conditions is a linear function at 0.04% of the torque. The sudden increase in torque is a result of cavitation in the pump. Figure 20 is a combined graph from the pump load graphs in M. Stopa *et al.* [84]. The original graphs are in Appendix A.

[7] Power. [Online]. Available: www.powermag.com. [Accessed 02 September 2014].

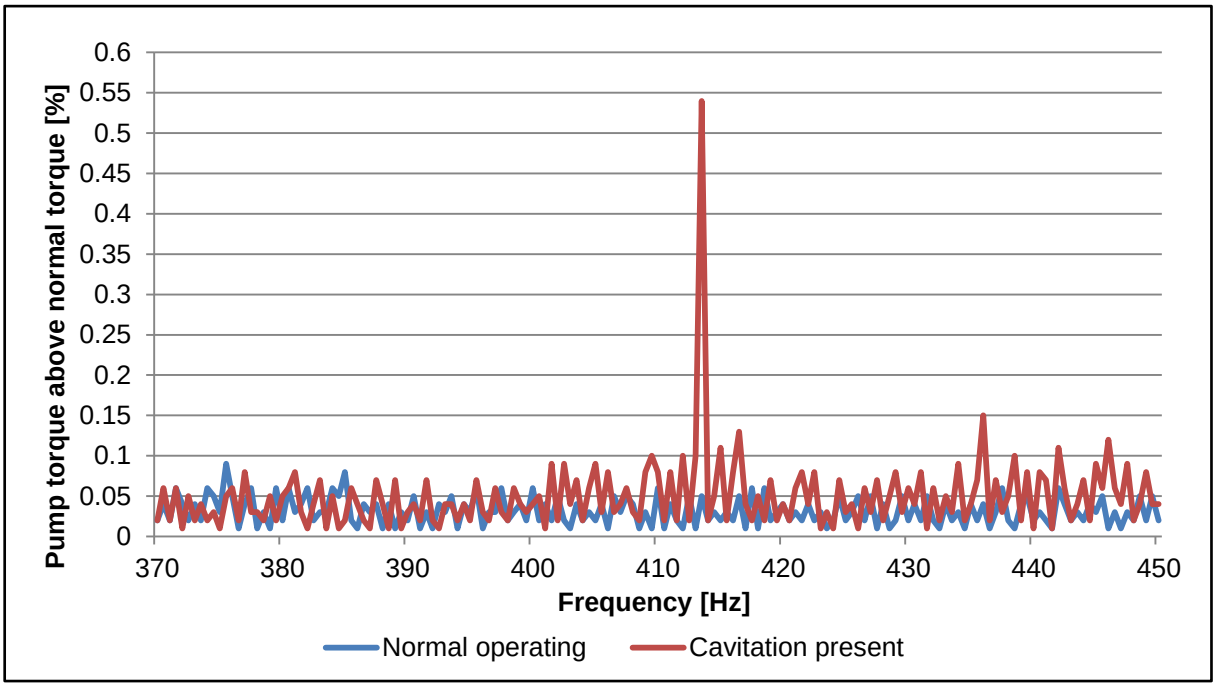

Figure 20: Pump load torque frequency spectrum

The hydrodynamic performance of a pump is immediately affected when cavitation is present in a pump [51]. In Figure 21 simplified graphs are shown from the pump cavitation graphs of D. Wu [85]. The head delivered, flow and rotational speed were measured for the same pump at low and high rotational speed during normal operation and with cavitation present. The suction pressure of the pump is adjusted to a low pressure with a vacuum pump creating cavitation. The original graphs can be found in Appendix A.

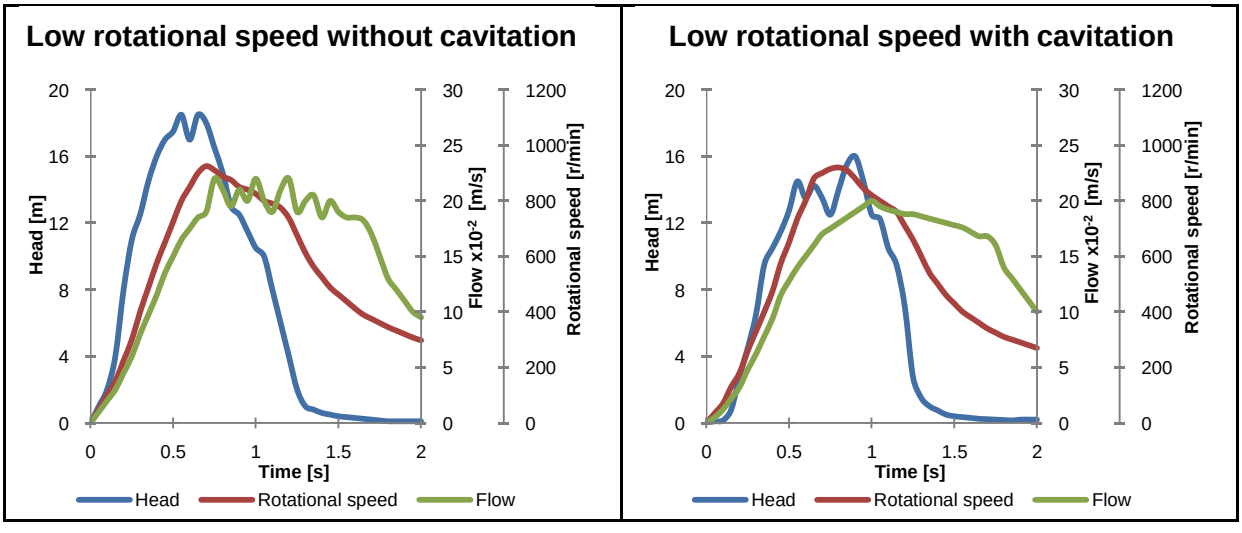

Figure 21: Various hydrodynamic performances of a pump with and without cavitation

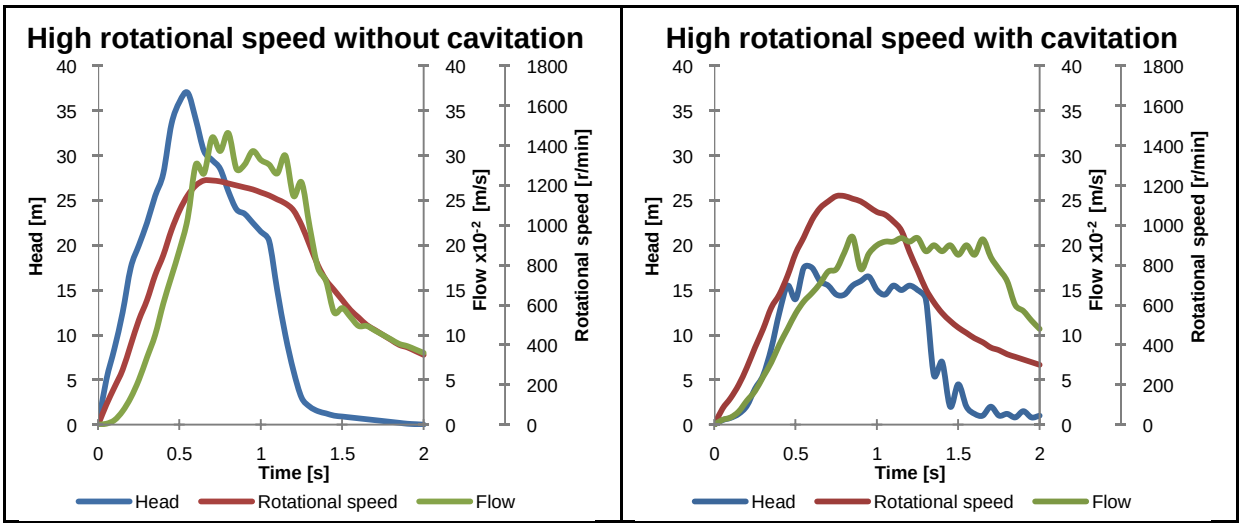

Figure 21 (continue): Various hydrodynamic performances of a pump with and without cavitation

Cavitation can be subdivided into three major stages according to the performance of the pump. The damage caused is directly proportional to the stage. The first stage is defined where a small change in the head is noticed. The second stage is when a dramatic change in the head is noticed. The third stage is when the cavitation is fully developed, with long bubbles present past the impeller [86].

Pump manufacturers do multiple tests to determine the Net Positive Suction Head required (NPSHr) to prevent cavitation. The normal operating curve of a pump is plotted. The inlet pressure of the pump is reduced in the system with a vacuum pump. As displayed in Figure 21, the hydrodynamic performance of a pump will decrease as soon as cavitation is present. The NPSHr is normally defined when the delivered head is 3% less than the normal operating conditions. The NPSHr of each pump is available on the pump specification supplied by the pump manufacturers. [46]

Cavitation occurs when the NPSHa is smaller than the NPSHr. The NPSHa is the potential head in the suction pipe minus the head of the vapour pressure of the fluid [84]. Equation2.5 can be used to calculate the NPSHa of a pump from the absolute suction pressure.

$$NPSHa = h_s - \frac{P_v}{\rho g} \qquad 2.5.$$

$NPSHa$	-	Net positive suction head available	m
h_s	-	Suction head	M
P_v	-	Vaporisation pressure	Pa
ρ	-	Fluid density	kg/m^3
g	-	Gravitational Constant	m/s^2

The potential suction head for the pump system in Figure 8 can be calculated from Equation 2.6 [84].

$$h_s = \frac{P_s}{\rho g} + H_{Ssi} - h_{sn} - 2h_{elb} - h_{fsp} \quad 2.6.$$

h_s	-	Suction head	m
P_s	-	Absolute suction pressure	Pa
H_{Ssi}	-	Static head of suction pipe	m
h_{sn}	-	Suction nozzle friction head	m
h_{elb}	-	Pipe elbow friction head	m
h_{fsp}	-	Suction pipe friction head	m

Observing Equation 2.4 where only the pump inlet and outlets are required to calculate the head of a pump. The NPSHa can thus be calculated through substituting the pump inlet conditions into Equation 2.5. Equation 2.7 illustrates how the NPSHa can be calculated from the inlet conditions [51].

$$NPSHa = \frac{P_i}{\rho g} + \frac{\dot{V}_i{}^2}{2g} - \frac{P_v}{\rho g} \quad 2.7.$$

$NPSHa$	-	Net positive suction head available	m
P_i	-	Inlet pressure	Pa
$\dot{V}_i$	-	Inlet velocity	m/s
P_v	-	Vaporisation pressure	m
ρ	-	Fluid density	kg/m^3
g	-	Gravitational Constant	m/s^2

To ensure cavitation does not occur, the NPSHa is often designed at NPSHr plus 0.6 m. This safety factor will limit the cavitation occurrence if the pump is operated outside the designed conditions. The suction flow is often restricted due to debris in the suction pipeline. This can result in a suction pressure dropping below the NPSHr [84].

2.6. Summary

The characteristics of a multistage centrifugal pump make it one of the most suitable pumps for dewatering a deep level mine shaft. Multistage centrifugal pumps have the capabilities to generate the pressure to overcome these high heads. Their proven reliability and robustness in severe conditions compensate for their cost in this application.

It is clear that neither condition, nor performance monitoring can be neglected when automating a pump. Condition monitoring is the key aspect protecting the pump against failure. Performance monitoring compliments condition monitoring to make a more informed decision on the condition of the pump. Both should be included in the pump automation program. This will not only ensure safe operation, but improve the reliability of the pump system.

The correct discharge valve for each pump should be specified in the design. Each valve type has an advantage for certain applications. The automation of the valve should be kept in mind when selecting the valve type for automation.

The damage caused by cavitation cannot be neglected. Internal damage has a direct impact on the life expectancy and efficiency of a pump. Short periods of cavitation also have a direct impact on the pump performance. Constant cavitation can result in a catastrophic failure and downtime.

The best practices for pump automation monitor the pump parameters to enable safe operation. Each instrument installed on the pump system monitors a specific parameter. These parameters were discussed and found necessary to monitor.

Chapter 3: Developing best practices for pump automation and control

In this chapter a case study is presented of a pump that failed after it had been automated. The pump failure was examined to determine the root cause of failure. Additional precautions and safety measures are considered to prevent a similar incident. The control philosophies for a dewatering system are discussed. An alternative method to determine pump efficiency in real-time is implemented.

3.1. Introduction

A pump automation project was implemented on a deep level mine in the West Rand, South Africa. The scope of work was to automate the dewatering system of the mine to enable load shift. Each automated pump was controlled with a dedicated Programmable Logic Controller (PLC). The PLCs were connected to a Supervisory Control And Data Acquisition system (SCADA) on surface for a graphical user interface. A real-time energy management system was used to control the pumps according to the dam levels.

The dewatering system of the mine consists of four pump chambers. The used hot water is collected at shaft bottom in a settler. The settler separates mining debris and the clear hot water into different reservoirs. Each pumping chamber has multistage centrifugal pumps and hot water dams. The pumping chambers are used in an upward cascading manner to dewater the shaft. Figure 22 shows the layout of the dewatering system of the mine.

3.2. Pump failure analysis

A multistage centrifugal pump on Intermediate Pumping Chamber Main shaft (IPCM) ceased during the implementation of the project. The pump was operated from the automated system underground after the automation had been commissioned. Several pump monitoring instruments and equipment were interlocked in the PLC program.

Unexpected failures of pumps are a major concern. It can result in damage to equipment, injury and even flooding. Flooding is a high environmental risk for the mining personnel. An additional concern is the maintenance cost of multistage centrifugal pumps. Refurbishment cost of a ceased multistage centrifugal pump can reach R 1-million.

Investigations were done to determine the root cause of failure, through examining the events leading to pump failure. If the causes of failure are known, additional safety systems can be investigated to prevent similar incidents.

3.2.1. Installed instrumentation and limits

Several condition monitor instruments were originally installed. Each instrument monitors a specific condition during start-up, running, shut-down or ready-to-start status of the pump. The installed instrumentation is discussed in the following sections.

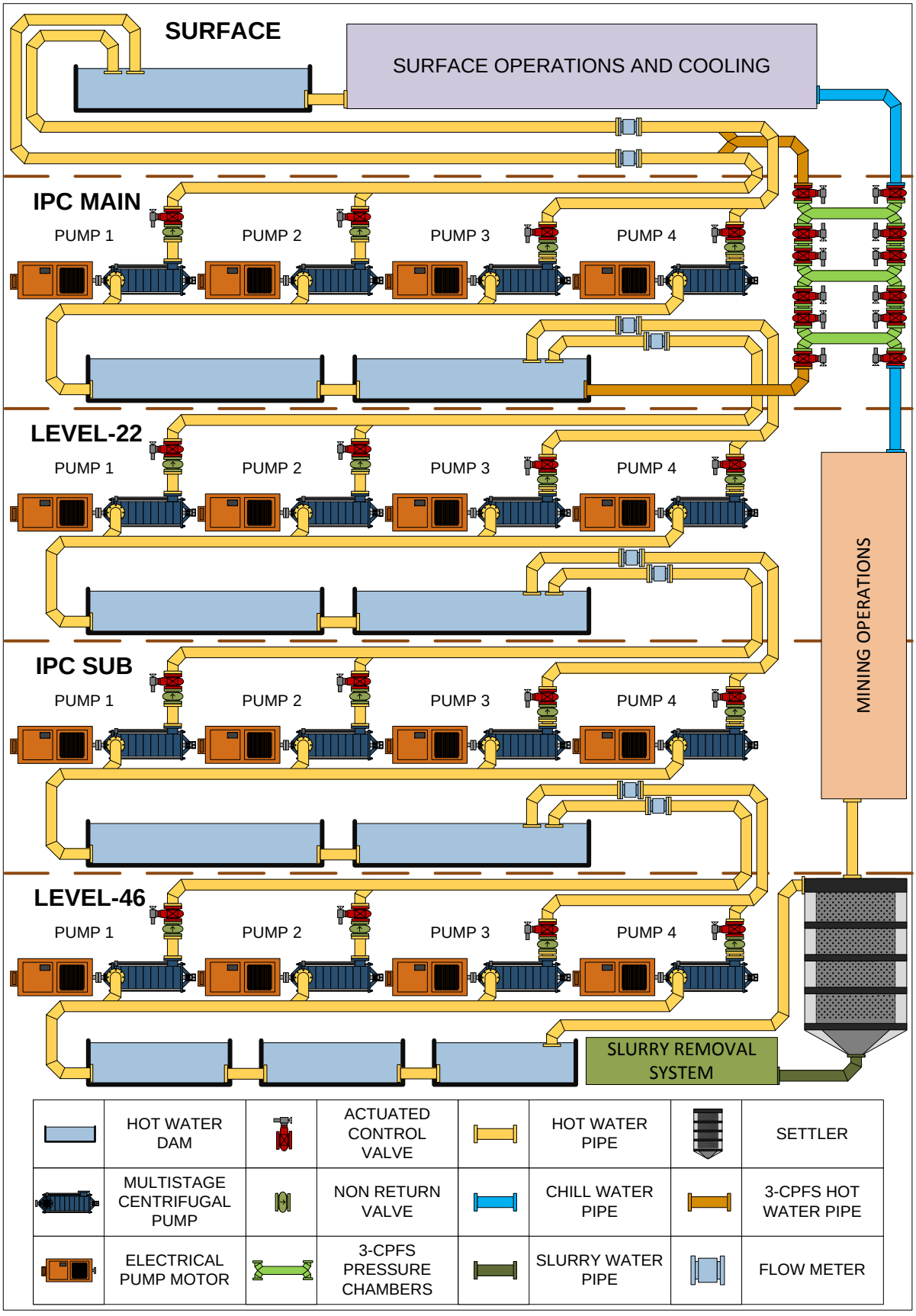

Figure 22: Dewatering system of the case study mine

Flow

A digital flow switch was installed on the suction column of the pump. The minimum flow was set manually on the flow switch. The flow switch ensured that the pump operated within the minimum flow parameters. The PLC was programmed to disable the flow switch for two seconds after the motor breaker had closed. This allowed the pump to generate enough flow during start-up without initiating a trip condition.

The pump motor uses chilled water from the refrigeration plant as cooling medium. A digital flow switch was installed on the inlet of the pump cooling water pipe. This ensured that the pump was cooled when the pump was operational.

Each pumping system consists of two discharge columns. Two pumps are connected in parallel feeding a column per pump station. An analog flow meter is installed on each discharge column of a pump station. The exact flow each pump delivers can only be determined if only one pump is operated per column.

A multistage centrifugal pump has a balancing chamber at the discharge side of the pump. Water enters the chamber between the shaft and the balance disc sleeve. This water acts as a thin film thrust bearing between the diffusor of the last stage and a balance disc in the balancing chamber. The pressure in the balancing chamber must not exceed half of the discharge pressure. To prevent a pressure build-up, a balance disc flow pipe connects the balancing chamber to the pump inlet.

An analog flow sensor was installed on the balance disc flow pipe of the pump. If the balance disc sleeve is worn out, the flow through the balance disc flow pipe will increase. This is also an indication of the wear on the internal components of the pump.

Pressure

These pumps had an efficiency monitoring system installed, which consisted of analog pressure sensors on the inlet and outlet of the pump. These pressure sensors were connected to the PLC. The pressure sensors used for performance monitoring, using the PLC to log the pressure values.

Power

A power meter was installed on the incomer panel of the pump. The power meter measures the power that each pump consumes. An accurate power measurement is required to determine the electricity cost saved during the load shift.

Vibration

Analog vibration sensors were installed on the motor and pump Drive-End (DE) bearings. The bearing housings were machine drilled and tapped to install the vibration sensors. Both vibration sensors were installed in the radial direction with respect to the shaft.

Temperature

Analog temperature probes were installed on the DE and the Non-Drive End (NDE) of both the motor and the pump. This will detect friction that is induced which will result in a temperature rise. The friction of the bearings can be a result of failing, incorrectly installed or incorrect operation of the pump.

The chilled water of the motor acts as a cooling medium for the air of the motor. The cooled air flows over the windings of the motor. The pump motor has internal winding temperature probes installed. The winding temperatures of all three phases were included in the PLC program.

Position switches and sensors

Position switches were installed on the suction butterfly valve of the pump. The switches were installed to detect if the valve is in the fully open or fully closed position. The PLC will prevent the pump from running if the valve is not in the fully open position. A trip condition will be initiated if the valve is closed when the pump is running. This will ensure the suction valve does not restrict the flow of the pump.

A proximity sensor was installed to detect the pump impeller displacement. The sensor was set mechanically according the float of the pump. The impeller of a pump moves due to thrust towards the suction intake when a pump is started. Impeller suction causes the thrust. The pump will thrust until the pressure in the balancing chamber is enough for the water to act as a thin film thrust bearing.

The motor has an internal position switch to detect if the cooling water of the motor leaks. A plate was installed underneath the cooling water pipe inside the air cooling system of the pump. The weight of the water from a leaking cooling water pipe will displace the plate and close the connection of the position switch.

An analog motor rotor displacement sensor was installed on the NDE of the motor. The thrust of the pump during start-up acts on the motor rotor. Once the pump is running at full load, the rotor must operate in the magnetic centre of the motor. This is the optimal position for the motor to operate. The rotor displacement sensor ensures that the motor is operated in its optimal position.

Alarms and trip

All of the instruments mentioned above were included in the PLC as part of an interlocking trip circuit when the pump failed. The alarm and trip are first set to the specification of the manufacturer. The normal operating conditions of a new pump are then monitored. If it is found less than specifications of the manufacturer, the alarm and trip set-points are decreased. This ensures that the pump does not operate outside its design parameters. Table 3 illustrates the programmed set-points in the PLC of each instrument.

Table 3: Alarms and trips of installed instrumentation

Instrument	Input	Unit	Alarm	Trip
Motor NDE Bearing Temperature	Analog	°C	75	80
Motor DE Bearing Temperature	Analog	°C	75	80
Motor DE Bearing Vibration	Analog	mm/s	4	8
Pump NDE Bearing Temperature	Analog	°C	75	80
Pump DE Bearing Temperature	Analog	°C	75	80
Pump DE Bearing Vibration	Analog	mm/s	4	8
Pump Inlet Pressure	Analog	kPa	N/A	1 600
Pump Outlet Pressure	Analog	kPa	N/A	16 000
Cooling Water Flow	Digital	Switch	Manual Setup: 3.4 l/s	
Pump Inlet Flow	Digital	Switch	Manual Setup: 85.9 l/s	
Motor Winding U Temperature	Analog	°C	115	120
Motor Winding V Temperature	Analog	°C	115	120
Motor Winding W Temperature	Analog	°C	115	120
Pump Suction Valve Open Position	Digital	Switch	Fully open position	
Pump Suction Valve Close Position	Digital	Switch	Fully close position	
Impeller Displacement	Digital	Proximity	Manual Setup: 3 mm	
Balance Disc Flow	Analog	l/s	40	45
Motor Air Temperature	Analog	°C	115	120
Motor Shaft Displacement	Analog	mm	N/A	<2 >8
Column Flow	Analog	l/s	N/A	

Discharge valve

The 250 mm nominal bore discharge gate valve was removed and refurbished. The stem and shoeblock were replaced during refurbishment. The bonnet of the gate valve was modified to fit a multi-turn actuator with a rating of 1800 Nm. The actuator open and close limit was set up manually. In this case the actuator used the number of bush rotations to determine the position of the gate in the valve body.

Human intervention

Although the pump is fully automated, human intervention is still needed. A typical daily task performed by mine personnel is filling the bearing oil cavity. Condition monitoring decreases the maintenance frequency but does not completely remove maintenance. The following safety equipment was installed to reduce human intervention incidents:

- Emergency stop at pump,
- Emergency stop on PLC panel,
- Pump lockout switch on PLC panel,
- Start-up warning siren,
- Red light to indicate running status,
- Blue light to indicate ready to start status,
- Green light to indicate a stop status, and
- Yellow light to indicate an alarm or trip.

The actuator, instrumentation, safety equipment and power meter were all interlocked in the PLC program. If any of the conditions monitored does not satisfy a safe pump operating condition, the pump will trip. An alarm with the trip condition description will be displayed on the HMI of the PLC. If the condition which initiated the trip is satisfied for safe pump operation, the PLC can be reset. If the unsafe condition persists, the PLC will prevent the pump from starting.

3.2.2. Events leading to pump failure

The connection between the shoeblock and stem failed, causing a separation during the opening of the discharge valve. The gate remained in the closed position. The actuator bush could still rotate freely, moving the stem to the open position. The actuator determined the position of the gate by the number of rotations of the bushes inside the actuator. An open position signal was received by the PLC.

Figure 23 displays a basic diagram of a gate valve. The shoeblock is the connection between the stem and the disc. The stem of the gate valve was only connected to the shoeblock with an approximately 10 mm circumferential weld on the top and bottom.

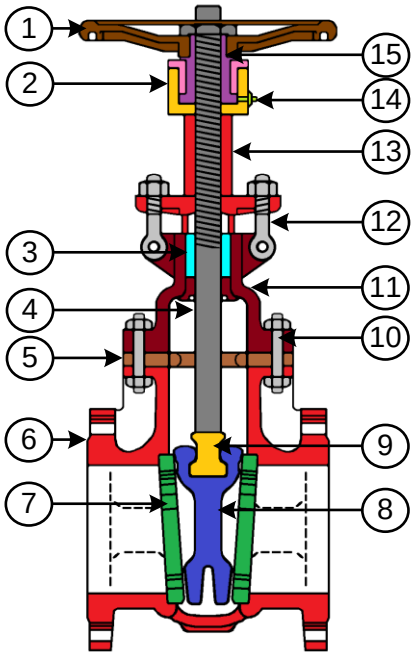

NR.	DESCRIPTION	NR.	DESCRIPTION
1	HANDWHEEL	9	SHOEBLOCK
2	GLAND	10	BONNET FASTENERS
3	PACKING	11	BONNET
4	STEM	12	YOKE FASTENERS
5	GASKET	13	YOKE
6	BODY	14	GREASE NIPPLE
7	SEAT RING	15	YOKE SLEEVE
8	DISC		

Figure 23: Gate valve diagram

Figure 24 illustrates the failed connection between the stem and shoeblock. Photo a in Figure 24 displays the bottom of the stem; photo b in Figure 24 displays the top of the shoeblock; photo c in Figure 24 displays the assembling of the component; and photo d in Figure 24 displays the gate. The connected stem and shoeblock slide into the key of the gate on the left to complete the assembly.

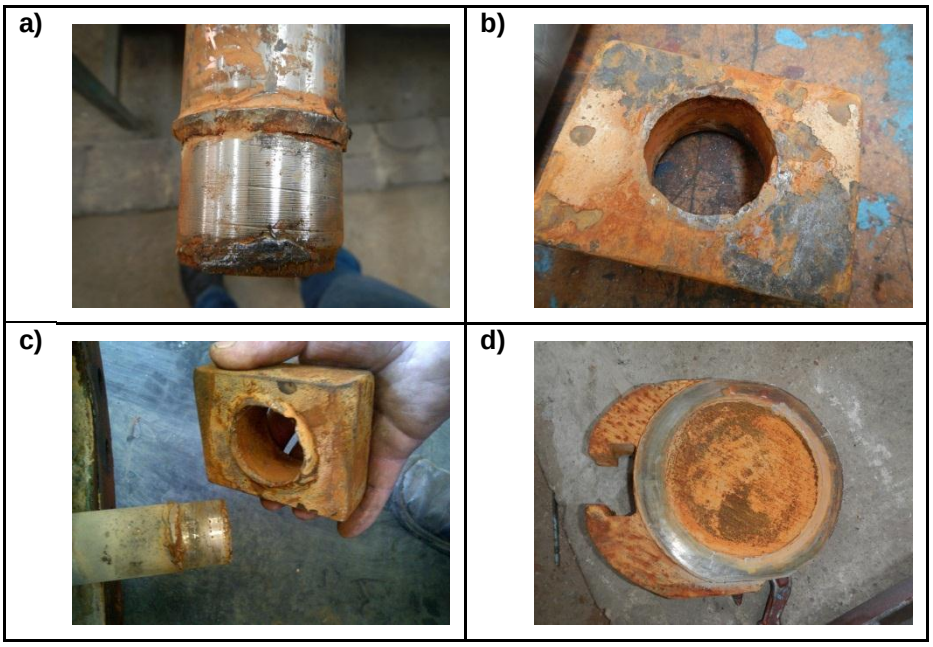

Figure 24: Gate valve a) spindle; b) shoeblock; c) spindle and shoeblock; and d) gate

A signal to close the motor circuit breaker was sent by the PLC. The motor started rotating the pump to initiate flow through the pump. The suction flow switch was disabled for approximately two seconds during the start-up sequence. This allowed the pump to generate flow before it tripped due to low or no suction flow.

The closed discharge valve resulted in no flow through the pump. Water is seen as an incompressible fluid. This resulted in the water volume inside the pump staying constant. The pump generated a pressure, as the design intended to deliver the head. The volume of the pump and columns are constant due their material properties. This resulted in a temperature rise from the mentioned constrains and Equation 3.1.

$$PVol = nRT \qquad 3.1.$$

P	-	Pressure	Pa
Vol	-	Volume	m^3
n	-	Amount of substance	Mol
R	-	Universal gas constant	J/mol.K
T	-	Temperature	K

The temperature rise resulted in expansion of the internal parts of the pump. The clearance between the internal parts is designed to a minimum to decrease internal pump pressure loss. The expansion led to friction between the rotating pump impellers and the stationary pump casing and diffusors. This resulted in a drastic secondary increase of the temperature.

3.2.3. Possible cause of valve failure

It is evident that the root cause of failure was the discharge valve that failed to open. The failure of the discharge valve resulted in a chain of events which resulted in pump failure. An investigation of the forces and pressures acting on the gate of the valve was launched to determine the possible reason of failure.

If the gate exceeds the close position, the gate is forced into the seat. If the gate was forced into the seat more force was required to open the valve. When the valve was opened for investigation, the gate was loose and could be moved freely by hand. This is an indication that the close limit of the actuator was set correctly and the gate was not forced into the seat.

Similar to the close limit, the actuator can cause damage to the valve if the open limit is set incorrectly. When the open position is exceeded, the shoeblock and gate is forced into the bonnet of the valve. The shoeblock is normally bent when the open limit is exceeded. Since the shoeblock was not bent, the open limit had been set-up correctly. Both the possibilities of the open and close limits set incorrectly were thus eliminated.

The torque limits of the actuator could have been set incorrectly. This would have resulted in the actuator applying more force than the valve was designed and manufactured to handle. If the sum of all forces applied to a body has an equilibrium force in one direction, the body will accelerate. This is shown with Equation 3.2.

$$F_{Eq} = ma \tag{3.2.}$$

F_{Eq}	-	Equivalent force	N
m	-	Mass	kg
a	-	Acceleration	m/s^2

The equilibrium force acting on the gate was zero, because the valve failed in a closed position. Another force must have been present to counteract the actuator force applied. The static friction force is the only force acting against the direction of the actuator force. This resulted in the zero equilibrium force of the gate. The static friction force is defined with Equation 3.3.

$$F_{sf} = F_N U_S \tag{3.3.}$$

F_{sf}	-	Static friction force	N
F_N	-	Normal force	N
U_S	-	Friction coefficient	-

The normal force, F_N acting on the gate of the valve is generated by the head of the water above the valve. The water creates pressure which acts on the gate of the valve. The pressure of the fluid at the discharge valve is defined with Equation 3.4.

$$P_H = \rho g H \qquad 3.4.$$

P_H	-	Pressure of head	Pa
ρ	-	Fluid density	kg/m^3
H	-	Head	m
g	-	Gravitational Constant	m/s^2

A Non-Return Valve (NRV) is installed between the pump and the discharge valve. Figure 25 displays the arrangement in with the valves are installed. The pump is stopped when the discharge valve is 5% open. This ensures the NRV seals properly and prevents the discharge valve from exceeding the maximum torque limit while closing. Some of the pressure is stored as potential pressure between the NRV and the gate valve.

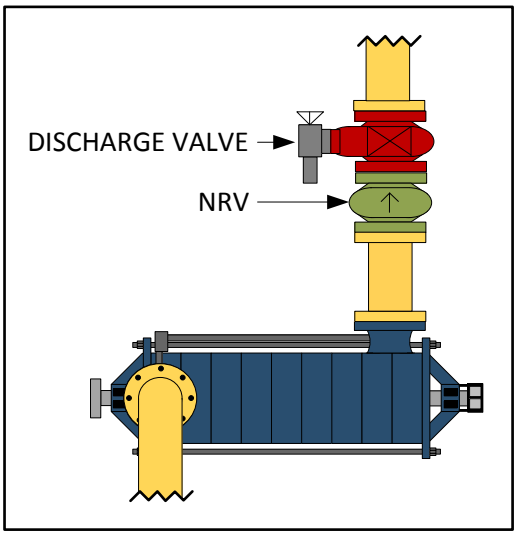

Figure 25: Discharge valve and NRV installed arrangement

If the NRV does not seal properly, the water leaks through to the pump. The potential pressure stored between the discharge valve and the NRV when the pump is stopped, will be lost. This results in a differential pressure across the valve. The differential pressure creates the normal force acting on the gate of the valve. The differential pressure across the valve is defined in Equation 3.5.

$$\Delta P_V = P_H - P_P \quad 3.5.$$

ΔP_V	-	Differential pressure across valve	Pa
P_H	-	Pressure of head	Pa
P_P	-	Stored potential pressure	Pa

The forces as a result of pressure inside a closed body, act perpendicular on the inner walls of the body. The diameter of the discharge valve gate is known. The force acting on the gate as a result of the pressure is defined with Equation 3.6. This force is also equal to the normal force acting on the gate of the valve.

$$F_N = \Delta P_V A \quad 3.6.$$

F_N	-	Normal force	N
ΔP_V	-	Differential pressure across valve	Pa
A	-	Area of the valve	Pa

Substituting Equation 3.4, 3.5 and 3.6 into Equation 3.3 gives the resultant force due to the pressure difference across the valve. Equation 3.7 illustrates the substituted equation. It is clear from the equation that the smaller potential energy is stored between the NRV and gate valve, the greater the friction force will be. The other variables can be seen as constant with the head at a maximum when the discharge column is full.

$$F_{sf} = (\rho g H - P_P) A \quad 3.7.$$

F_{sf}	-	Static friction force	N
ρ	-	Fluid density	kg/m^3
H	-	Head	m
g	-	Gravitational Constant	m/s^2
P_P	-	Stored potential pressure	Pa
A	-	Area of the valve	Pa

This shows that if the torque limit of the actuator was set incorrectly, another force must have been present preventing the gate from moving. The secondary force was a result of a leaking NRV creating a differential pressure across the valve. There were no other forces found to act as the reaction force.

3.2.4. Pump disassembled examination

Figure 26 displays a diagram of a six stage centrifugal pump. The components of the pump are numbered and displayed in the table of the figure. The figure shows where the

components of the pump are located. A 12-stage centrifugal pump has similar components, only with double the number of stages.

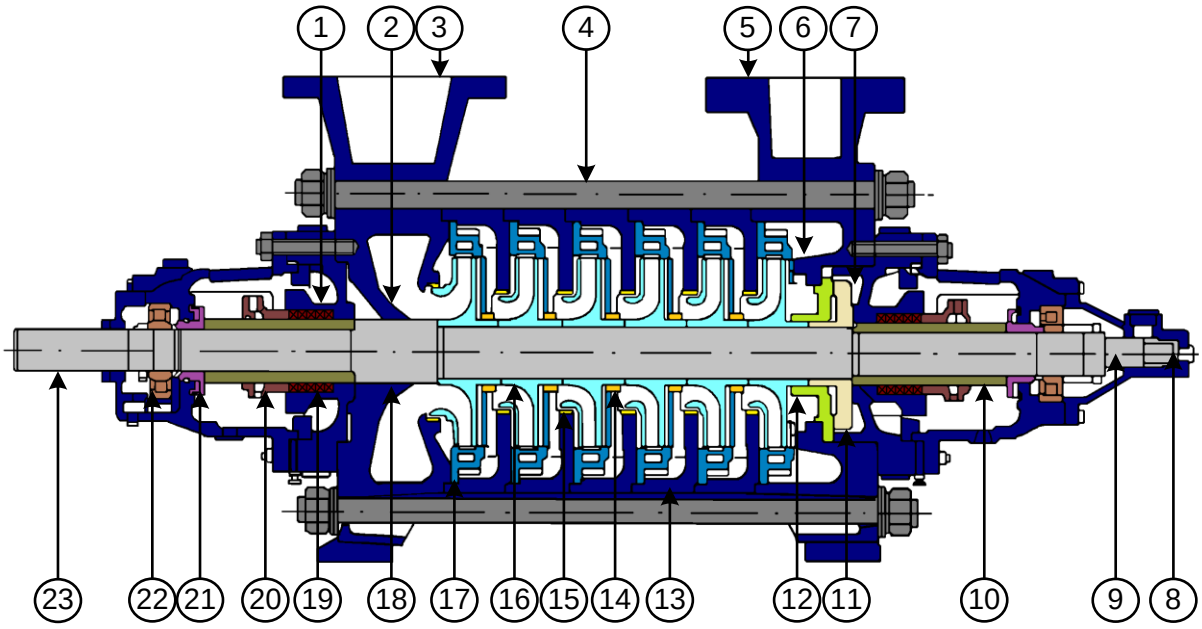

NR.	DESCRIPTION	NR.	DESCRIPTION
1	STUFFING BOX HOUSING	13	STAGE CASING
2	INLET CASING	14	WEAR RING
3	INLET	15	WEAR RING
4	ASSEMBLY FASTENER	16	IMPELLER
5	OUTLET	17	DIFFUSOR
6	OUTLET CASING	18	SHAFT
7	BALANCE DISC CHAMBER	19	PACKING
8	IMPELLER DISPLACEMENT	20	PACKING GLAND
9	PUMP NDE	21	O-RING
10	SHAFT SLEEVE	22	BEARING
11	BALANCE DISC	23	PUMP DE
12	BALANCE RING		

Figure 26: Six stage centrifugal pump diagram

The seized pump was sent for repairs. Access was arranged to do a visual examination of the pump when it was disassembled. The pump had only been installed and operated for two months before it seized. It was assumed that any visible sign of damage found on the pump was caused by the recent failure.

The casing neck ring is a stationary component installed on the pump casing. It acts as protection between the pump casing and the shroud of the rotating impeller. The clearance between the impeller neck and the casing neck ring for normal operation is 0.2 mm on each

side. The small clearance improves the efficiency of the pump through limiting internal losses.

Figure 27 displays the inlet neck and eye of a single impeller with the neck ring of the specific stage. The neck ring was fused to the hub of the impeller. This is a clear indication that the internal components of the pump expanded. A temperature rise of the fluid caused the internal components to expand.

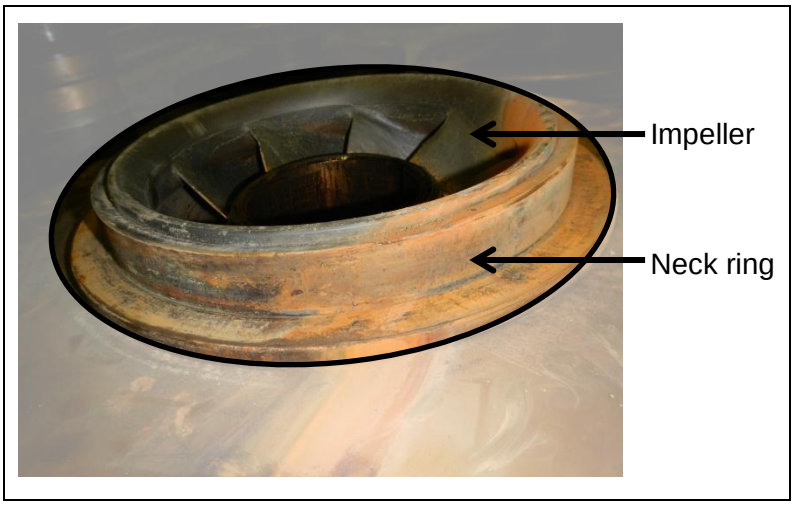

Figure 27: Impeller eye and neck with ceased neck rings

Figure 28 displays the outlet neck of an impeller hub. The damage was also caused through expansion, similar to the inlet neck in Figure 27. The hub made contact with the stationary diffusor of the pump while rotating. This caused friction between the hub and the diffusor which resulted in damage.

Figure 28: Outlet neck of an impeller hub

Signs of cavitation were visible on the internal components of the pump. Figure 29 displays a sign of cavitation on the casing of the pump. The casing is installed after the diffusor and

before the inlet of the next impeller. The erosion in the casing was caused by the imploding bubbles.

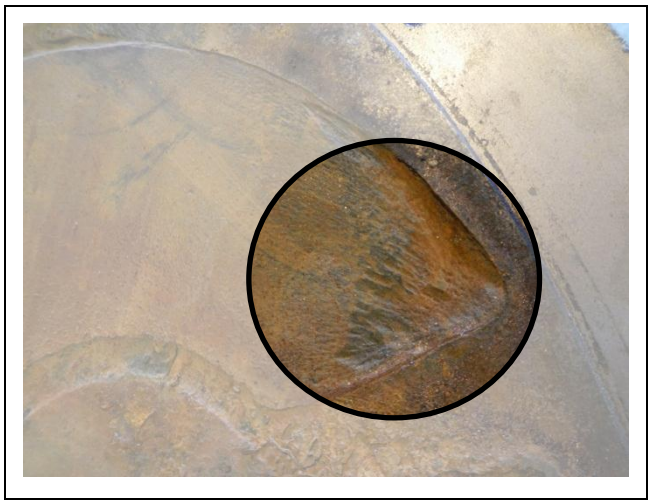

Figure 29: Sign of cavitation on casing

Cavitation occurs when the static pressure drops below vapour pressure. The inlet of the pump was not restricted, thus the pressure could not have been below vapour pressure. The reason for cavitation was that the temperature exceeded the vapour temperature at the specific pressure. This resulted in vapour forming in the water.

The failed discharge valve induced a pressure increase on the outlet side of the pump. This pressure resulted in an additional force being applied on the outlet of each impeller. The force caused the balance disc to make contact with the outlet casing. Figure 30 displays the wear found on the outlet casing.

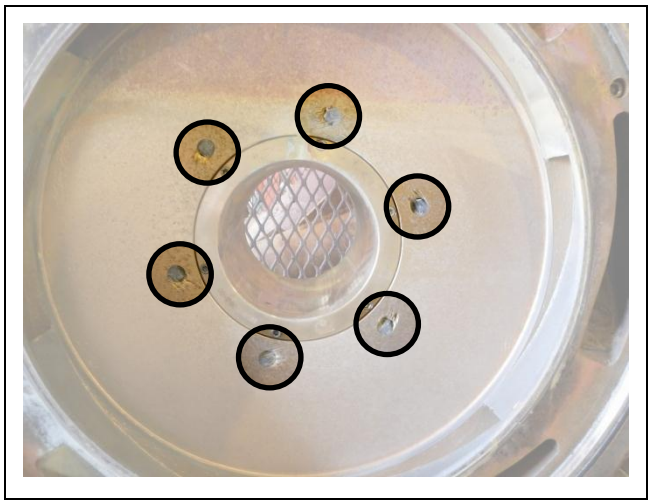

Figure 30: Friction on the outlet casing due to balance disc

The balance disc wear is manufactured with a bronze wear ring and a steel wear ring. The minimum thickness of a balance disc wear ring is 37 mm. This prevents the impeller shrouds

from colliding with the pump casing. Table 4 compares the thickness of a new balance disc wear ring to the one removed from the failed pump. It is clear that the pump operated within the specified thrust distance.

Table 4: Balance disc wear thickness

Ring	New thickness [mm]	Ceased pump thickness [mm]
Bronze ring	20	19.38
Steel ring	20	19.85
Total	40	39.23

3.2.5. Unsuccessful prevention

Automation of the pump chamber included pump monitoring instrumentation. The installed instrumentation should have protected the pump against failures. The instrumentation installed to protect the pump from the condition leading to overheating and cavitation was investigated. The inability of these instruments to protect against failure was determined.

Temperature sensors on bearings

It was clear from the investigation that the pump ceased due to overheating. The only temperature monitoring sensor installed on the pump was on the DE and NDE of the pump. The other temperature sensors monitor the pump motor temperatures. This temperature will not be influenced by the internal temperature of the pump.

The shaft is the only direct connection between the internal parts and the bearings of the pump. An air channel between the pump casing and bearing housings acts as a temperature isolator. Heat transfer from the internal components to the bearings is minimal and will not create a pump trip condition.

Vibration sensors on the drive ends

Signs of cavitation were also detected on visual inspection of the pump components. Cavitation can be detected with vibration sensors. The pump had one vibration sensor installed in the radial direction on the DE bearing. The purpose of the vibration sensor is to detect if the pump shaft is vibrating during operation.

Figure 12 clearly illustrates the vibration spectrums of different defects in a pump. The amplitude of the maximum vibration between normal operating and with cavitation is the same. The frequency of vibration is changes for the two conditions. The vibration sensor is interlocked for a maximum amplitude vibration. This result in the vibration sensor will not initiate a trip if cavitation is present inside a pump.

Position of the discharge valve gate

The actuator of the discharge valve uses the number of rotations to determine the position of the gate. The actuator raises the stem through rotating the bush inside the actuator. This acts as a screw jack gear system and raises the gate inside the valve. The body of the valve guides the gate to prevent it from rotating.

The broken connection between the gate and the spindle made that the spindle could still move freely. The actuator received an open position signal because the actuator completed the number of turns. This prevented the PLC to initiate the trip sequence for a close discharge valve.

Flow switch on suction column

Zero to low flow through the pump was caused by the discharge valve that failed to open caused. The flow switch is activated in the PLC program two seconds after the motor breaker closes. It should have initiated the trip sequence. The minimum required flow set manually on the flow switch was met. This caused the pump to continue to run with low flow.

When the efficiency of a pump starts to deteriorates, the minimum flow is not delivered. Mine personnel often reduce manual set limit on the flow switch when it is insufficient. This prevents the PLC to initiate the trip sequence and allow for pumping. The reduced limit on the flow switch did not detect the low flow through the pump when the valve failed.

Discharge pressure

The main purpose of the installed discharge pressure was to monitor the performance of the pump. A trip set-point for the pressure was programmed into the PLC. The maximum rated pump discharge pressure is 12.3 MPa at a low flow. The trip set-point of the pressure was set at 16.0 MPa. The pump was not capable to generate enough pressure to reach the trip set-point.

3.3. Improved design to prevent failure

The pump failure is proof that the automation and safety circuit of the pump did not cater for all failure conditions. The current practice in which the client specifies automation has to be improved to prevent similar incidents. Immediate precautions had to be taken because the automation project was already commissioned. Several solutions were investigated to prevent similar incidents.

3.3.1. Differential pressure over discharge valve

The evident proof of the presence of a differential pressure across the discharge valve led to the first solution. It was proposed that a pressure sensor be installed between the NRV and the discharge valve and another sensor after the discharge valve. This could be used to determine the differential pressure across the valve.

The NRV and the discharge valve flanges are directly next to each other. Installing a pressure sensor between the valves was impossible. Installing the pressure sensor between the pump and the NRV will not measure the differential pressure across the discharge valve. The NRV will act as pressure isolation.

Further investigation of the discharge valve application showed that pressure equalising valves were available. Figure 31 illustrates a gate valve with a manual bypass valve. By opening the bypass valve before opening the main valve, the pressure across the valve will be equalised. These types of valve are designed for high pressure application, which often has a differential pressure.

Figure 31: High pressure gate valve with pressure equalizing bypass[8]

The pressure differential will only be created if the NRV leaks. If the NRV leaks and the bypass valve remains in the open position, the discharge column will be drained. In this case the bypass valve has to be in the closed manually. This defies the purpose of automation if the bypass valve has to be opened manually. The cost of the new valves and automating the bypass valve is not feasible.

[8] Xinhai Valve. [Online]. Available: www.xhvalves.com. [Accessed 02 September 2014].

It was found that most NRVs have small flow when leaking, resulting in a long leakage period. More torque is usually required to open the discharge valve if the pump does not operate for more than 24 hours. Equalising of the differential pressure across the valve was thus programmed into the PLC. The PLC opens the discharge valve to 10% every 30 minutes when the pump is not operated. This minimises the differential pressure across the valve.

3.3.2. Redesign shoeblock connection

The weld connection between the spindle and shoeblock was proved to be insufficient when a differential pressure was present. The connection was redesigned to withstand greater transfer force to the gate. Block thread was machined on both the stem and the shoeblock. The shoeblock was screwed onto the stem. Figure 32 shows the redesigned connection.

Figure 32: Block thread on spindle and shoeblock

A locking pin was also inserted through the shoeblock into the stem. This not only provided additional strength, but also kept the shoeblock from rotating. When the assembly was completed, a 10 mm circumferential weld was also applied on the top and bottom.

3.3.3. Additional temperature probes

Installing additional temperature probes to monitor the temperature of the fluid was investigated to prevent both conditions. The input energy of the pump will result in a temperature rise of the fluid at the pump outlet. The maximum temperature of the fluid is found at the outlet of the pump. A temperature probe was installed at outlet of the pump to monitor the temperature fluid.

Each stage of a multistage pump increases the pressure of the fluid. The minimum pressure of the fluid is at the inlet of the pump. The vapour temperature of the fluid can be determined by using the minimum pressure of the pump and its thermodynamic properties. If the

maximum pressure at the outlet exceeds the fluid vapour pressure, the PLC must initiate the trip sequence.

Further investigations showed that the pump efficiency could be determined through the differential temperature of the inlet and outlet fluid. Multiple methods can be used to calculate the efficiency from the differential temperature. An additional temperature probe was installed at the pump inlet to monitor the temperature of the fluid.

Both the temperature probes were installed on the pipe pieces at the pump inlet and outlet. A certified high pressure welder installed these pockets on the pipes. High pressure pockets, machined from a solid stainless steel rod, were installed into the sockets. Both the socket and pocket ensure that no leakage occurs at the installation. The pockets also protect the temperature probes against the high pressure and flow. Figure 33 displays the installed sockets, pockets and temperature probes on the pump.

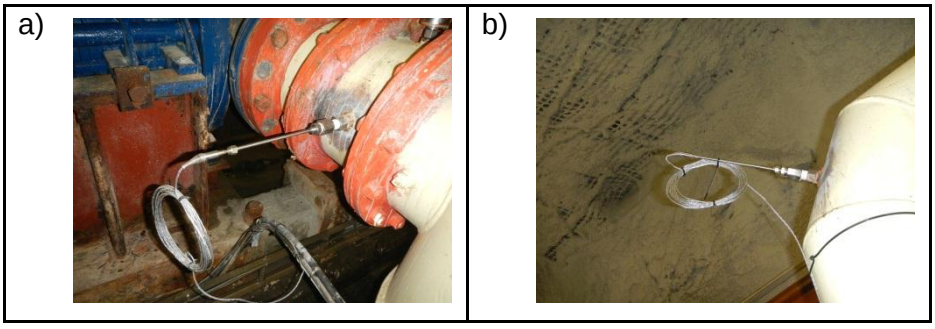

Figure 33: Additional temperature probes: a) Inlet; and b) Outlet

Three of the pockets installed on the discharge of the pump failed after installation. The specification was re-checked to ensure they were acceptable for the application. It was found that the pockets were not manufactured according to the design. The manufacturer replaced all 32 installed pockets.

If a similar incident would repeat itself, there would be little or no flow through the outlet of the pump. The temperature probe on the outlet was installed 1.8 m from the pump outlet. Little or no heated fluid would reach the temperature probe. A true indication of the internal fluid temperature would not be measured with the temperature probe.

A third temperature probe was installed on the balance disc flow pipe. Low flow at the pump outlet would result in an increased flow through the balance disc flow pipe with an increased temperature. Figure 34 displays the additional temperature probe installed on the balance disc flow.

Figure 34: Temperature probe on balance disc flow

Figure 35 displays the installed locations of the additional temperature probes. These parameters were interlocked in the PLC program. A trip will be initiated if the vapour temperature of the fluid was exceeded at the specific pressure.

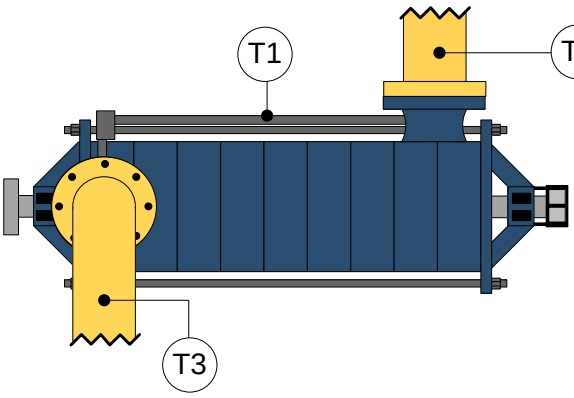

NR.	DESCRIPTION
T1	BALANCE DISC FLOW TEMPERATURE
T2	PUMP OUTLET TEMPERATURE
T3	PUMP INLET TEMPERATURE

Figure 35: Additional temperature probes installed locations

3.3.4. Actuator limits

The actuator is the source of the force applied to the stem. Another force must be present for the force that the actuator applies to the stem to result in failure. The force that the actuator applies to the stem is determined by the amount of torque. The torque of the actuator was limited to 30% of its maximum rated torque.

The open and close limits of the actuator were also verified. Incorrect configured open or close limits can result in damage to the stem, shoeblock, gate, seats and actuator.

Maximum torque is required for initial opening of the valve. As soon as the pressure across the valve is equalised, a minimum of 5% of the rated torque is required to move the gate. The minimum torque is required to overcome the internal friction of the valve and actuator. If the connection between the spindle and shoeblock fails, the friction will decline, resulting in reduced torque. An under torque limit of 5% was set on the actuator during gate movement.

3.3.5. Suction flow sensor protection

The suspicion of tampering with the suction flow sensor led to a password protection investigation. A digital installed flow switch was installed on the suction of the pump. The trip set-points of digital instruments were set manually on the instrument. A digital instrument only returns an open or close feedback. This results that the trip set-point cannot be interlocked in the PLC program.

The installed suction flow switch could only be locked instead of password protected. Minimum flow was set and locked on the flow switches according to tested flows of each pump. The locking and unlocking procedure could not be changed. It is of utmost importance that only authorised personnel receive the procedure.

3.4. Optimised pump control

The automated pump system allowed for remote safely control of the pump system. To maximise potential savings, a dynamic pump scheduling program was implemented. The program determines the pump schedule according to the real-time dam levels. The pump load is reduced with the program to a minimum during the more expensive electricity peak periods. Several interlocks are programmed into the software to ensure the water is managed safely.

3.4.1. Input parameters

The more expensive electricity peak periods are from 7:00 to 10:00 and 18:00 to 20:00. The mine requested to extend the period of minimum pump load. The minimum pump load is programmed from 6:45 to 10:00 and 16:45 to 20:00. Defining the correct control limits will create enough capacity to extend the peak periods.

The full storage potential of mine dams is seldom used. The settlers do not remove all the debris from the water, which settles in the clear water dams. The minimum dam levels of the

dams are thus increased. To reduce the risk of flooding the maximum dam levels are also limited. Table 5 displays the maximum and minimum specified dam limits at this mine.

Table 5: Maximum and minimum dam limits

Pump chamber	Minimum dam level [%]	Maximum dam level [%]
IPCM 3-CPFS Off	30	95
IPCM 3-CPFS On	60	95
Level-22	30	95
IPCS	50	90
Level-46	20	95

The 3-CPFS and the pumps on IPCM use the same dewatering column. This increases the risk of failure due to the pressure and decreases the system efficiency. The pumps must be limited to a maximum two when the 3-CPFS is running.

3.4.2. Control dams

All pump chambers have more than one dam. The total dam storage capacity is determined through the availability of the dams. The dams of each pump chamber are connected with a pipe and an isolation valve. During normal operation the isolation valves are open. The pump schedule is determined with a control dam. The control dam level is calculated from the average dam levels of the dams available.

Hot water dams are often contaminated with mud. The mud acts as a corrosion agent on the pumps when it is pumped with water. This results in additional wear on the internal parts of the pumps. The mud has a direct influence on the minimum dam level and storage capacity. The isolation valve is closed when the specific dam is drained to clean and remove the mud. Isolated dam levels are excluded from the control dam average.

3.4.3. Hold commands

The 3-CPFS is not controlled with the dynamic pump scheduling program. The 3-CPFS has four pump running statuses and a pause status. Different combinations of the statuses result in different amounts of flow delivered. Table 6 displays the flow the 3-CPFS deliver for different pump status combinations.

Table 6: 3-CPFS flow from its pump status combinations

Pump 1	Pump 2	Pump 3	Pump 4	Paused	Flow [l/s]
1	1	-	1	-	320
-	-	1	1	-	140
-	-	-	-	1	0

If any of the four pumps or the pause status is active, the 3-CPFS is seen as running in the dynamic pump scheduling program. The program has a different control philosophy for when the 3-CPFS on or off. The transition between the 3-CPFS pump combinations often results in an off status. This affects the program and activates the incorrect control philosophy. A hold command was used to ensure the correct status of the 3-CPFS was incorporated in the program during the transition periods.

The hold tag uses a countdown timer to hold the pump status. It will return the pump status when the pump is running. It is programmed to hold the pump running status for the set period of time after the pump has stopped. The period of each timer can be defined in the program. The countdown timer resets when a pump running status is received. Figure 36 displays an example of a 30 minute hold command.

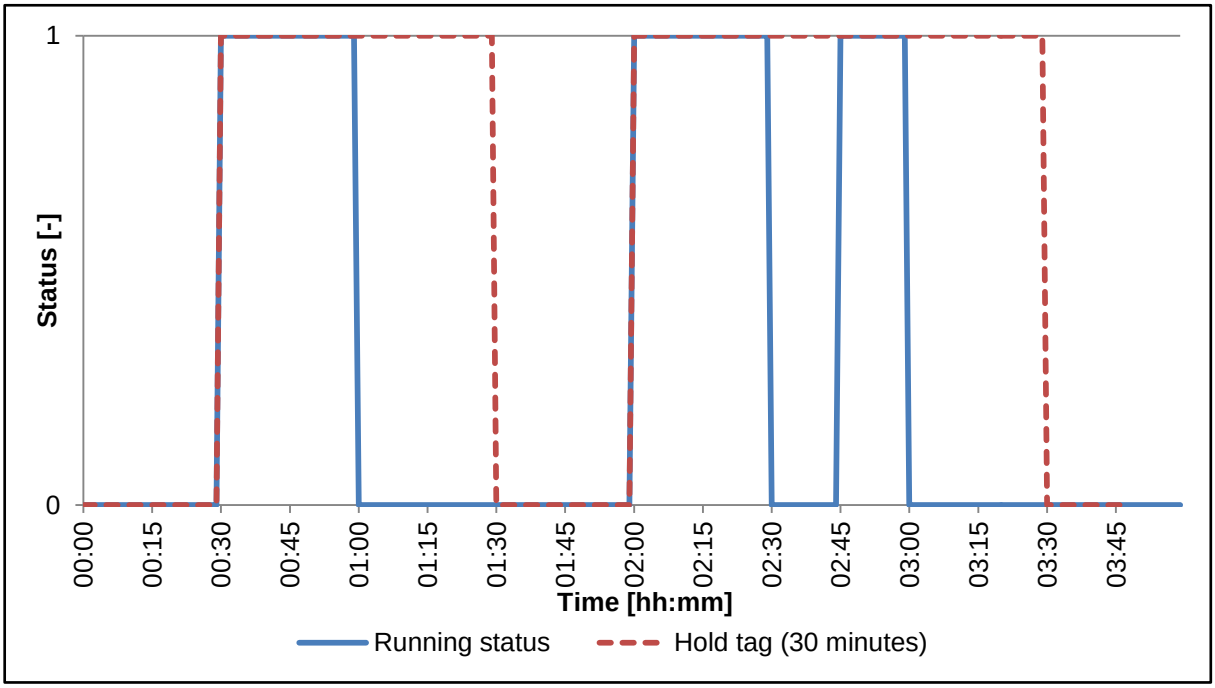

Figure 36: Hold command example

The actions of the hold command are explained in Table 7. The table must be used with Figure 36 to understand correctly.

Table 7: Explanation of hold command action

Time	Status	Hold	Timer Action
00:00	0	0	Off initial status
00:30	1	1	Resets
01:00	0	1	Starts
01:30	0	0	Ends
02:00	1	1	Resets

Table 7 (continue): Explanation of hold command action

Time	Status	Hold	Timer Action
02:30	0	1	Starts
02:45	1	1	Resets
03:00	0	1	Starts
03:30	0	0	Ends

3.4.4. Upstream control

The dynamic pump scheduler is used to control the pumps of a pump chamber. It uses the upstream control dam level as the primary control parameter. A Minimum Dam Level (MDL) is defined for the daily profile. The MDL is programmed according to the daily tariff periods as showed in equation 3.8. This result in the maximum dam storage capacity is available during peak periods to schedule the minimum number of pumps.

$$MDL_t = f(hh{:}mm) \tag{3.8.}$$

MDL_t	-	Minimum defined daily profile	%

A Control Offset (CO) is defined for the daily profile. The CO is added to the MDL to create the Control Range (CR) as displayed in equation 3.9. This is the optimum range for the dam level to be when the peak periods start to allow minimum pump load for the longest period.

$$CR_t = MDL_t + CO_t \tag{3.9.}$$

CR_t	-	Control range calculated daily profile	%
MDL_t	-	Minimum defined daily profile	%
CO_t	-	Control offset defined daily profile	%

A daily profile Top Offset (TO) is defined per dynamic pump scheduler. The number of TO's is determined with the number of pumps available for the pump chamber. The first TO is added to the CR, and from the second TO it is added to the previous TO. This defines the dam levels at which an additional pump will be scheduled. Equation 3.10 displays how the TO is calculated.

$$TO(n_{pa}-1)_t = CR_t + (n_{pa}-1)TO_t \tag{3.10.}$$

$TO(n_{pa}-1)_t$	-	n^{th} top offset calculated daily profile	%
n_{pa}	-	Number of pumps available	-
CR_t	-	Control range calculated daily profile	%

A Bottom Offset (BO) is similar defined to the TO. The first BO is deducted from the MDL, from the second BO, it is deducted from the previous BO. This defines the dam levels at which one less pump will be controlled. Equation 3.11 displays how the BO's are calculated.

$$BO(n_{pa}-1)_t = MDL_t - (n_{pa}-1)BO_t \qquad 3.11.$$

$BO(n_{pa}-1)_t$	-	nth top offset calculated daily profile	%
n_{pa}	-	Number of pumps available	-
MDL_t	-	Minimum defined daily profile	%
CO_t	-	Control offset defined daily profile	%

The scheduler aims to control the dam level between the MDL and CR. The number of pumps will increase if the dam is filled and each time the dam level exceeds the CR or a TO. The increase in the number of pumps will decrease the rate at which the dam is filled or starts to drain. The number of pump will decrease if the dam is drained and each time the dam level exceeds the MDL or a BO. The dam will start to fill or drain slower.

Figure 37 is a graphic illustration of the offsets of IPCM with the 3-CPFS off. The smaller MDL during the off-peak and standard periods will increase the pump load during this period. This enables the pumps to be stopped in the peak period due to available dam capacity and the higher MDL. The smaller TO during the off-peak maximise the pump load during this period. This results in most of the water being transferred during the less expensive time periods. The dam level control limits are displayed in Figure 37.

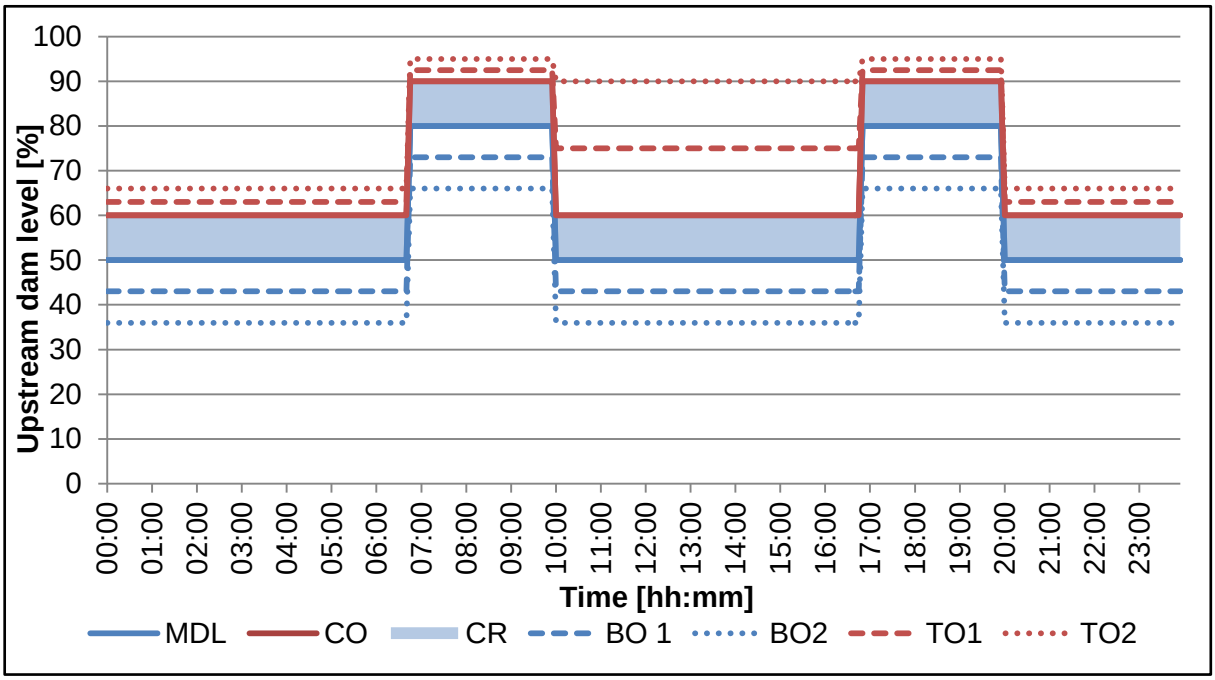

Figure 37: Optimised offsets IPCM with 3-CPFS off

Table 8 displays the defined varying dam limits during a 24-hour profile. The MDL is increased with 30% during the more expensive peak periods. This allows for the stopping of the pumps during this period.

Table 8: Optimised offsets for IPCM with 3-CPFS off

Start [hh:mm]	End [hh:mm]	MDL [%]	BO [%]	CO [%]	TO [%]
00:00	6:44	50	7	10	3
06:45	9:59	80	7	10	5
10:00	16:45	50	7	10	15
16:46	19:59	80	7	10	5
20:00	23:59	50	7	10	3

The 3-CPFS has a higher control privilege. The offsets of the pumps are adjusted when a hold command running status is received from the 3-CPFS. A higher dam level is maintained on IPCM to ensure the maximum potential of the 3-CPFS is utilised. Figure 38 displays the input parameters of IPCM when the 3-CPFS is running. The optimised control schedules for the other three levels can be found in Appendix C.

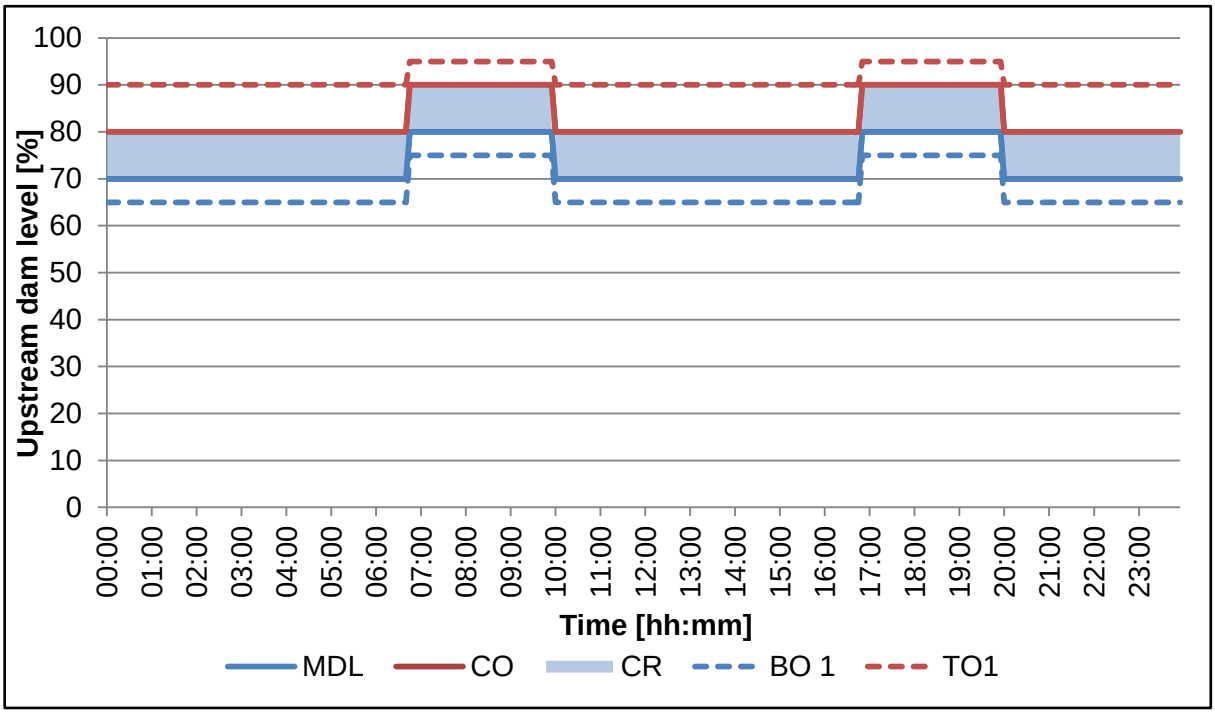

Figure 38: Optimised offsets IPCM with 3-CPS on

Table 9 displays the defined input when the 3-CPFS is running. The higher MDL during the standard and off-peak periods allows for maximum operation of the 3-CPFS.

Table 9: Optimised offsets for IPCM with 3-CPS on

Start [hh:mm]	End [hh:mm]	MDL [%]	BO [%]	CO [%]	TO [%]
00:00	6:44	70	5	10	10
06:45	9:59	80	5	10	5
10:00	16:45	70	5	10	10
16:46	19:59	80	5	10	5
20:00	23:59	70	5	10	10

3.4.5. Stable Values

The dam levels of an automation project are usually determined with ultra-sonic level transmitters or pressure transmitters. Both these sensors determine the dam level relevant to their installed positions. A small fluctuation is often found with both transmitters. The fluctuation can interfere with the pump control. Stable values are used to prevent pump cycling due to this fluctuation.

Stable values can be described as trailing memory tags. The two types of stable values used are top stable and bottom trailing types. The top stable value remains at the last maximum value the dam level has reached when the actual value starts to decrease. The top stable will decrease at the same rate of the dam level, when the difference between the top stable and actual value is equal to the set limit. When the dam level starts to increase, the top stable will remain the minimum value reached. The top stable will increase with the actual dam level when the actual dam level is equal or larger than the minimum value reached.

The stable values used for the control dams are shown in Table 10. This prevents the pumps from cycling due to dam level fluctuation. Pump cycling increases pump maintenance as mentioned in Section 1.4.

Table 10: Stable values of control dams

Control dam	Stable 1	Stable 2
Surf	10	10
IPCM	15	15
Level-22	5	5
IPCS	5	5
Level-46	5	5

Figure 39 graphically displays a top stable and bottom stable values with the actual dam level. Both are set to a 10% stable value. The stable values were set equal to the actual at the start.

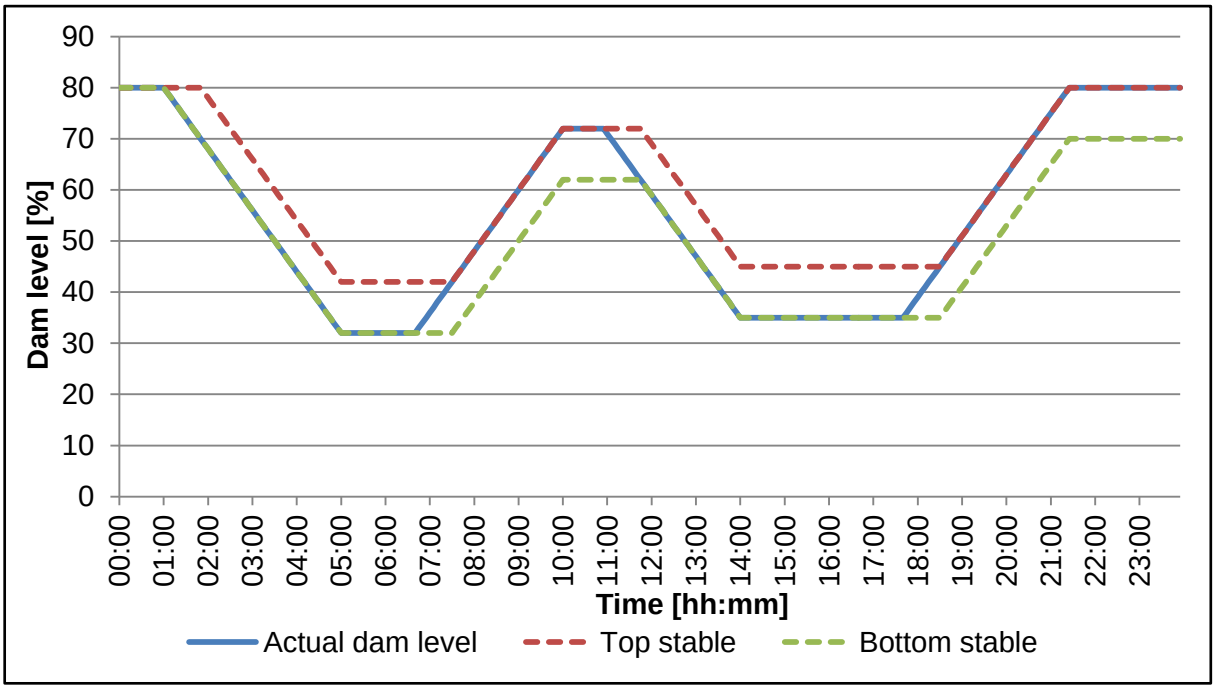

Figure 39: Stable value example

3.4.6. Number of pumps

The upstream control relies on the water balance being kept in the optimal range with all the pumps available. As this is only achievable in an ideal world, an additional safety precaution is required. The downstream dam level is also monitored with the pump scheduler. This will prevent the downstream dam from flooding as a result of a high inflow.

The downstream dam level limits the maximum number of pumps available to schedule. If both the upstream and downstream dam levels are almost full, the maximum number of pumps is set to the number of pumps available. This will pump the excess water to the surface as a precaution measure. The running status of 3-CPFS also influences the number of pumps available to schedule on IPCM.

The number of pumps available is adjusted with multiple if-functions, hold commands and stable values. Table 11 illustrates the different parameters and results for IPCM. The table is used per column from the first to the last. The applicable situation is selected in each column as described in the column heading. Only an option from the row of the previous selected situations can be selected in the subsequent column. The maximum number of pumps available to schedule is returned in the last column. The maximum number of pumps tables for the other three levels can be seen in Appendix C.

Table 11: Maximum number of pumps for IPCM

Pumps available	3-CPFS hold status	IPCM ST1	Level-22 pump status	Surface ST1	Surface ST2	Maximum number of pumps
>2	1	>95	N/A	N/A	N/A	2
		<95	2	>95	>100	0
				>95	<100	1
				<95	<100	2
		<95	1	>95	>100	0
				>95	<100	0
				<95	<100	1
		<95	0	>95	>100	0
				>95	<100	0
				<95	<100	0
	0	-	-	>95	>100	1
				>95	<100	2
				<95	<100	3
2	1	>95	N/A	N/A	N/A	2
		<95	2	>95	>100	0
				>95	<100	1
				<95	<100	2
		<95	1	>95	>100	0
				>95	<100	0
				<95	<100	1
		<95	0	>95	>100	0
				>95	<100	0
				<95	<100	0
	0	-	-	>95	>100	1
				>95	<100	2
				<95	<100	2
1	1	>95	N/A	N/A	N/A	1
		<95	2	>95	>100	0
				>95	<100	1
				<95	<100	1
		<95	1	>95	>100	0
				>95	<100	0
				<95	<100	1
		<95	0	>95	>100	0
				>95	<100	0
				<95	<100	0
	0	-	-	>95	>100	1
				>95	<100	1
				<95	<100	1
0	N/A	N/A	N/A	N/A	N/A	0

3.4.7. Enhancing of control

The control parameters explained in the previous sections are the optimised parameters. The optimised parameters were achieved through a series of simulation from a basic model. Small adjustments were made with each simulation until the optimum was achieved.

The offsets for the basic model are achieved with a water balance equation. It is important to convert the dam level percentage to water volume for the calculation. Equation 3.12 illustrates how to determine the dam levels to enable a maximum load shift for the basic model.

$$DL_{end} = \frac{V_D(DL_{Start}) - n_{p\_out}\dot{Q}_{p\_out}t + n_{p\_in}\dot{Q}_{p\_in}t + t\dot{Q}_{settler}}{V_D} \quad 3.12.$$

DL_{end}	-	Dam level at the end of period	%
DL_{Start}	-	Dam level at the start of period	%
V_D	-	Dam volume	l
DL_{Max}	-	Maximum dam level available	%
n_{p_out}	-	Number of pumps draining dam	-
$\dot{Q}_{p\_out}$	-	Flow per pump draining dam	l/s
t	-	Time	s
n_{p_in}	-	Number of pump feeding dam	-
$\dot{Q}_{p\_in}$	-	Flow per pump feeding dam	l/s
$\dot{Q}_{settler}$	-	Flow of settler feeding dam	l/s

It was found to be the easiest to start optimising the control from the deepest level and work upward per level. This is due to the settler often only feeding the deepest level. The flow from the settlers can be seen as constant for the purposes of the model. The pumps feeding the subsequent level vary the inflow rate of the subsequent level which influences the pump control.

3.5. Real-time efficiency calculation

The control of a pump system can be optimised if the efficiency of each pump is known. Including pump efficiencies in the running schedule of the pumps can realise potential energy savings. Although the most efficient pump is the most energy efficient, the pump load must be distributed evenly between the pumps. This ensures the efficiency of all the pumps will deteriorate on an equal basis. Efficiency of a pump could be verified through analysing the pump history and performance.

The efficiency of a multistage centrifugal pump can be determined relative to the input power of the motor. The efficiency is the power delivered by the pump divided by the input power of the motor. Equation 3.13 shows how the efficiency is calculated [21].

$$\eta = \frac{\rho Q H g}{P_m} \tag{3.13.}$$

η	-	Efficiency	%
ρ	-	Fluid density	kg/m^3
Q	-	Volume flow	m^3/s
H	-	Head	m
g	-	Gravitational constant	m/s^2
P_m	-	Motor input power	W

Temperature probes installed in the suction and discharge column can be used to measure the temperature rise across the pump. Equation 3.14 is obtained through substituting the temperature rise across the pump into Equation 3.13 and simplifying with thermodynamic laws [87].

$$\eta = \frac{1}{\frac{C_p}{v}\left(\frac{\Delta T}{\Delta P} - \mu\right)} \tag{3.14.}$$

η	-	Efficiency	%
C_p	-	Specific heat constant	J/kg.K
v	-	Specific volume	m^3/kg
ΔT	-	Differential temperature across pump	°C
ΔP	-	Differential pressure across pump	Pa
μ	-	Joule-Thompson coefficient	K/Pa

The efficiency of the pumps is determined in real-time using the dynamic pump scheduling program. Equation 3.14 was programmed into the software to determine the efficiency. The differential pressure and temperature across the pump are required for the equation.

The specific volume was determined from varying inlet temperatures and pressures. Figure 40 displays the result of the specific volumes. The specific volume is on the vertical axis against the temperature on the horizontal axis. The thermodynamic data was found in Thermophysical Properties of Fluid System, National Institute of Standards and Technology [88]. The thermodynamic table can be found in Appendix D.

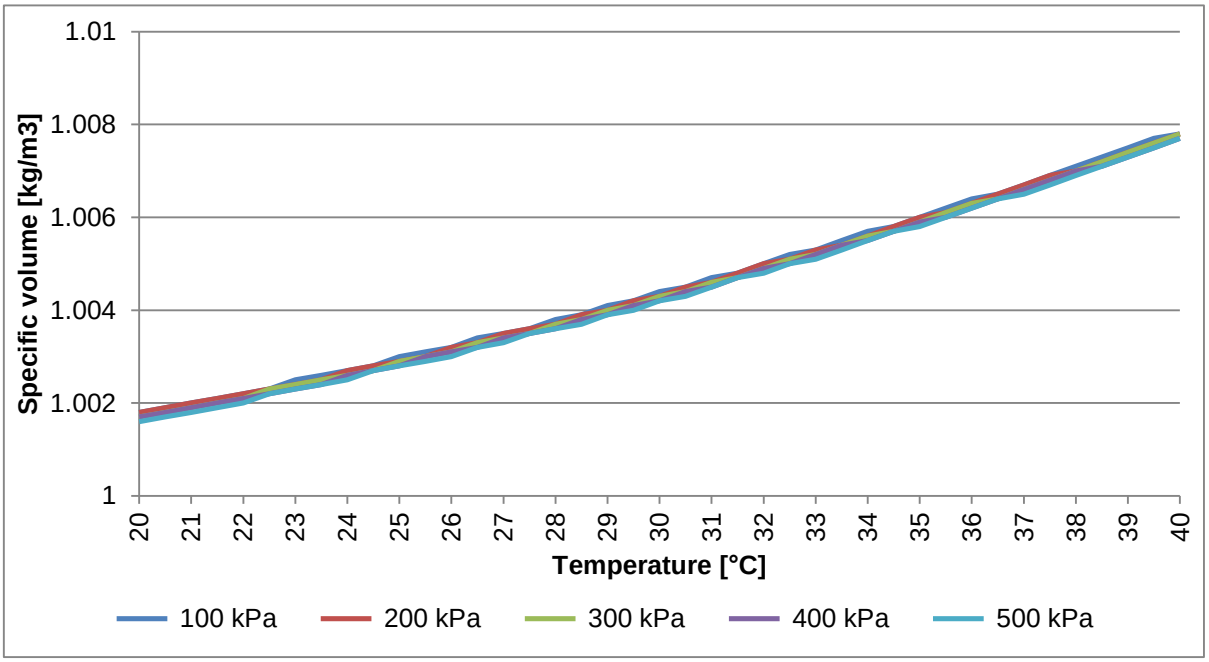

Figure 40: Water specific volume for varying temperatures and pressures

The specific heat was determined similar to the specific volume at varying inlet temperatures and pressures. Figure 41 displays the result of the specific heat. The specific volume is on the vertical axis against the temperature on the horizontal axis.

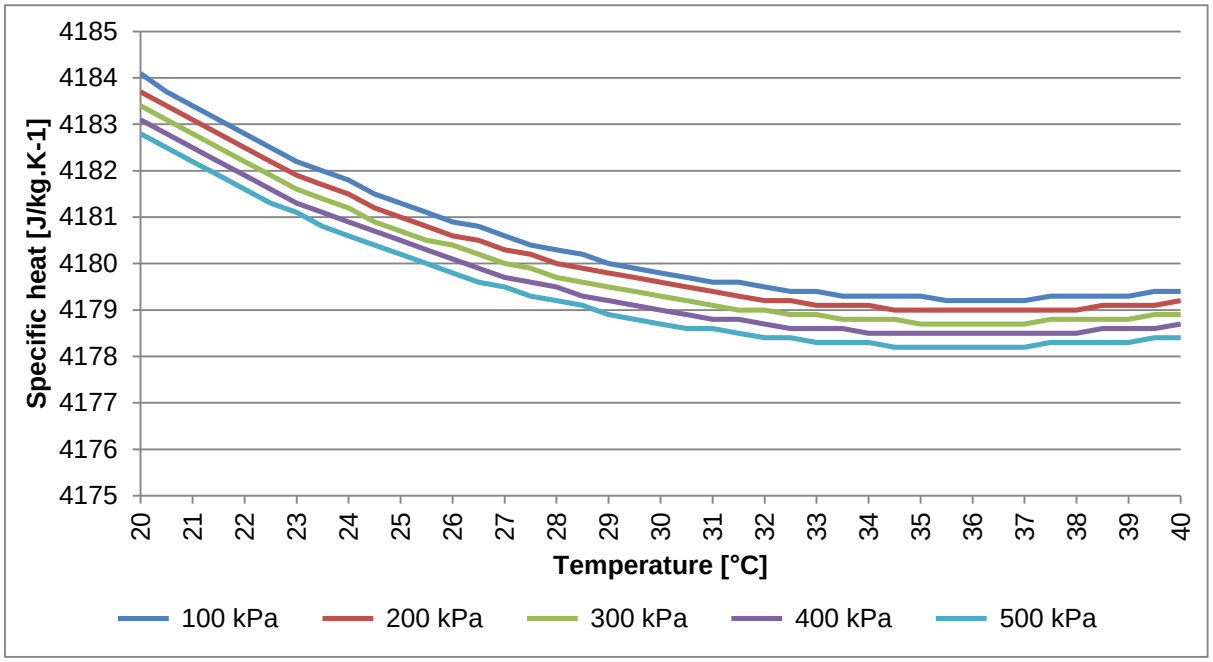

Figure 41: Water specific heat constant for varying temperatures and pressures

The Joule-Thompson coefficient was determined from the varying inlet temperatures. This result is displayed in Figure 42. The Joule-Thompson coefficient is on the vertical axis against the temperature on the horizontal axis. It was found that varying the pressure had an

insignificant effect on the coefficient. The plots for the varying pressure could not be noticed on the graph and are assumed to be equal.

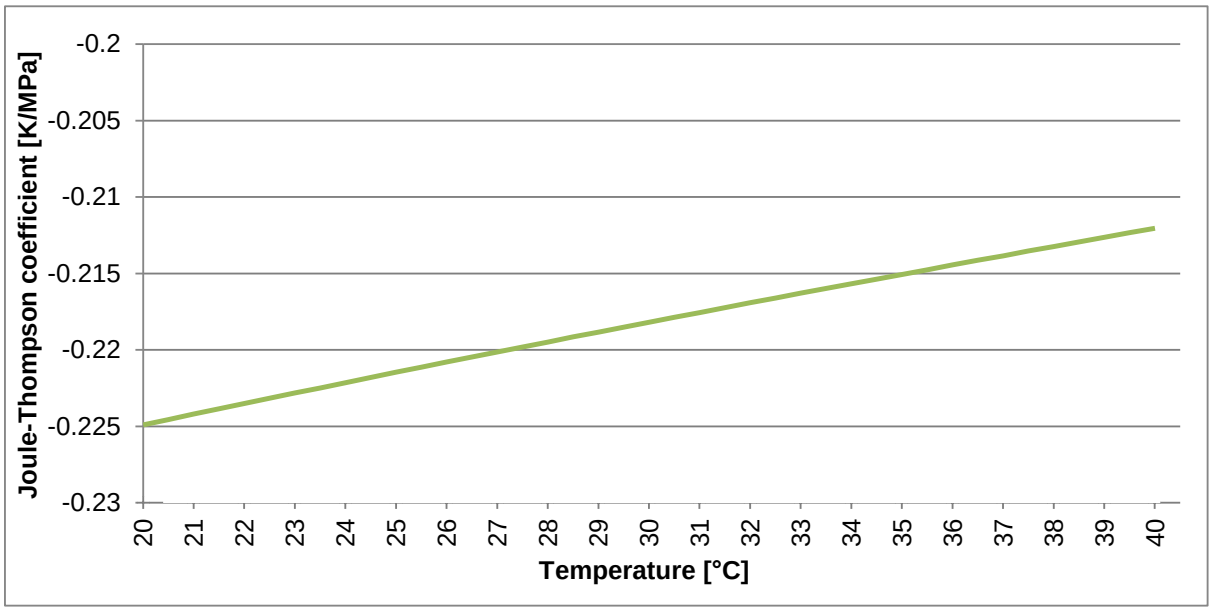

Figure 42: Water Joule-Thompson coefficient for varying temperatures and pressures

Figure 43 displays the pump efficiency calculated with Equation 3.14. The correct thermodynamic variables were obtained from the thermodynamic tables. A differential temperature of 1°C and pressure of 8 MPa were set over the pump. The maximum deviation is 0.0134% for the varying pressures.

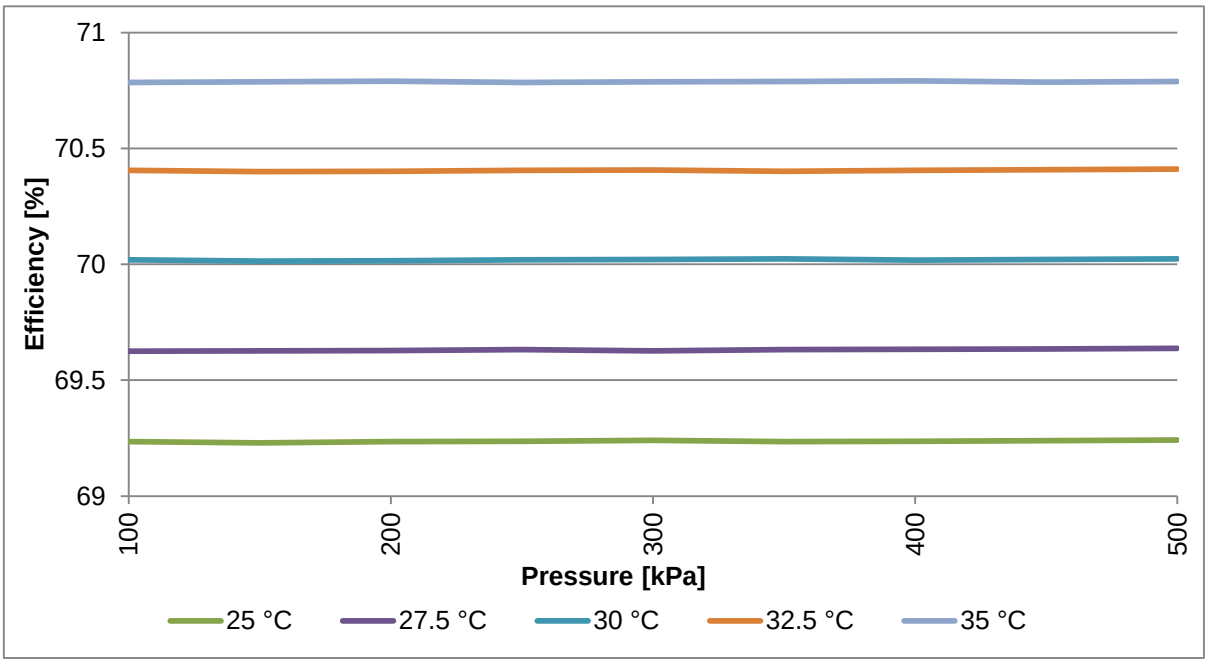

Figure 43: Pump efficiency for varying temperatures and pressure

From Figure 43 it is evident that the pressure does have a significant influence on the efficiency calculation of a pump. The variables can be determined according to the inlet temperature only. Table 12 displays the water thermodynamic properties that were programmed onto the software for the varying temperatures.

Table 12: Programmed water thermodynamic properties

Inlet temperature [°C]	Specific Volume [dm^3/kg]	Specific heat [$J/kg.K^{-1}$]	Joule-Thompson coefficient [K/MPa]
< 20.00	1.0017	4183.4	-0.225
21.00 - 21.49	1.0019	4182.8	-0.224
21.50 - 21.99	1.0020	4182.5	-0.224
22.00 - 22.49	1.0021	4182.2	-0.224
22.50 - 22.99	1.0023	4181.9	-0.223
23.00 - 23.49	1.0024	4181.6	-0.223
23.50 - 23.99	1.0025	4181.4	-0.222
24.00 - 24.49	1.0026	4181.2	-0.222
24.50 - 24.99	1.0027	4180.9	-0.222
25.00 - 25.49	1.0029	4180.7	-0.221
25.50 - 25.99	1.0030	4180.5	-0.221
26.00 - 26.49	1.0031	4180.4	-0.221
26.50 - 26.99	1.0033	4180.2	-0.220
27.00 - 27.49	1.0034	4180.0	-0.220
27.50 - 27.99	1.0035	4179.9	-0.220
28.00 - 28.49	1.0037	4179.7	-0.219
28.50 - 28.99	1.0038	4179.6	-0.219
29.00 - 29.49	1.0040	4179.5	-0.219
29.50 - 29.99	1.0041	4179.4	-0.219
30.00 - 30.49	1.0043	4179.3	-0.218
30.50 - 30.99	1.0044	4179.2	-0.218
31.00 - 31.49	1.0046	4179.1	-0.218
31.50 - 31.99	1.0047	4179.0	-0.217
32.00 - 32.49	1.0049	4179.0	-0.217
32.50 - 32.99	1.0051	4178.9	-0.217
33.00 - 33.49	1.0052	4178.9	-0.216
33.50 - 33.99	1.0054	4178.8	-0.216
34.00 - 34.49	1.0056	4178.8	-0.216
34.50 - 34.99	1.0057	4178.8	-0.215
35.00 - 35.49	1.0059	4178.7	-0.215
35.50 - 35.99	1.0061	4178.7	-0.215
36.00 - 36.49	1.0063	4178.7	-0.214
36.50 - 36.99	1.0064	4178.7	-0.214
37.00 - 37.49	1.0066	4178.7	-0.214
37.50 - 37.99	1.0068	4178.8	-0.214

Table 12 (continue): Programmed water thermodynamic properties

Inlet temperature [°C]	Specific Volume [dm^3/kg]	Specific heat [$J/kg.K^{-1}$]	Joule-Thompson coefficient [K/MPa]
38.00 - 38.49	1.0070	4178.8	-0.213
38.50 - 38.99	1.0072	4178.8	-0.213
39.00 - 39.49	1.0074	4178.8	-0.213
39.50 - 39.99	1.0076	4178.9	-0.212
> 40.00	1.0078	4178.9	-0.212

The efficiency was used to determine the starting priority of each pump per pump chamber. Additional electricity cost savings can be realised through starting the pumps from most to least efficient in the peak and standard period. The least efficient pump is scheduled to start first during the off-peak period to distribute the pump load evenly.

In order to ensure the pumps do not cycle when the efficiency changes, the priority should only be updated once a day according the efficiencies. The daily average pump efficiency of each pump was saved to a memory tag. Each pump priority was programmed to update daily between 00:00 and 00:15 to its efficiency memory tag of the previous day.

The correct efficiency will only be calculated when the pump is running. When the pump is not running, the differential pressure and temperature will be insignificant. This results in the incorrect efficiency is averaged for the day. The efficiency of the pumps will also be incorrect if a pressure sensor or temperature probe fails. The average was interlocked to return the calculated pump efficiency when the list of conditions below is satisfied. If a condition is not satisfied, the efficiency memory tag was averaged.

- Pump is running,
- Suction pressure larger than 100 kPa,
- Discharge pressure larger than 100 kPa,
- Discharge pressure larger than suction pressure,
- Suction temperature between 20 and 40°C,
- Discharge temperature between 20 and 40°C, and
- Discharge temperature larger than suction temperature.

Mines often replace or refurbish a pump when the efficiency is less than 55%. The efficiency of a new pump can be up to 80%. When a pump is replaced, the average of the memory tag from the removed pump will decrease the efficiency of the new pump. The calculated pump efficiency will overwrite the memory tag if the difference between the calculated pump efficiency and efficiency memory tag is larger than 10% for longer than 10 minutes. Figure 44 displays graphically how the pump efficiency is calculated.

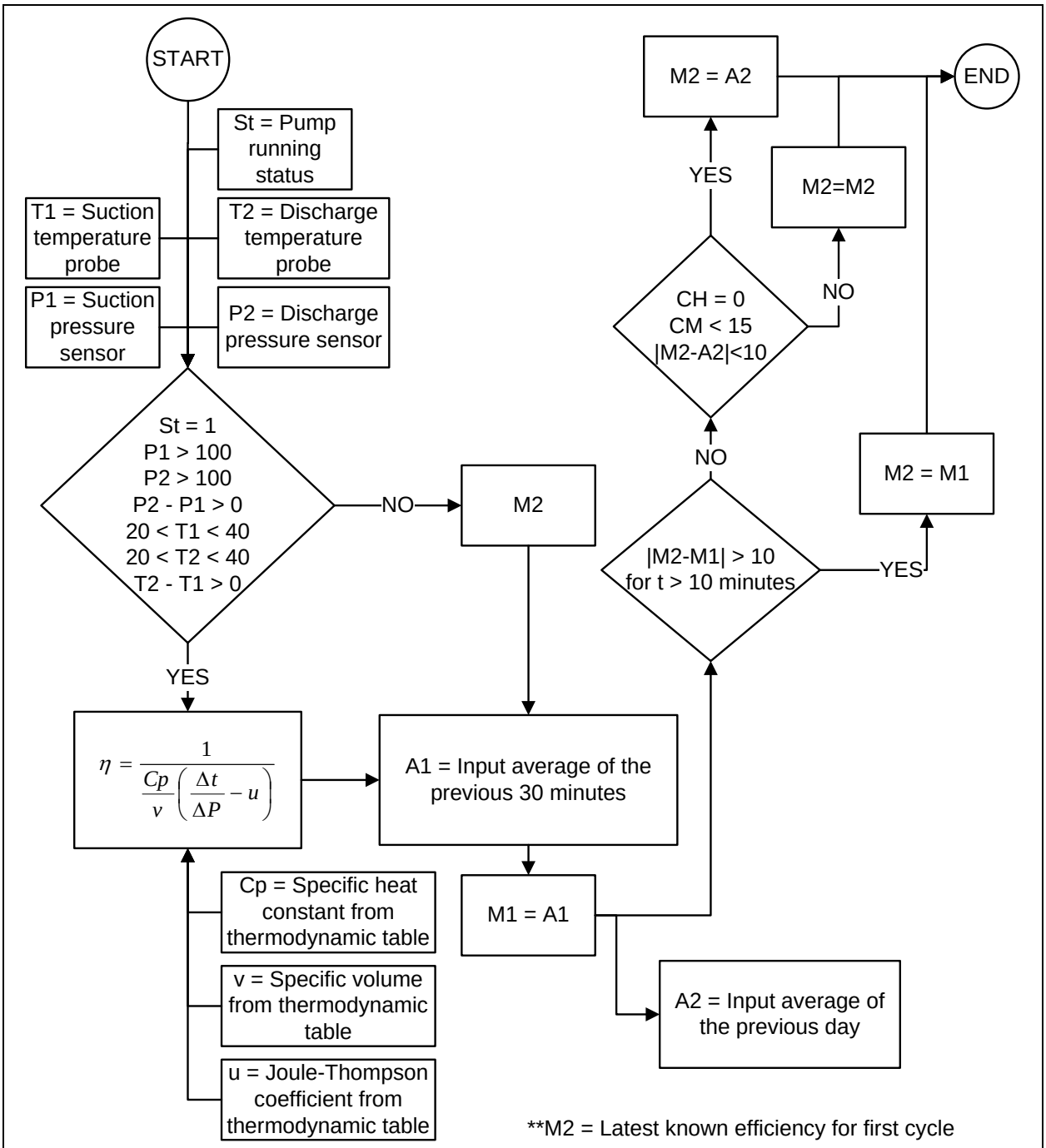

Code		Description	Code		Description
St	-	Pump running status	U	-	Joule-Thompson coefficient
T1	-	Suction temperature	A1	-	Average tag one
T2	-	Discharge temperature	A2	-	Average tag two
P1	-	Suction pressure	M1	-	Memory tag one
P2	-	Discharge pressure	M2	-	Memory tag two
Cp	-	Specific heat constant	CH	-	System current hour
v	-	Specific volume	CM	-	System current minute

Figure 44: Real-time efficiency calculation tree

3.6. Summary

The current best practice to automate a pump system in the case study was proved insufficient to protect the pump against failure. Additional safeties and trip circuits were installed on the pump to prevent failure from a similar incident.

The automated pump system made it possible to implement a real-time pump scheduling program. The program creates spare dam capacity during the off-peak and standard periods to shift the pump load out of the peak periods, using the predefined dam levels to prevent the flooding and ensure it is done safely. The 3-CPFS was interlocked in the program to ensure optimal electricity savings is achieved.

A method was implemented to determine the pump efficiency in real-time. This was achieved with the additional installed instrumentation. The efficiency can realise additional cost savings through utilising the more efficient pump in the more expensive electricity periods.

Chapter 4: Results of improved design and control

In this chapter the results of the installed instrumentation of a pump are shown. The additional precautions and safety measures are verified to determine if it will prevent a similar incident. Pump running statuses are discussed with the implemented control philosophies. The real-time efficiencies of the pumps calculated are shown.

4.1. Introduction

The instrumentation, control philosophies and efficiency calculations discussed in the previous chapter have to be verified. Data from each pump PLC was logged on a two minute interval with the dynamic pump schedule program. The interval was adjusted finer where needed.

The data from the system will be displayed graphically for illustration purposes. This allows for a detailed analysis of the results. It also enables the detection of unsafe or abnormal condition.

4.2. Analysis of instrumentation data

Daily profiles of the installed instrumentation are used to determine the running conditions of the pumps. Daily profiles for a typical day of the analog instrumentation of pump 1 on Level-22 are shown. To analyse the condition of the pump correctly, all the data received form the instrumentation must be analysed simultaneously.

Figure 45 displays the daily pump running profile. The pump running status is on the vertical axis against the time on the horizontal axis. The pump status must be kept in mind when analysing the data of the instrumentation.

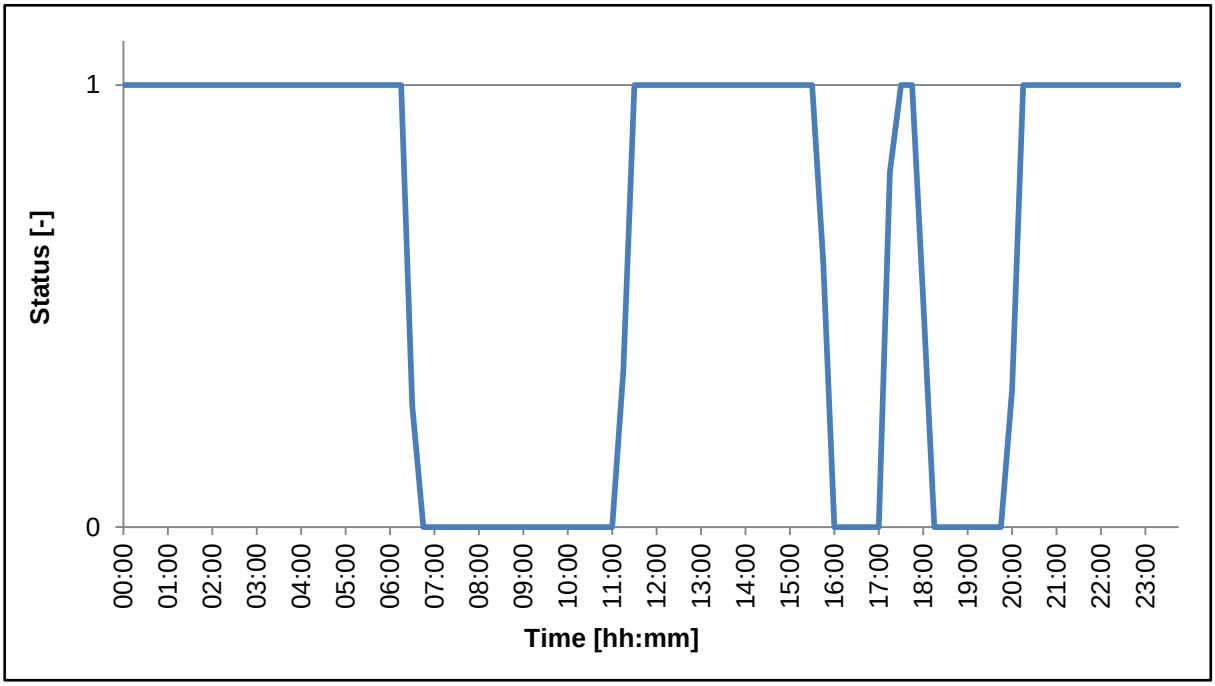

Figure 45: Pump running status daily profile

Figure 46 displays the daily position of the discharge valve profile. The position is on the vertical axis against the time on the horizontal axis. The discharge valve is controlled with an actuator. The valve opens and closes automatically when the start or stop signals are send.

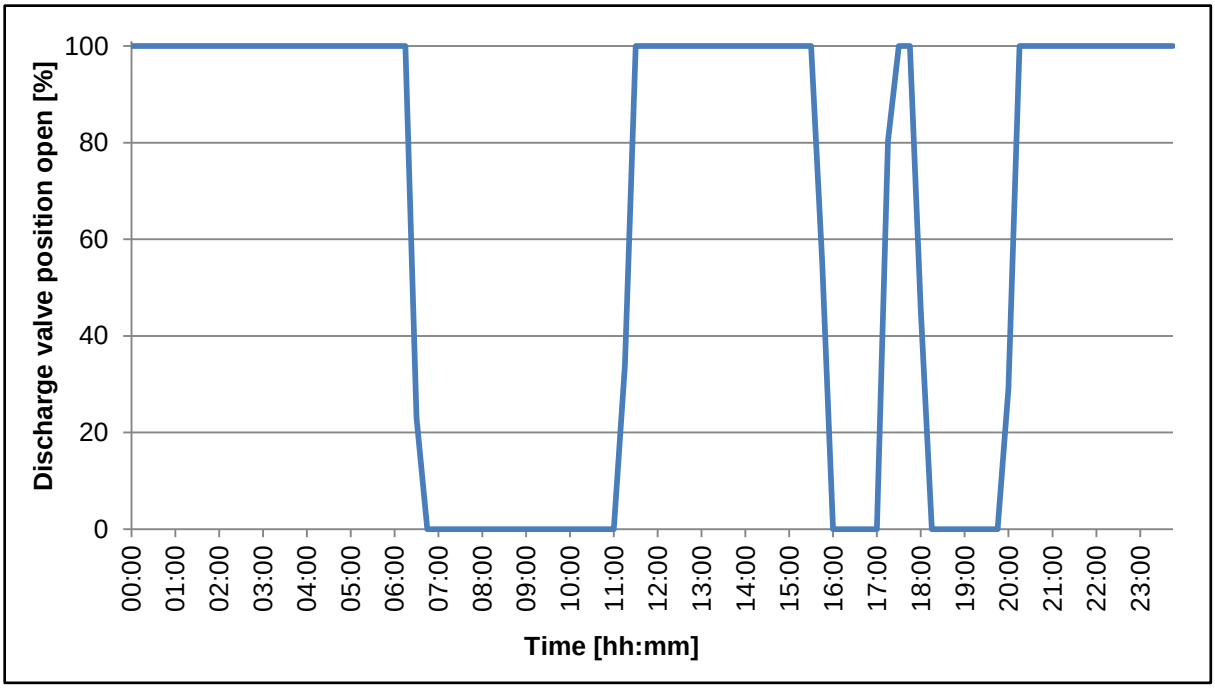

Figure 46: Pump discharge valve position daily profile

Figure 47 displays the daily flow the pump delivers. The flow is on the vertical axis against the time on the horizontal axis. The flow is used to determine the pump efficiency.

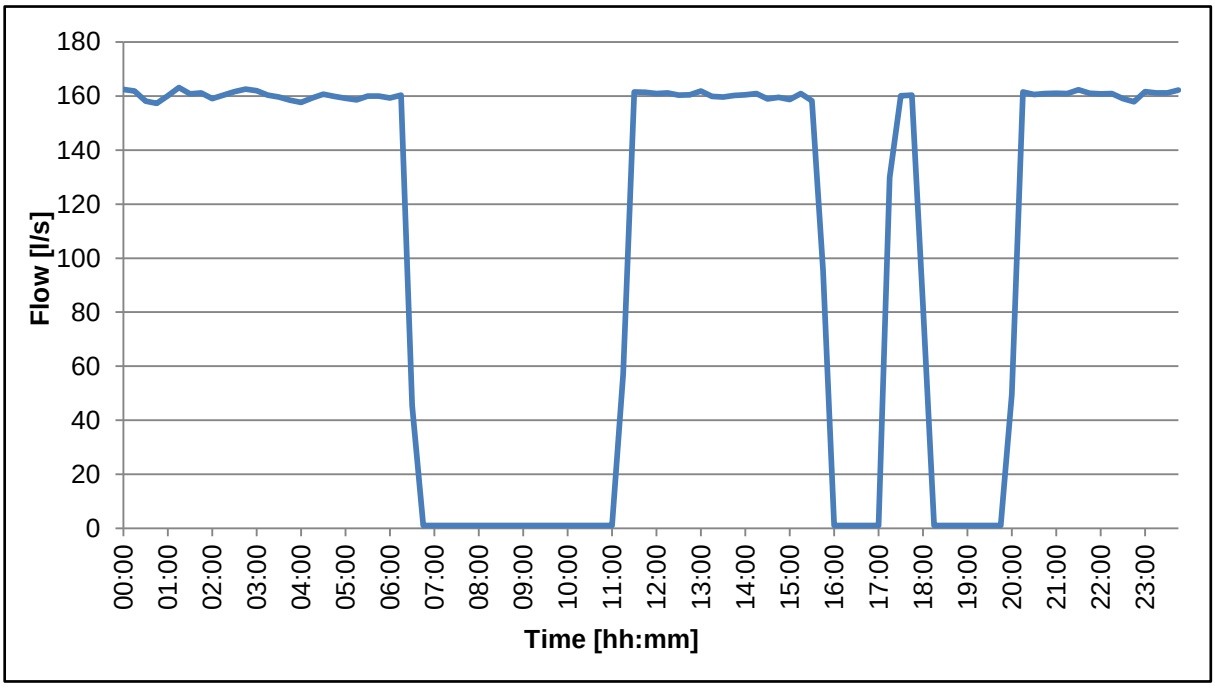

Figure 47: Pump flow daily profile

Figure 48 displays the balance disc flow vertical axis against the time on the horizontal axis. The PLC is set to activate an alarm at 40 l/s and initiate the trip sequence at 45 l/s.

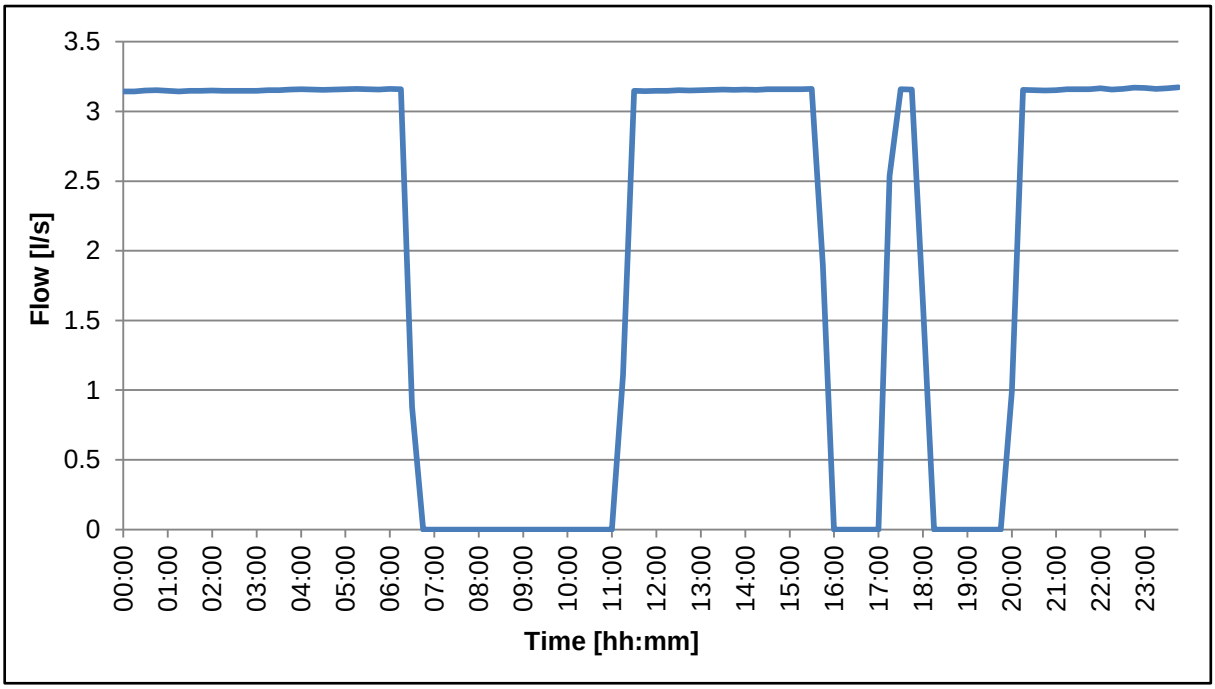

Figure 48: Pump balance disc flow daily profile

Figure 49 displays the daily profile of the pump and motor bearings temperature. The temperature is on the vertical axis against the time on the horizontal axis. The PLC is set to activate an alarm at 75°C and initiate the trip sequence at 80°C.

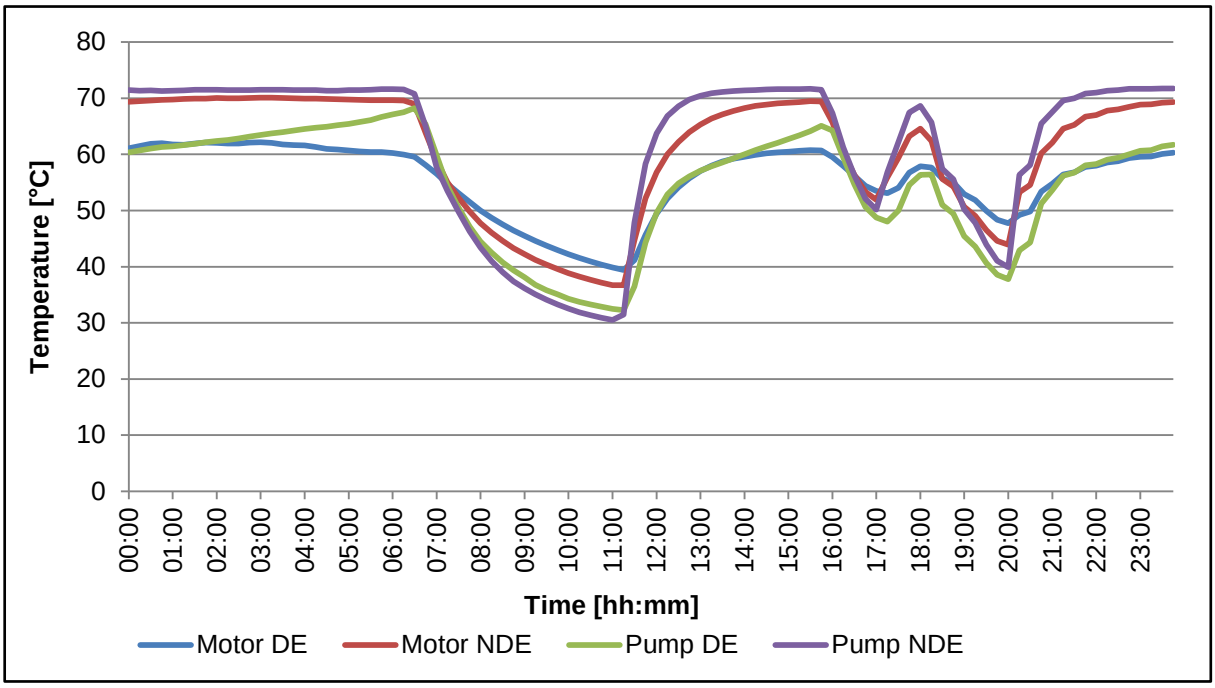

Figure 49: Pump and motor bearing temperatures daily profile

Figure 50 displays the motor windings temperature vertical axis against the time on the horizontal axis. An alarm will be activated at 115°C and trip sequence initiated at 120°C.

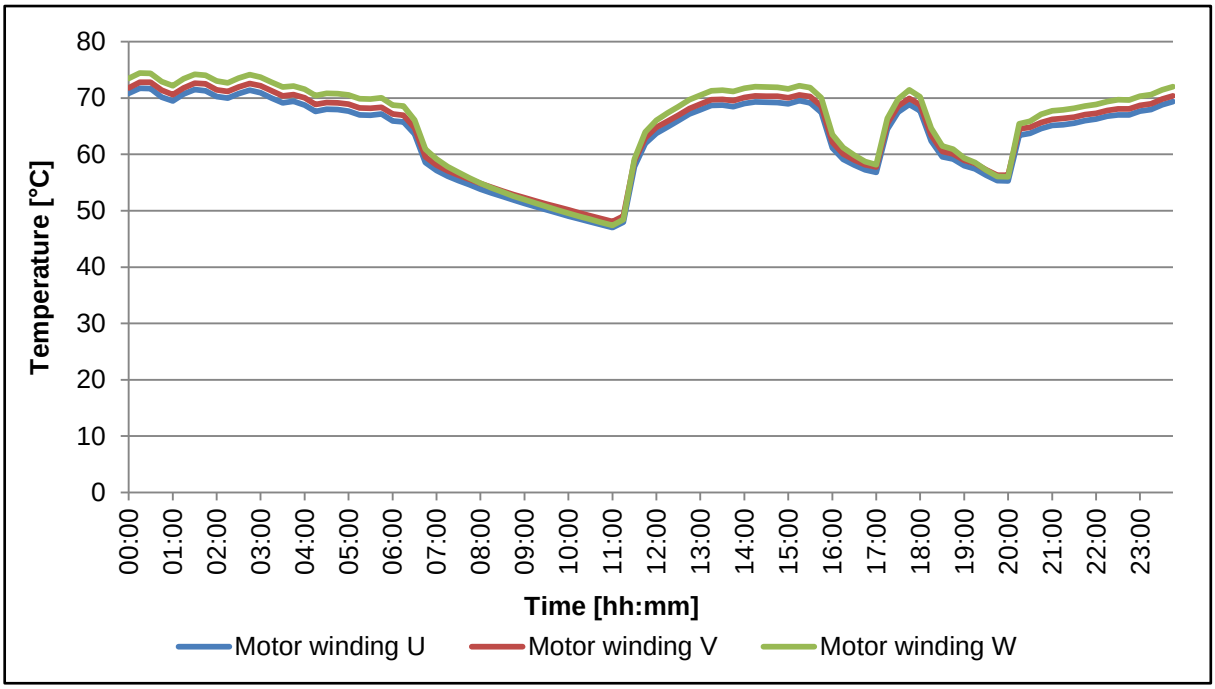

Figure 50: Motor winding temperatures daily profile

Figure 51 displays the daily pump and motor DE vibration profile. The vibration velocity is on the vertical axis against the time on the horizontal axis. The PLC is set to activate an alarm at 4 mm/s and initiate the trip sequence at 8 mm/s.

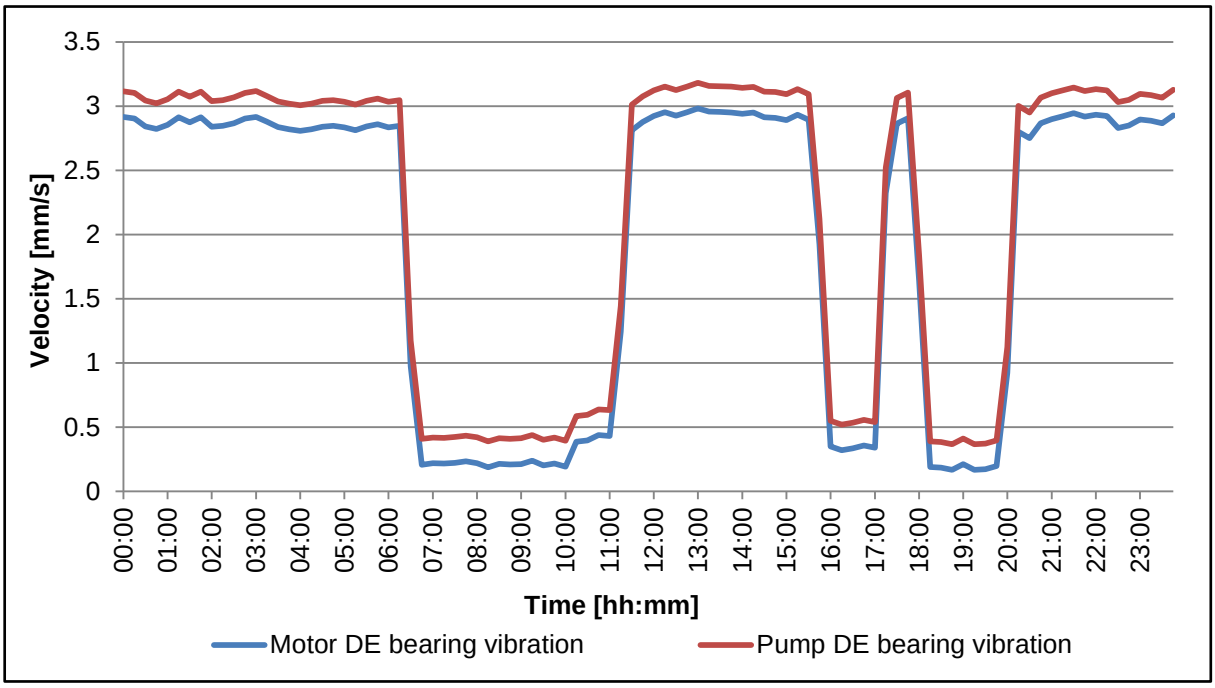

Figure 51: Pump and motor DE vibration daily profile

Figure 52 displays the daily pump suction and discharge profiles. The pressure is on the vertical axes against the time on the horizontal axis.

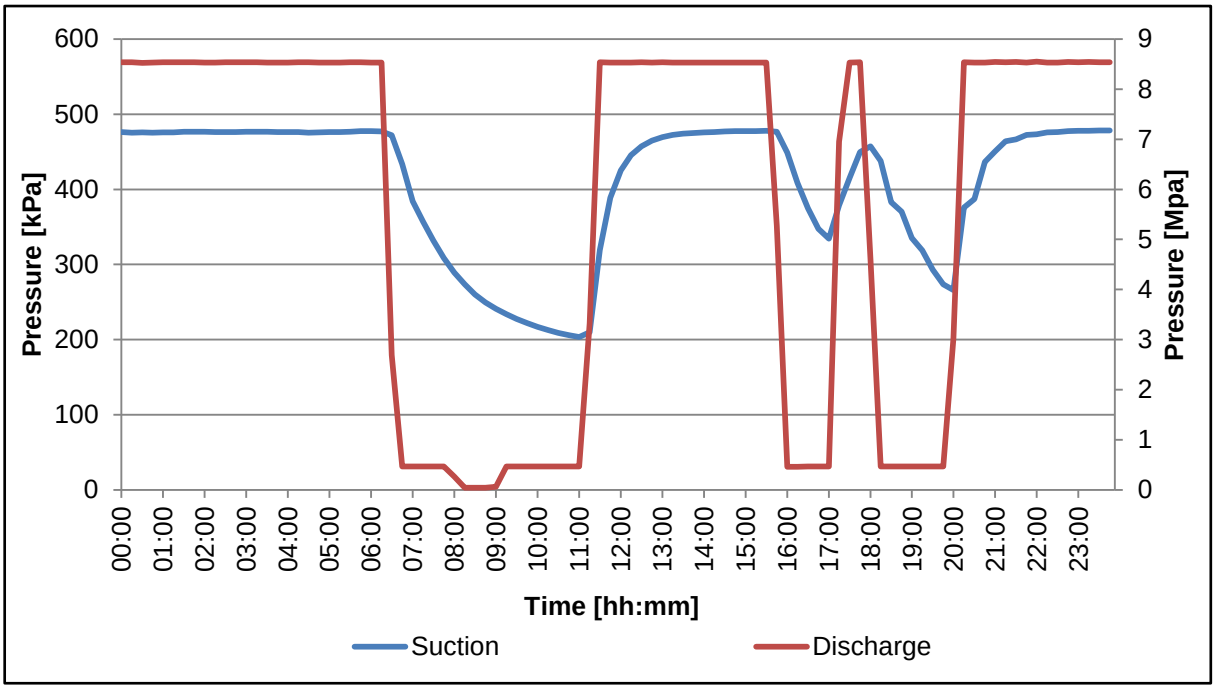

Figure 52: Pump suction and discharge pressure daily profile

Figure 53 displays the daily pump suction, discharge and balance disc temperature profiles. The temperatures are on the vertical axis against the time on the horizontal axis. The PLC will activate an alarm if any of the temperatures exceeds 40°C and trip sequence at 45°C.

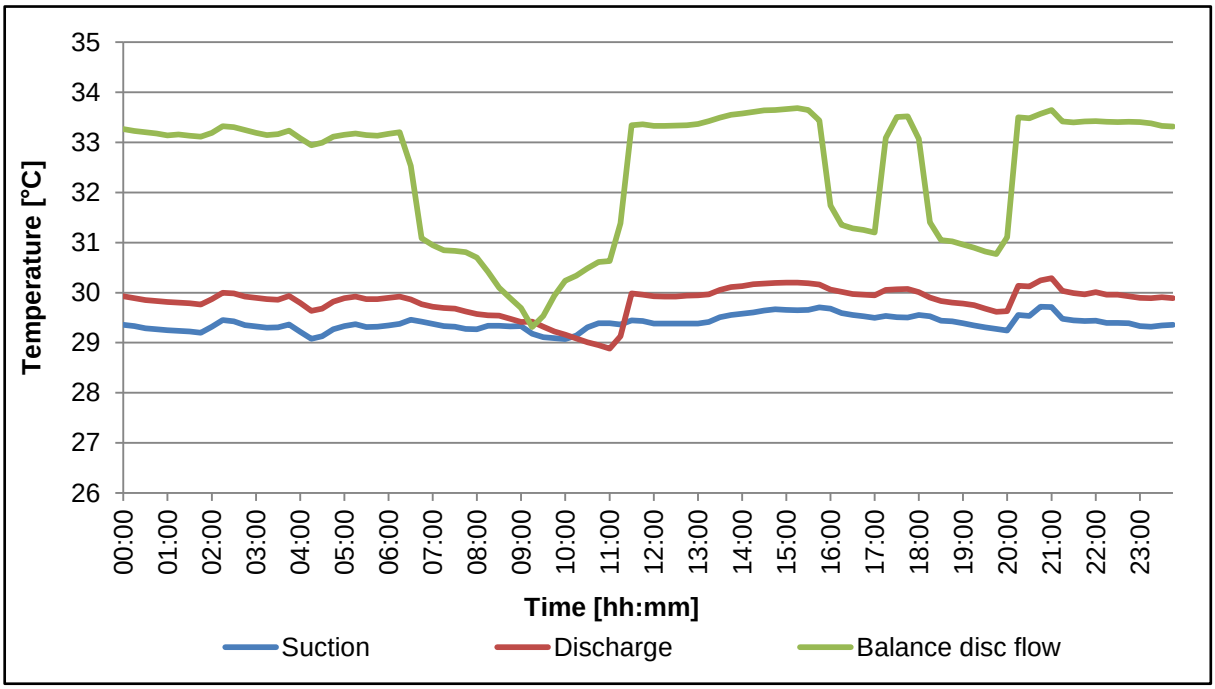

Figure 53: Pump suction, discharge and balance disc temperature daily profile

Figures 45 to 53 display the daily pump running data of the analog instruments. It is clear from the data that the pump operates within safe operating limits as defined by the client. The limits on the PLC are also set within an acceptable range to activate an alarm or initiate the trip sequence if the limits are reached.

4.3. Overheat and cavitation failure prevention

The daily profile graphs are an illustration of the typical pump operating parameters. A smaller log interval was used to determine if the additional instrumentation installed will prevent failure due to overhead and cavitation. A more detail examination could be done on the parameters from the smaller intervals.

The refurbishment cost of the pump that failed was almost R 1-million. Repeating the same scenario to test if the additional instrumentation will prevent failure is not feasible. A safe test method was used to determine if the additional instrumentation would detect overheating and cavitation during low flow.

The pump motor starts when the discharge valve is only 20% open. This result in a small period of low flow until the valve is fully open. Observing all instrumentation during this period will give an indication if the instrumentation will detect overheat and cavitation during low flow. There were no significant results during the starting period because when the pump generated a discharge pressure the valve was already fully open.

The stop sequence was used with a similar method. The pump motor only stopped when the discharge valve is 5% open. During the closing period, the pump was already running at full load. This period was then used to examine the instrumentation results.

Figure 54 displays the pump motor running status during the stop sequence. The status is on the vertical axis against the time on the horizontal axis.

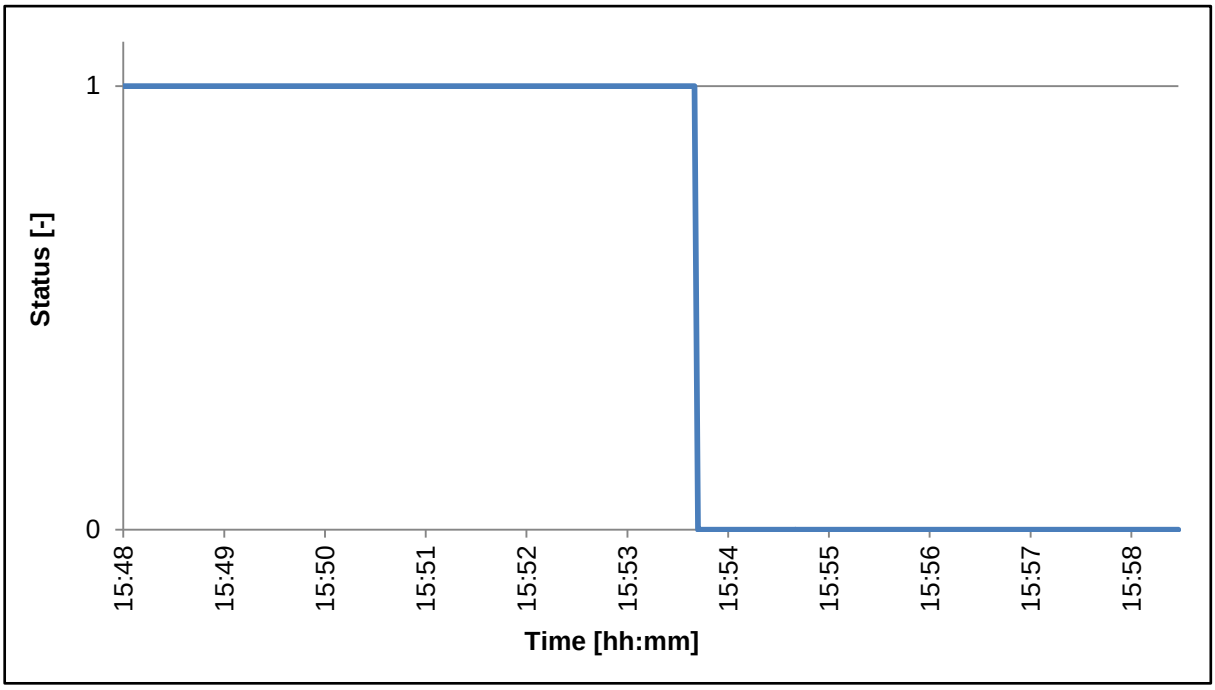

Figure 54: Pump stop sequence motor running status

Figure 55 displays the discharge valve position during the pump stop sequence. The discharge valve position percentage open is on the vertical axis against the time on the horizontal axis. The actuator requires approximately 1 minute and 30 seconds to close the valve from fully open. Also note that the motor running status was also stopped at 5% from Figures 54 and 55.

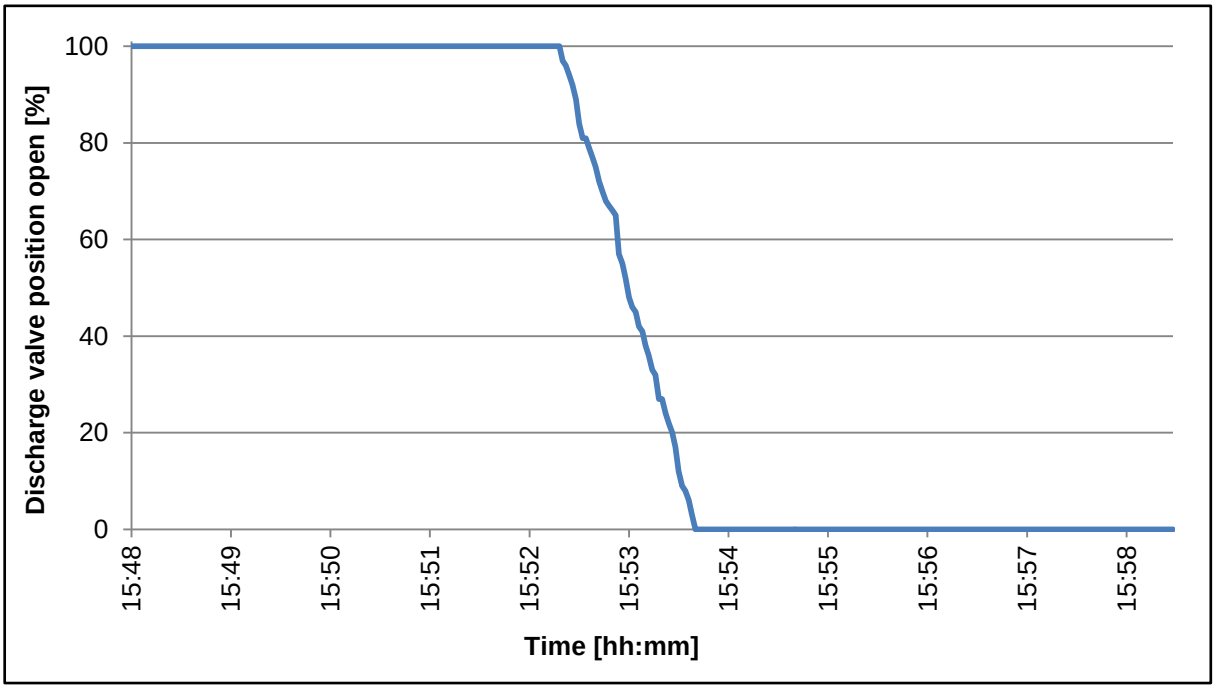

Figure 55: Pump stop sequence discharge valve position

Figure 56 displays the pump flow during the stop sequence. The flow is on the vertical axis against the time on the horizontal axis. The closing discharge valves only started to influence the flow delivered when the valve had reached 15%. At 5% when the motor was stopped, the flow was reduced to 87.09 l/s. This limited the amount of water hammer in the system.

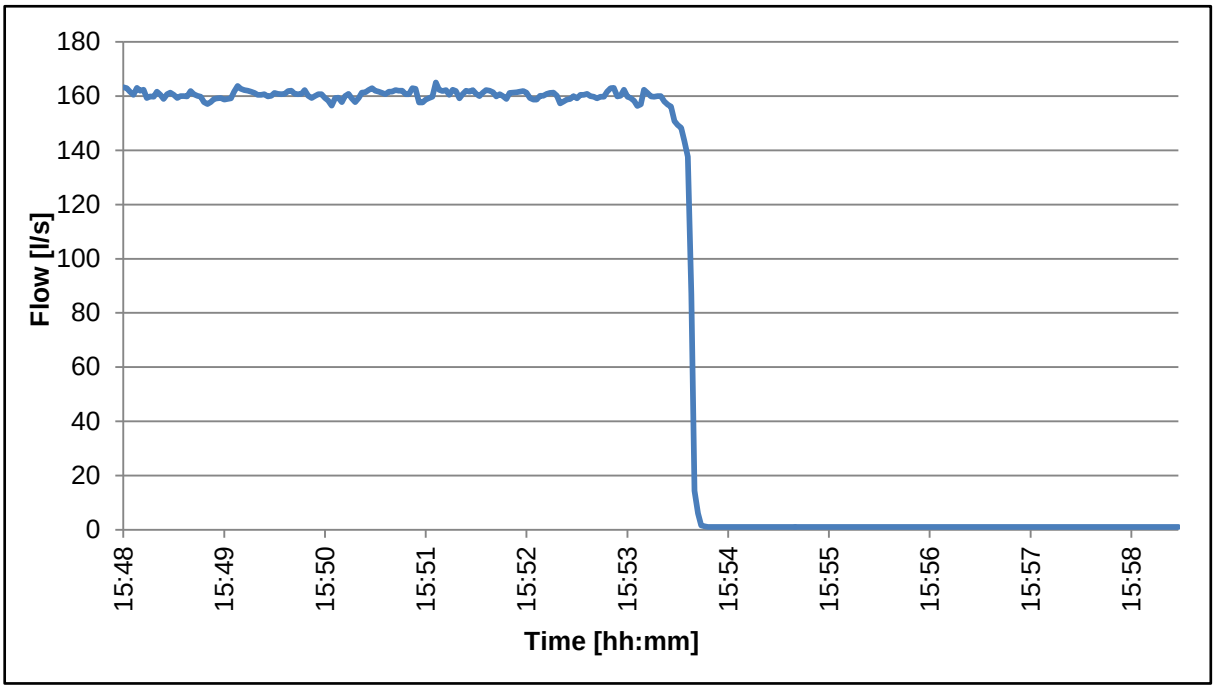

Figure 56: Pump stop sequence flow

Figure 57 displays the pump and motor bearing temperatures during the stop sequence. The temperature is on the vertical axis against the time on the horizontal. The bearings tend to cool as soon as the motor is stopped. The pump DE temperature trend does however differ from the other bearings. In the bearing daily profile, Figure 49, the temperature of the same bearing acted irregularly compared to the others. It is expected that the bearing was damaged.

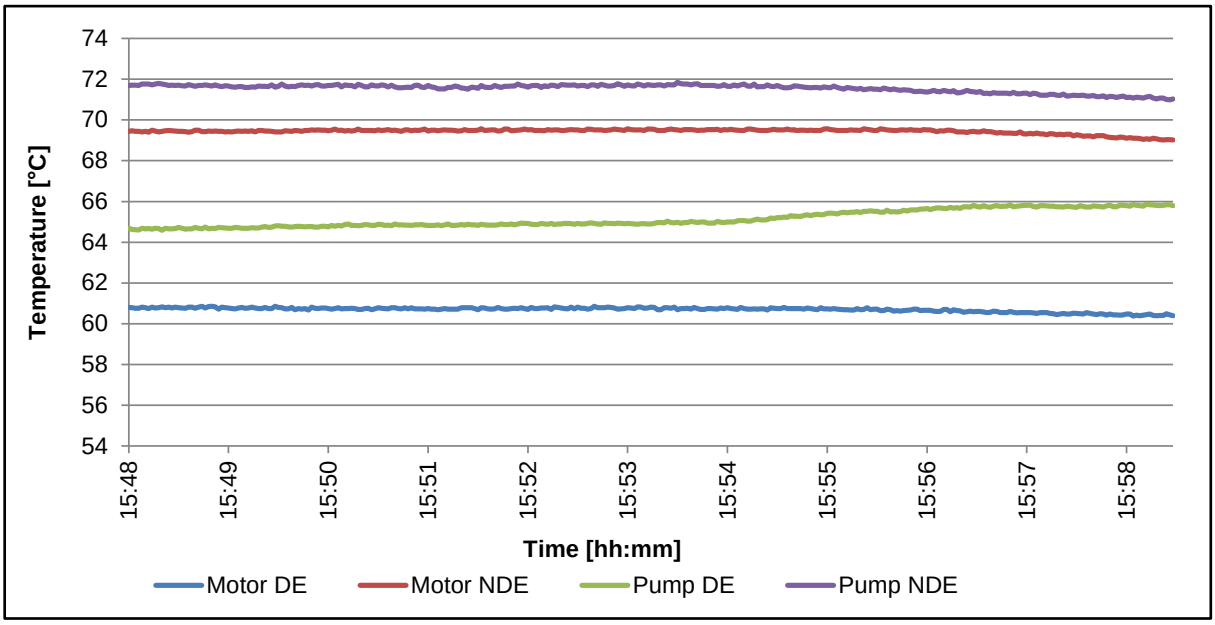

Figure 57: Pump and motor stop sequence bearing temperatures

Figure 58 displays the motor winding temperatures during the stop sequence. The temperature is on the vertical axis against the time. The windings start to cool when the motor is stopped.

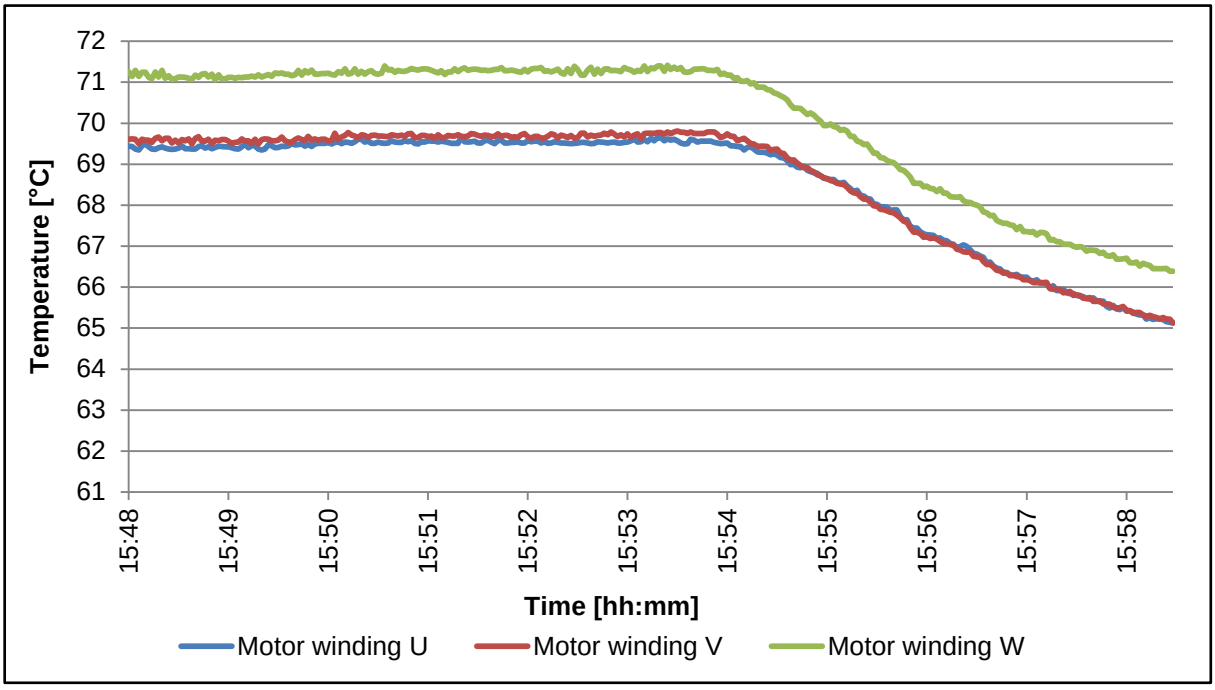

Figure 58: Motor stop sequence winding temperature

Figure 59 displays the pump and motor DE bearing vibrations during the stop sequence. The vibration velocity is on the vertical axis against the time on the horizontal axis. The increase of vibration on the bearings during the stop sequence is an indication of a damaged bearing. This can be the same pump DE bearing with the temperature rise.

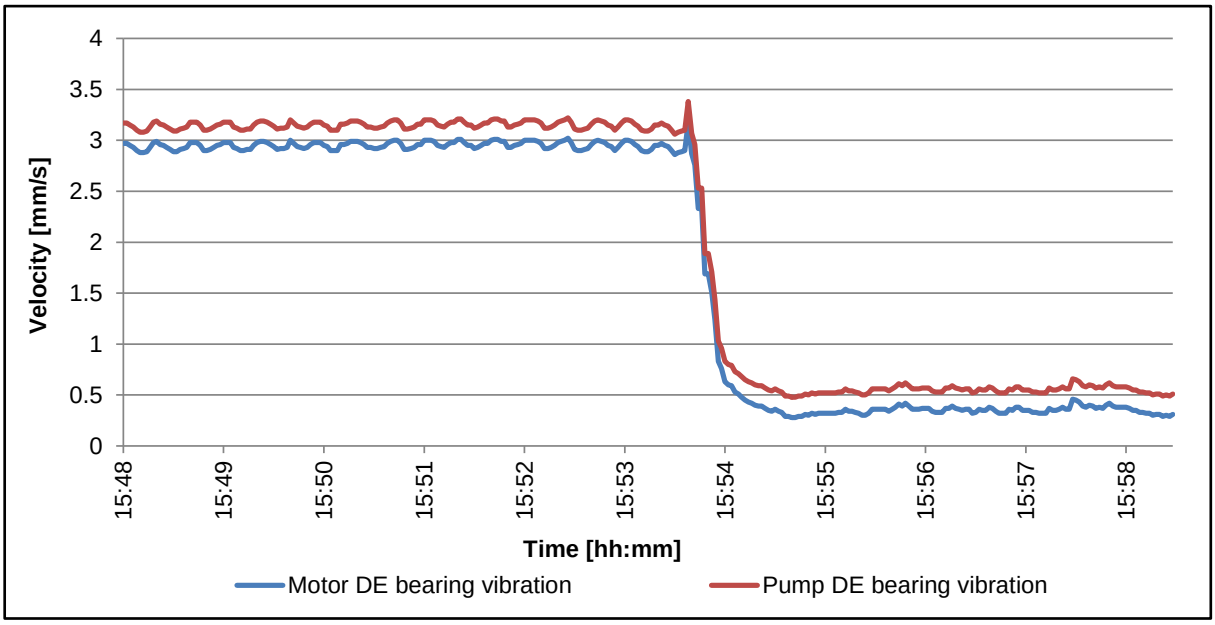

Figure 59: Pump and motor stop sequence DE bearing vibration

Figure 60 displays the balance disc flow during the stop sequence. The flow is on the vertical axis against the time on the horizontal axis. The balance disc flow increases when the discharge valve closes. This is a result of the pressure increase at the discharge.

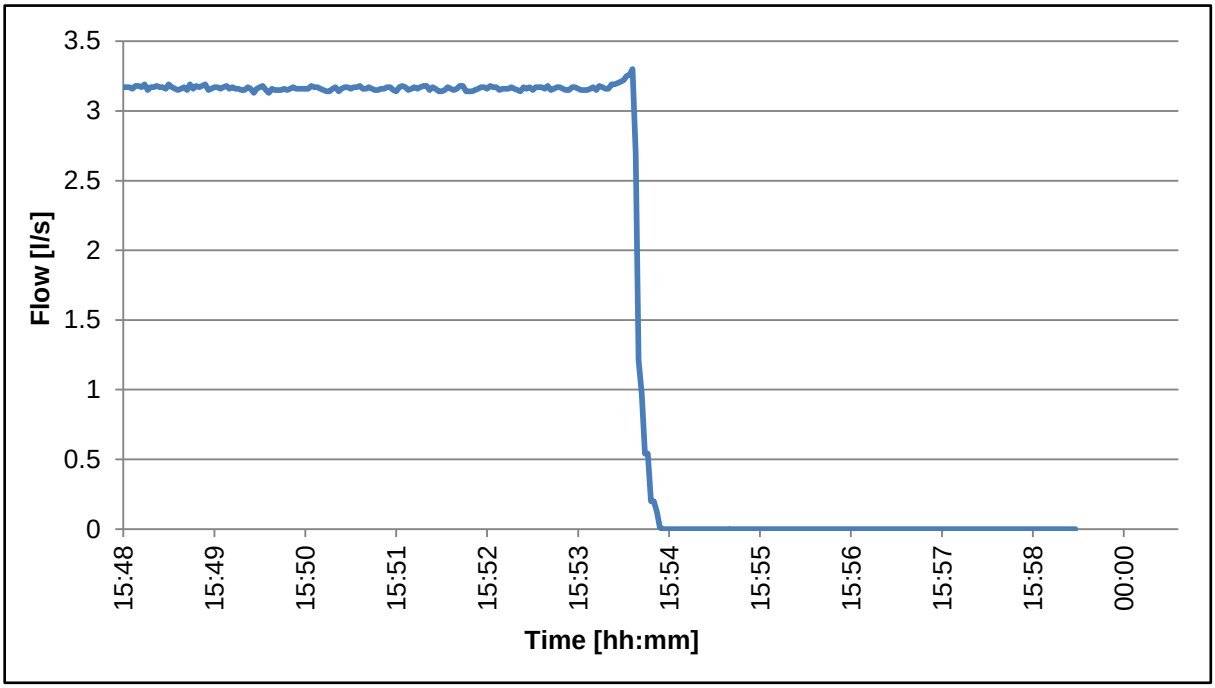

Figure 60: Pump stop sequence balance disc flow

Figure 61 displays the suction and discharge pressure during the stop sequence. The pressure is on the vertical axes against the time on the horizontal. Both the suction and discharge pressure increase when the valve starts to close. The discharge pressure tends to be equal to the suction pressure when the motor stops.

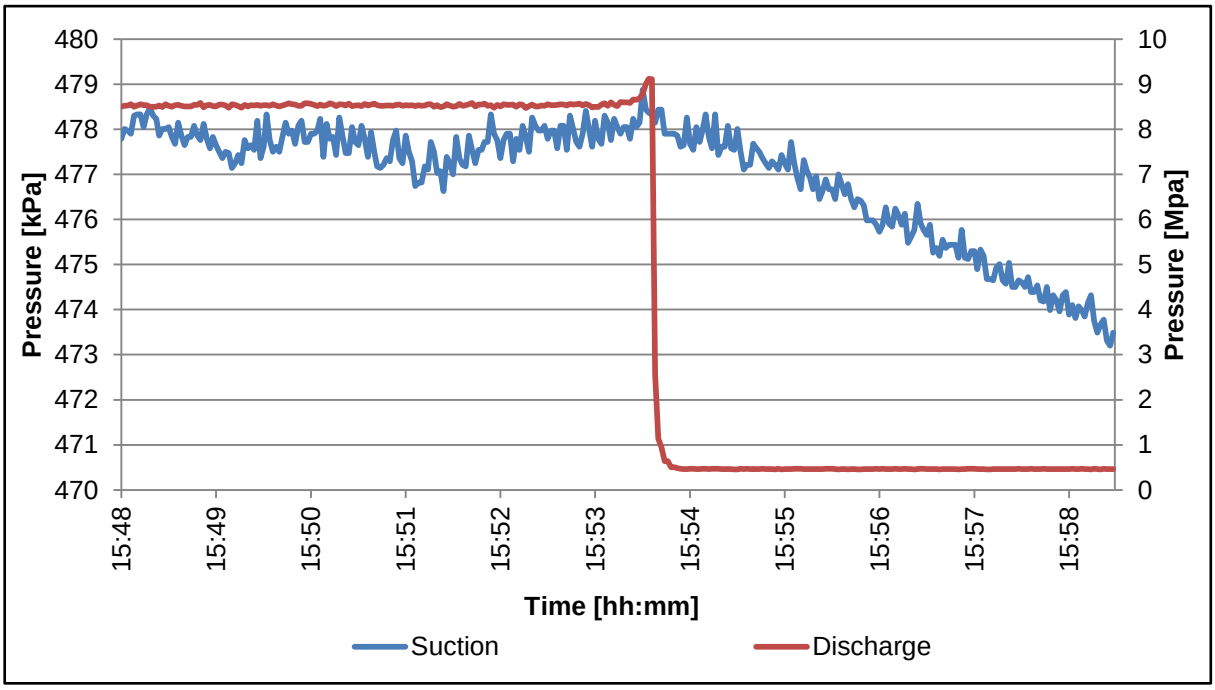

Figure 61: Pump stop sequence suction and discharge pressure

Figure 62 displays the suction, discharge and balance flow temperature during the stop sequence. The temperature is on the vertical axis against the time on the horizontal axis. The balance disc flow temperature decreases when the motor is stopped. The discharge temperature remains constant. The suction temperature starts to increase when the valve reaches 5% open.

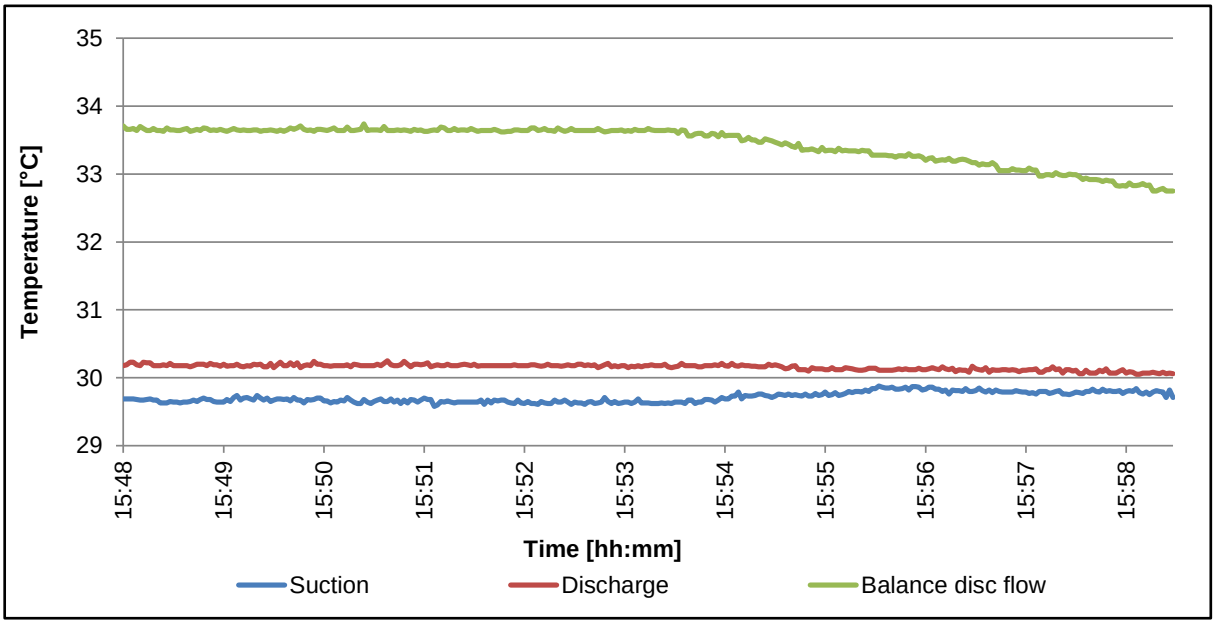

Figure 62: Pump stop sequence suction, discharge and balance disc flow temperatures

Figure 63 displays the suction temperature and valve position during the stop sequence. The temperature and discharge valve open percentage are on the vertical axes and the time on the horizontal axis.

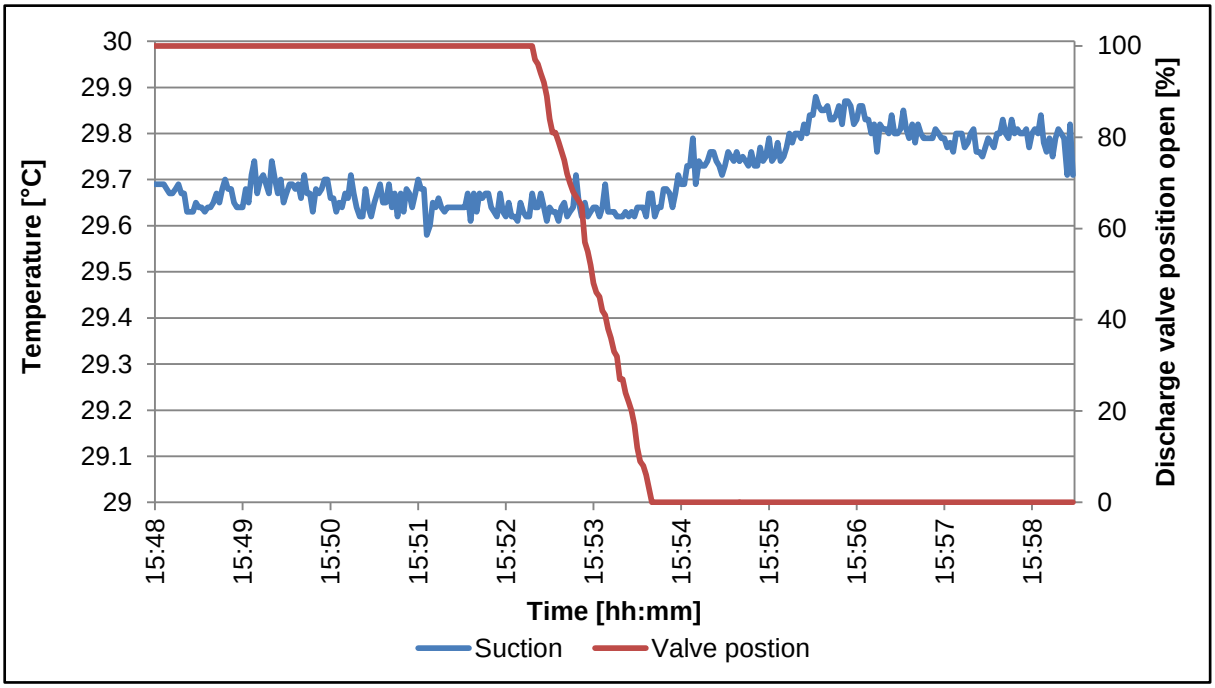

Figure 63: Pump stop sequence suction temperature

The suction temperature increases when the discharge valve closes. This is due to the low flow through the pump. If the pump continues to run with low flow, this temperature will increase until the trip temperature is reached. The PLC will then initiate the trip sequence, protecting the pump from failing from overheating and cavitation.

4.4. Real-time pump control results

The results of the pump statuses were used to determine if the real-time pump scheduling performed a load shift successfully. The pump schedule, different control philosophies and interlocks results are examined.

4.4.1. 3-CPFS incorporation

Figure 64 displays the pump and pause status of the 3-CPFS. The alteration between the statuses is due to the chilled water available on surface. The 3-CPFS statuses have a direct impact on the control philosophy of IPCM.

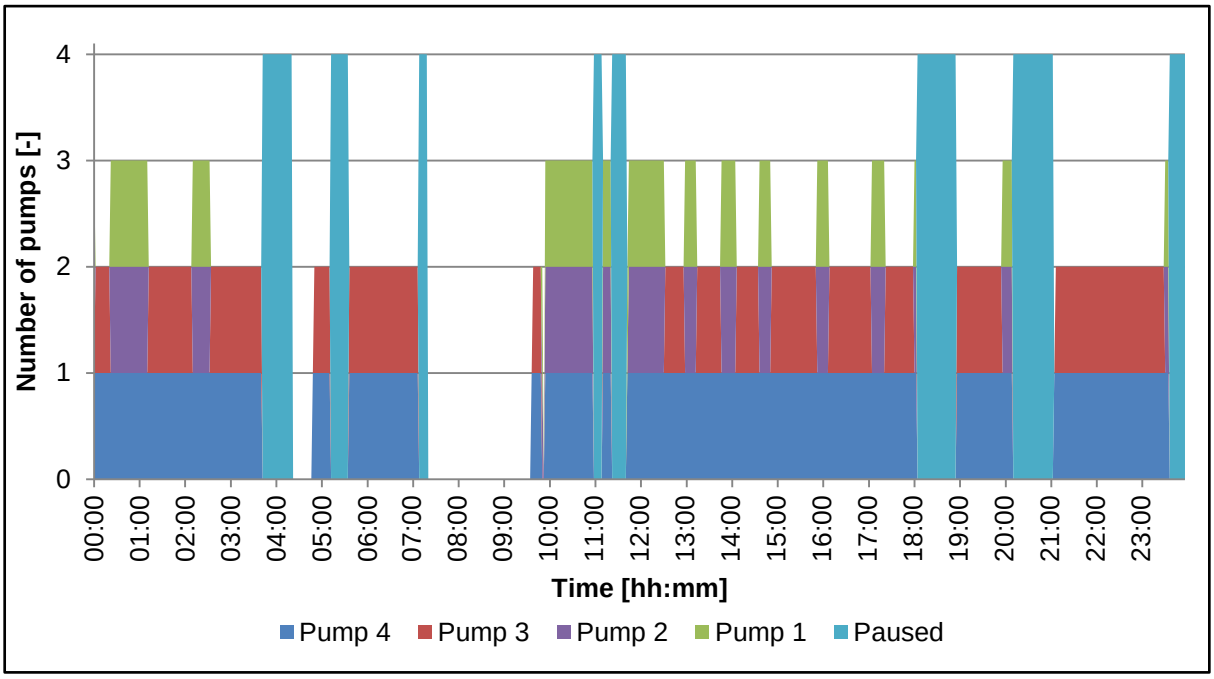

Figure 64: 3-CPFS pump and pause status 24 hour profile

The transition periods between the statuses often result in an off status for the 3-CPFS. A hold tag was used to prevent the control philosophy of IPCM to change. Figure 65 displays the hold tag results. The returned hold status is used to determine if the 3-CPFS is operated.

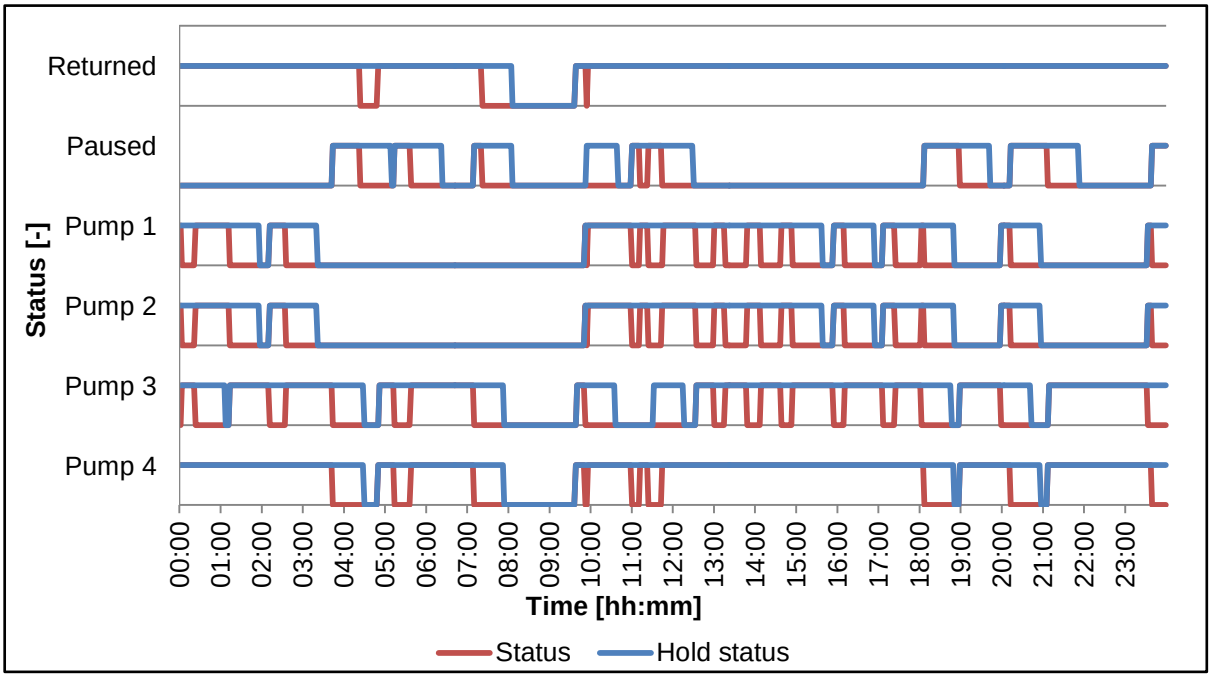

Figure 65: 3-CPFS pump, pause, hold and return status 24 hour profile

It is clear at 4:30 and 9:30 that the hold tag prevented IPCM to alter the control philosophy when an off status was received from the 3-CPFS. At 8:00 the 3-CPFS was off for a long

enough period to change the control philosophy. The hold tag was found functional for this purpose.

4.4.2. Pump chamber control

The different control philosophies of each pump chamber resulted in different pump schedules. The control philosophies incorporated the minimum and maximum dam levels for each pump chamber. The pump offsets ensured that the dam levels were controlled within the limits and to create enough dam capacity to perform a load shift.

Figure 66 displays the schedule, maximum number of pumps and dam level of IPCM. The maximum number of pumps was limited according to the control philosophy when the hold running status was received. From 8:00 to 9:40 when the hold status was off, the scheduler could have scheduled the maximum number of pumps if required.

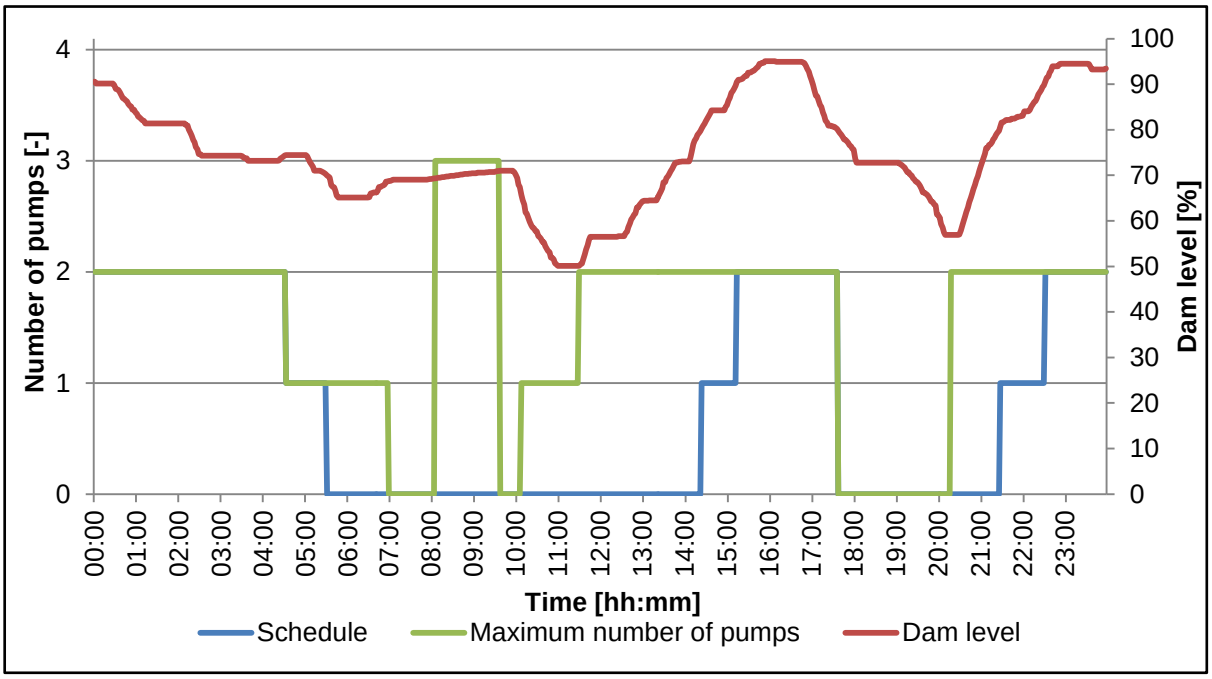

Figure 66: IPCM schedule, maximum number of pumps and dam level 24 hour profile

To ensure the maximum potential of the 3-CPFS is harvested, the maximum number of pumps is limited to the number of pumps running on Level-22 when the 3-CPFS is running. This is to prevent the pumps from draining the dam and limit of the 3-CPFS. This is seen at 4:30, 7:00, 10:00, 11:30 and 20:20. At 17:00 the number of pumps was zero on Level-22, but the schedule of IPCM continued at two until the 15% bottom stable of IPCM was less than 95%, actually 80%. This is an additional safety measure to ensure the dam levels are controlled within safe limits.

Figure 67 displays the schedule, maximum number of pumps and dam level of Level-22. According to the control philosophy, the maximum number of pumps must be limited when the 15% bottom stable value of IPCM exceeds 90% to prevent flooding. This is shown from 0:00 to 2:30, 15:15 to 18:00 and 22:30 to 24:00. The maximum number of pumps is increased when the stable value is less than 90%, resulting that the actual dam level has to be less than 75%.

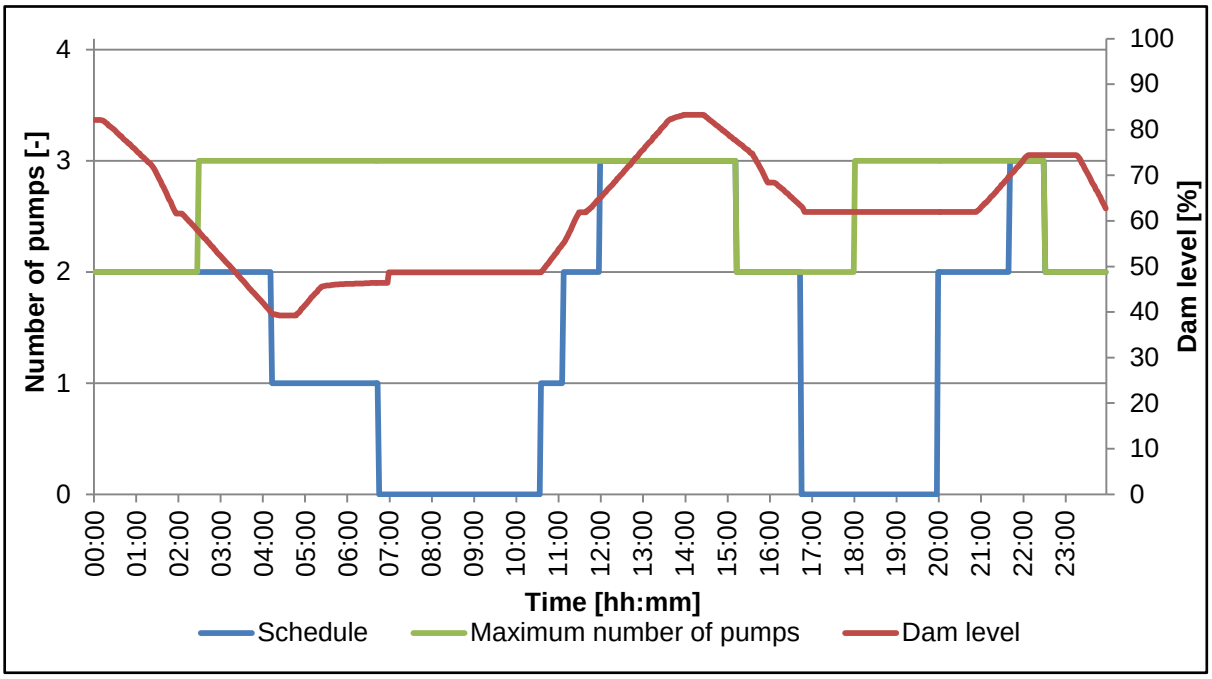

Figure 67: Level-22 schedule, maximum number of pumps and dam level 24 hour profile

The schedule, maximum number of pumps and dam level of IPCS main are displayed in Figure 68. A load shift was still possible with only 40% of the dam capacity available in which to control. This was achievable because the only inflow was from the pumps of Level-46. If the pumps on Level-46 were off, the dam level remained constant.

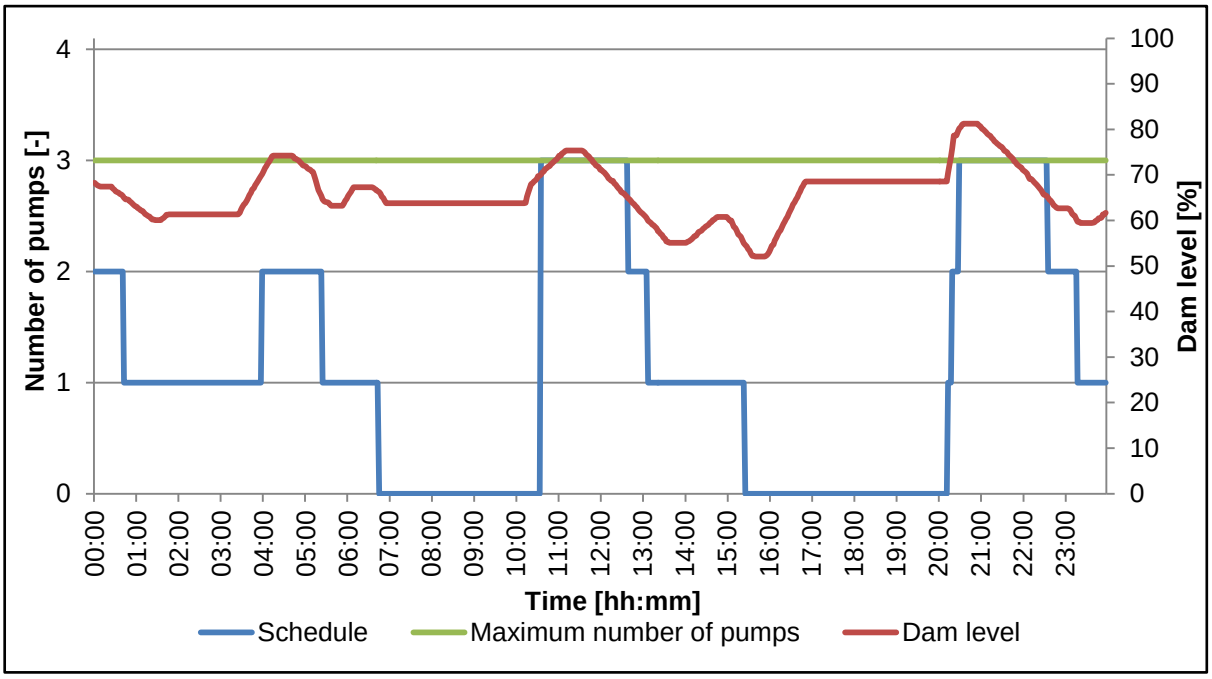

Figure 68: IPCS schedule, maximum number of pumps and dam level 24 hour profile

Figure 69 displays the schedule, maximum number of pumps and dam level of Level-46. The maximum available dam capacity is required before the peak periods to accommodate the inflow from the settlers. The control philosophy made it possible to stop all the pumps in both peak periods.

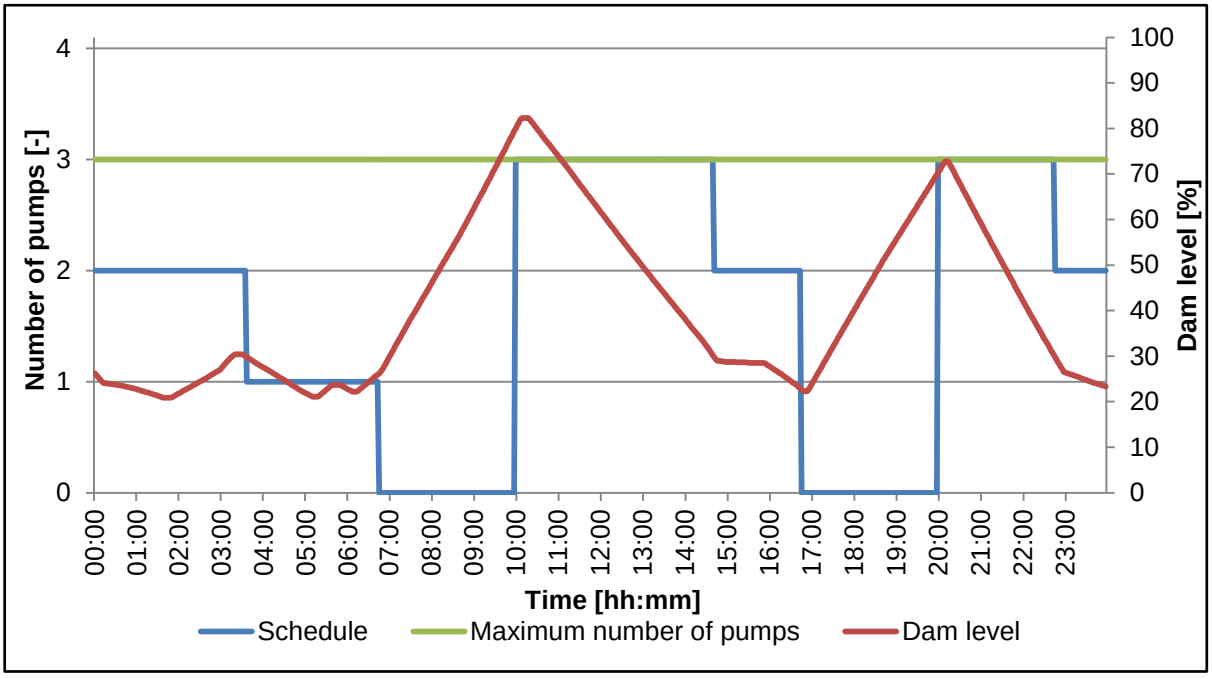

Figure 69: Level-46 schedule, maximum number of pumps and dam level 24 hour profile

4.4.3. Electricity cost savings

The results of pump schedules for a 24-hour profiles illustrated that each level control philosophies made load shifting possible. The electricity consumption of all the pumps have to be included in the electricity cost saving calculation.

A baseline of the pump power was established before the project was implemented. This was used to determine the amount of load shifted out of the peak period. The baseline was determined from a three month period to ensure it was an accurate reflection of the pump power consumption.

A load shift project is energy neutral. This implies that the total power consumption of the measured profile and the baseline have to be equal. Due to the daily variation in the amount of water pumped, the baseline has to be scaled according to the total power consumed per day. Figure 70 displays the total power consumption for the same day as the schedule graphs, baseline and the scaled baseline for the relevant day.

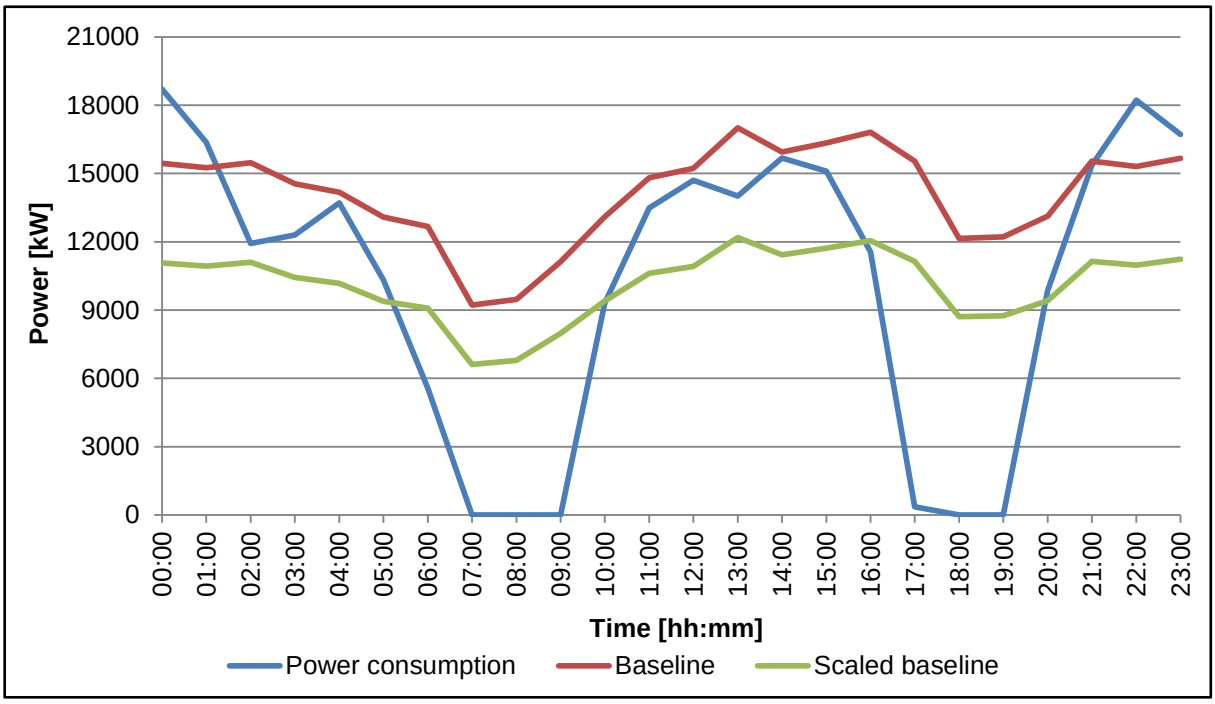

Figure 70: Total power consumption of pumps, baseline and scaled baseline

The daily electricity cost saving is calculated from the hourly difference between the actual power consumption and the scaled baseline. This difference is then multiplied by the ToU electricity price structure. Table 13 displays the values of the total power, baseline, scaled baseline, ToU electricity tariff structure for summer and winter weekday and the total electricity cost savings. The tariff is determined according to the 2014/2015 Megaflex tariff in

a transmission zone smaller than 300 km and an incomer voltage between 500 V and 66 kV [29].

Table 13: Daily electricity cost saving achieved

Time	Total power [kW]	Scaled baseline [kW]	Weekday winter tariff [c/kWh]	Weekday winter cost saving [R]	Weekday summer tariff [c/kWh]	Weekday summer cost [R]
00:00	18 701	11 071	35.77	-2 729	30.97	-2 363
01:00	16 365	10 935	35.77	-1 942	30.97	-1 682
02:00	11 924	11 100	35.77	-295	30.97	-255
03:00	12 303	10 433	35.77	-669	30.97	-579
04:00	13 705	10 168	35.77	-1 265	30.97	-1 095
05:00	10 326	9 379	35.77	-339	30.97	-293
06:00	5 556	9 085	65.87	2 325	49.92	1 762
07:00	0	6 611	217.44	14 376	72.34	4 783
08:00	0	6 791	217.44	14 765	72.34	4 912
09:00	0	7 981	217.44	17 354	72.34	5 773
10:00	9 306	9 394	65.87	58	49.92	44
11:00	13 487	10 620	65.87	-1 889	49.92	-1 432
12:00	14 706	10 914	65.87	-2 498	49.92	-1 893
13:00	14 009	12 190	65.87	-1 198	49.92	-908
14:00	15 676	11 430	65.87	-2 797	49.92	-2 120
15:00	15 104	11 724	65.87	-2 227	49.92	-1 687
16:00	11 555	12 054	65.87	329	49.92	249
17:00	354	11 143	65.87	7 107	49.92	5 386
18:00	0	8 705	217.44	18 928	72.34	6 297
19:00	0	8 755	217.44	19 038	49.92	4 371
20:00	9 866	9 408	65.87	-302	49.92	-229
21:00	15 370	11 143	35.77	-1 512	30.97	-1 309
22:00	18 220	10 978	35.77	-2 591	30.97	-2 243
23:00	16 717	11 236	35.77	-1 960	30.97	-1 697
Total	**243 249**	**243 249**		**70 068**		**13 792**

The current optimised control has a daily electricity cost saving on a typical winter weekday of R 70 000 and on a summer weekday approximately R 13 800. The ToU tariff structure does not have a peak period on weekends or public holidays. The total annual savings for the project is only determined from the total cost savings of weekdays. The year 2014 has a total of 186 summer weekdays and 64 winter weekdays. The annual estimated electricity cost saving in 2014 can reach R 7-million.

The actual savings achieved for the project for the year 2014 is displayed in Table 14. The minimum saving achieved was used for the outstanding months of the year. The control schedule was only followed from February. The total electricity cost saving for the year 2014 achieved and predicted at about R 6-million.

Table 14: Savings achieved and minimum saving predicted in 2014

Month in 2014	Electricity cost saving [R]	Load shifted from peak period [MW]
January	0	0.00
February	233 951	8.05
March	279 248	8.49
April	252 709	8.04
May	224 687	5.86
June	1 241 916	7.12
July	1 340 384	6.18
August	1 451 128	7.79
September (Minimum saving achieved)	224 687	5.86
October (Minimum saving achieved)	224 687	5.86
November (Minimum saving achieved)	224 687	5.86
December (Minimum saving achieved)	224 687	5.86
Total	**5 922 711**	

The estimated electricity cost savings reached 85% of the maximum savings. Bearing in mind that the projected savings were set to the minimum and in January no load shift was performed. The average load shifted from the peak period was 6.82 MW, and the target for the project was 5.58 MW.

4.5. Real-time efficiency results

The real-time pump efficiency results of the pump were found to be higher than the maximum efficiency the pump manufacturers specify. A daily running average efficiency of 84.06% was calculated when observing an individual pump. The maximum efficiency for a multistage centrifugal pump is 83%. Figure 71 displays the 24-hour profile for the efficiency of a pump using Equation 3.14 and the installed instrumentation.

The efficiency can only be calculated when the pump is running. Zero efficiency was returned when the pump was off. It is evident from the graph that an efficiency of 84% is returned from the equation.

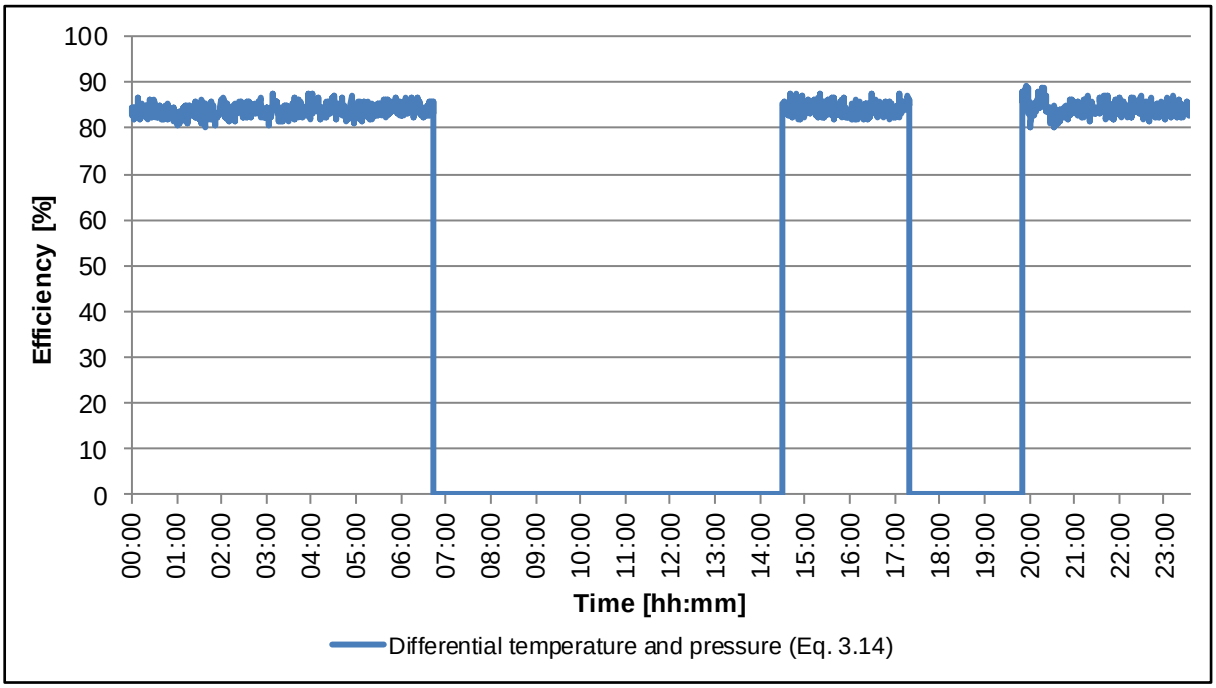

Figure 71: Pump efficiency calculated with differential temperature and pressure

The unrealistic efficiency obtained from the differential temperature led to an investigation. The system was designed for two pumps to transfer water in one column. Each of the dewatering columns had a flow meter installed. This resulted that Equation 3.13 could be used to verify the efficiency results obtained. The static head was known, the flow could be used when only one pump per column was running and the power was measured. Figure 72 displays the pump efficiency verified with the static head, flow and power efficiency.

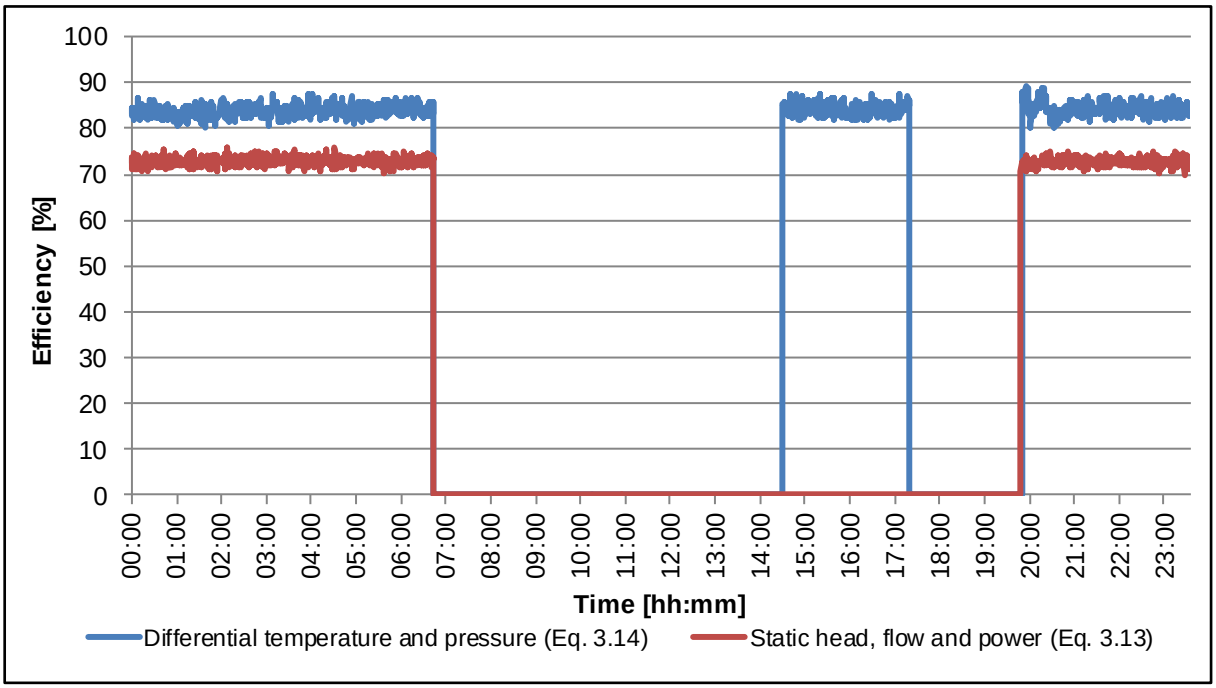

Figure 72: Pump efficiency verified with static head, flow and power efficiency

Similar to Figure 71, zero efficiency was returned when the pump was not running. Zero efficiency was also returned during the period from 14:30 to 17:15. The second pump in the same column was also operated in this period. This resulted in that the flow of the pump could not be obtained. The average daily efficiency of the static head, flow and power is 72.81%.

The static head in the previous efficiency calculation is used to determine the pressure of the fluid required. This enabled verification of installed pressure sensors. The static head pressure can be substituted with the measured pressure in Equation 3.13. Figure 73 displays the efficiency determined from the pressure sensors, flow and power.

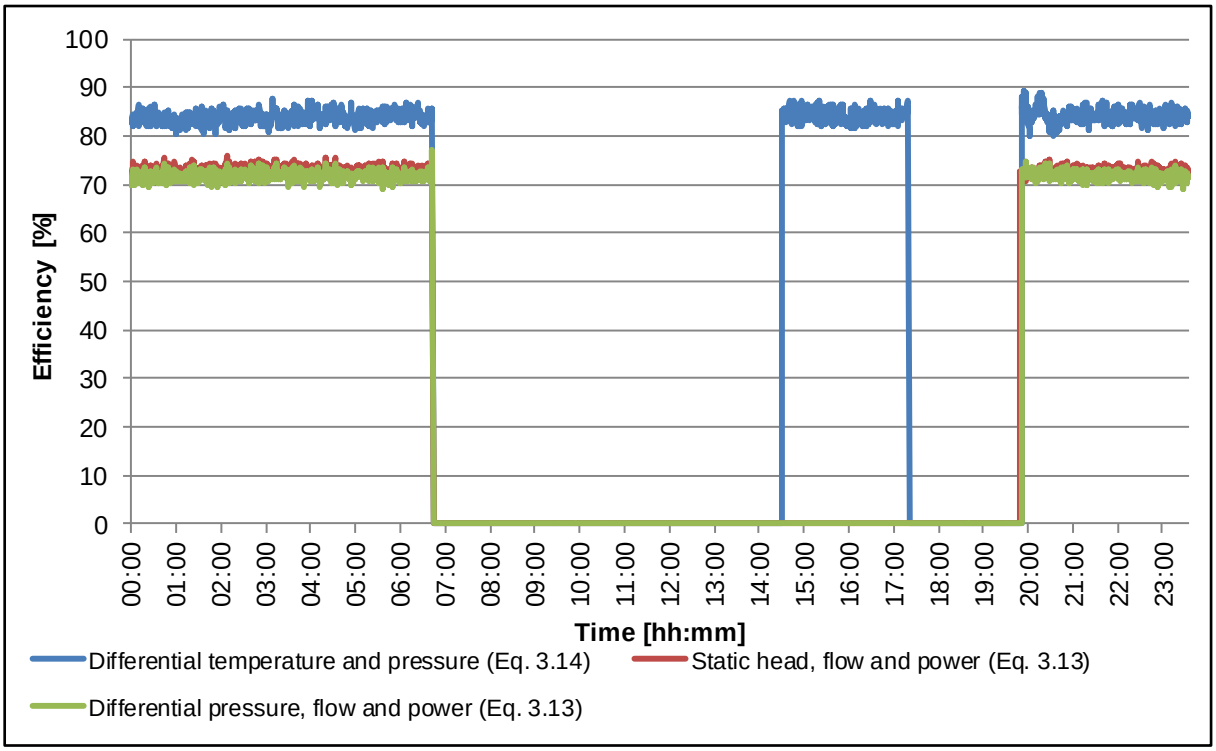

Figure 73: Pressure sensors verified with pump efficiency

It is clear that the data received from the pressure sensors were correct if compared to the static head. The average daily efficiency using the differential pressure, flow and power is 71.82%. The difference between the static head and pressure sensor results is 1.01%.

The last method to verify the efficiency results was to use the result of the current installed efficiency system. The efficiencies of the pumps were reported on a monthly basis. The efficiency of the specific pump was 74%. Figure 74 displays the efficiencies verified with the installed system efficiency compared to the other efficiency results.

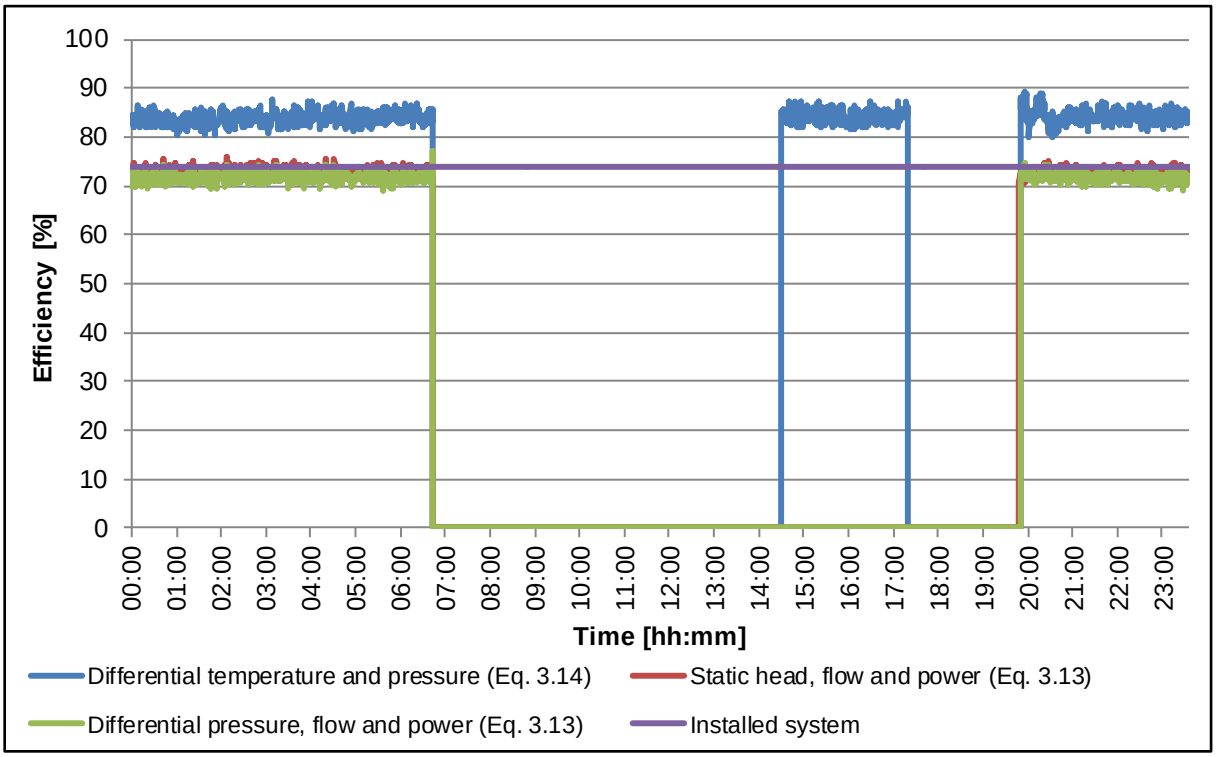

Figure 74: Pump efficiency verified with the installed system

The efficiency calculated with Equation 3.14 is a function of the differential temperature, pressure and the thermodynamic properties. From Figures 72 to 74 it is evident that the pressure sensors are correct. The thermodynamic properties are determined from a thermodynamic table. This leaves the differential temperature to be the only parameter being incorrect.

The specification sheets from the manufacturers show that a 3-wire PT1000 temperature probe has a tolerance of ±(0.30+0.005 |t|); |t| is the measured temperature [89]. The operating temperature of the temperature probes range from 26°C to 30°C. The average tolerance that can be expected is 0.44°C per temperature probe.

It was determined that a value of 0.31546°C must be added to the differential temperature in Equation 3.14 to give the same daily average of 74.0%. This adjustment is within the tolerance of the installed temperature probes. The results of the adjusted temperature are shown in Figure 75.

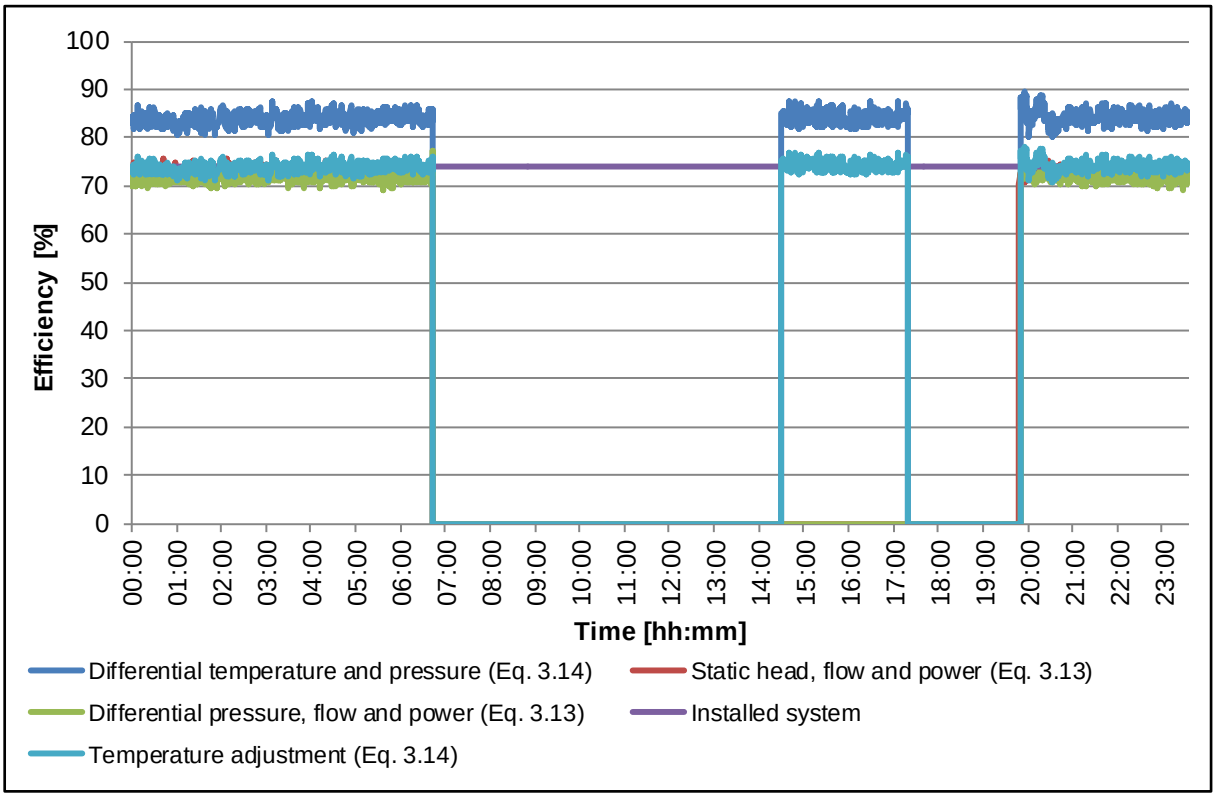

Figure 75: Pump efficiency with temperature adjustment

It is evident from Figure 75 that the temperature adjustment corrects the efficiency to the correct value when the pump is running. Calculating the efficiency with Equation 3.14 also gives the advantage to calculate the efficiency even when more than one pump is operated in the same column.

Temperature adjusted pump efficiencies

The tolerances of each temperature probe are different. This results in the temperatures of all the pumps having to be calculated individually. The daily adjustment of the pumps was calculated for a one work week test period. Pump 1 on IPCM discharge pressure sensor was not operational, pump 4 on IPCM did not run, and pump 1 to 3 on Level-46 had a communication failure during the test period. The temperature adjustments for the pumps during the test period are displayed in Figure 76.

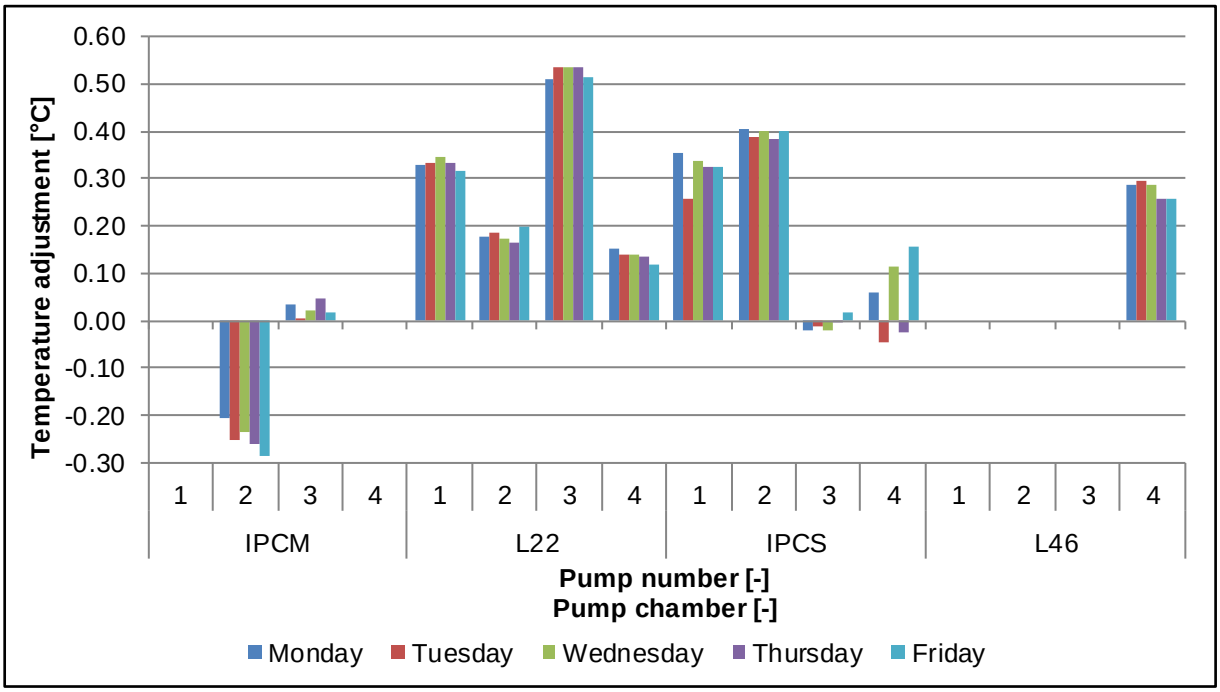

Figure 76: Daily temperature adjustments for the efficiencies

The installed temperature probes have a specified tolerance of ±0.44°C. This implies that the maximum temperature adjustment can be up to 0.88°C. The maximum is possible if the suction temperature probe is -0.44°C and the discharge temperature probe is +0.44°C. The temperature adjustments in Figure 76 are within the maximum tolerance of the temperature probes.

The temperature adjustment was set to the average of the adjusted temperature during the test period. The results of the temperature adjusted efficiencies are displayed in Table 15.

Table 15: Temperature adjusted pump efficiency results

Pump chamber	Pump number	Installed system efficiency [%]	Eq. 3.14 efficiency [%]	Temperature adjustment [°C]	Eq. 3.14 temperature adjusted efficiency [%]	Deviation between installed and adjusted efficiency
IPCM	1	79.00	Discharge pressure sensor failure.			
	2	74.00	67.78	-0.25	73.12	0.88
	3	72.00	72.39	0.02	71.82	0.18
	4	70.00	Pump not operated during test period.			
Level-22	1	74.00	84.07	0.33	73.56	0.44
	2	66.00	70.59	0.18	66.37	-0.37
	3	69.00	84.38	0.53	68.71	0.29
	4	71.00	74.16	0.14	70.48	0.52

Table 15 (continue): Temperature adjusted pump efficiency results

Pump chamber	Pump number	Installed system efficiency [%]	Eq. 3.14 efficiency [%]	Temperature adjustment [°C]	Eq. 3.14 temperature adjusted efficiency [%]	Deviation between installed and adjusted efficiency
IPCS	1	74.00	84.62	0.32	74.12	-0.12
	2	70.00	81.77	0.40	70.13	-0.13
	3	77.00	77.50	-0.01	77.76	-0.76
	4	72.00	76.54	0.05	74.99	-2.99
Level-46	1	61.00	Communication failure.			
	2	70.00	Communication failure.			
	3	77.00	Communication failure.			
	4	70.00	77.10	0.28	69.50	0.50

The maximum deviation between the installed system and the temperature adjusted efficiency is 2.99. The temperature adjustment of the pump in question fluctuated the most in Figure 76. The temperature probes of the specific pump have to be investigated.

The other pumps have a maximum deviation of 0.88. Efficiencies of pumps are used as a trend line over a period of time. When a minimum limit is reached or a sudden large depreciation in the efficiency is present, the pump must be refurbished or replace. The deviation of 0.88 is in an acceptable range.

4.6. Summary

The data of the installed instrumentation is analysed in this chapter. It is clear that the installed instrumentation will prevent failure of the pump in normal operating conditions.

The similar failure conditions could not be repeated due to the risk involved. A low flow scenario was represented when the pump was stopped. The valve closed to 5% when the pump motor was stopped. This allowed for testing of the additional instrumentation. It was evident that the suction temperature probe would detect the temperature increase due to the low flow. The installed instrumentation did not show a condition to trip the pump.

The results of the control philosophy of the pumps showed a noticeable electricity cost saving. The savings achieved and projected for 2014 was R 6-million. This was achieved through optimising the control schedule of the pump. The pump load in the expensive peak periods was reduced. This was achieved through preparing the dam correctly in the less expensive off-peak and standard periods.

The pump efficiencies were calculated with the additional temperature probes installed. This allowed calculating the efficiencies of each individual pump in real-time. The efficiencies were calculated incorrectly. Using the output power over the input power and the installed system the efficiencies could be verified. The temperature sensors were found to be correct. The efficiencies were then adjusted with the temperature to ensure the efficiencies were calculated correctly.

Chapter 5: Conclusion, recommendations and research opportunities

In this chapter a conclusion on the results obtained is made. The results also make it possible to suggest alterations to the project. From this study several opportunities for further studies are identified. These opportunities are also discussed in this chapter.

5.1. Conclusion

This study focused on the automation and control of mine dewatering systems. A case study was presented on a project done on a pump dewatering system of the mine. During implementation a pump failed after it had been automated and commissioned. The automation of the pump was investigated to protect pumps from failing in similar operating conditions.

From the literature study it is explained which condition of a pump must be monitored to prevent failure. The instrumentation according to the current best practice was found mandatory for pump automation. This can be seen from the results of the installed instrumentation displayed for a daily operating profile. It is evident from the operating profiles that the installed instrumentation will prevent failure from the conditions they were intended to monitor.

The connection between the shoeblock and the discharge valve failed during the start-up sequence. This resulted in a period of low flow which caused a temperature increase and cavitation in the pump. The installed instrumentation was not able to detect the abnormal operating conditions.

The failure of the automated pump proved additional precautions must be taken to prevent similar failure. The intricate investigation of the pump failure made it possible to identify the root cause of failure. This made it possible to make the following improvements to the current best practice:

1. Equalising differential pressure across the discharge valve through opening it to 10% every 30 minutes when the pump is not running.
2. Redesigning the shoeblock connection to increase the force it can transfer.
3. Additional temperature probes were installed to measure the temperature increase of the water across the pump.
4. Setting of an under torque limit on the actuator to ensure the gate is opening.
5. Locking the flow switch to prevent unauthorised personnel from lowering the trip limit.

The control of the automated dewatering system proved to be feasible. Informed control decisions could be made through interlocking all the control parameters from a centralised system. This was made possible with the automation of the pumps and including the dam levels and 3-CPFS status. The pump control graphs illustrate the dam levels remained in the safe specified ranges.

The total electricity cost saving for the year 2014 achieved and predicted is R 6-million through minimising pumping in the peak periods. This is more than half of the total automation cost. This proves that in a period of two years the initial automation cost will have been repaid with savings from electricity usage. The control also included the running status of the installed 3-CPFS. This ensures that the maximum potential of the 3-CPFS is harvested and the pump load is shifted safely.

The savings were calculated, using the pump running status only. Additional savings were achieved with the 3-CPFS that was not included in these savings. The control of the dam schedules ensured that the operation 3-CPFS was increased. The dam levels were prepared correctly to ensure the maximum potential of the 3-CPFS was realised.

The installed instrumentation did make it possible to calculate the pump efficiencies. The suction and discharge pressure sensors were used to determine the total head each pump developed. The additional suction and discharge temperature probes were used to determine the temperature increase across the pump. A formula found in the literature derived from Thermodynamic principles was used to calculate the efficiency. The increase of temperature is an indication of efficiency losses.

This allowed calculating the efficiency of each individual pump when it was operated. The efficiencies were verified by comparing the power input with the power output and the current installed efficiency system. The temperature was adjusted and the efficiencies were within 5% of the verified efficiencies.

Three aspects of the dewatering system were investigated in this study. All three were proved to be successful within an acceptable range. Additional instrumentation was added according to the best practice to automate a pump system to improve the reliability. This allowed for safe control from the surface to realise electricity cost savings.

5.2. Recommendations

It is recommended that automated pumps must include the best practice instrumentation as discussed in this study. The conditions they monitored must be interlocked according to the manufacturer. If the operating conditions are less, the limits can be reduced to initiate the stop sequence at an earlier stage.

The pressure across the discharge valve must be equalised when there is a possibility for a differential pressure. This will prevent the pressure from holding the gate in the closed position resulting in additional forces to be applied. The pressure equalising can be easily performed through altering the control software.

Refurbishment of equipment is usually less expensive than replacing it with new equipment. When equipment is refurbished, it is recommended to ensure it meets the original design specifications. If the specifications are not met, design improvements must be made. It is also recommended to improve the connection, between the shoeblock and spindle, of refurbished gate valves to prevent failure.

The additional temperature probes to measure the temperature increase across the pump is recommended for pump automation. The redundancy of the automation is increased from protecting the pump against low flow. This is achieved when multiple instruments monitor the same condition. If one of the instruments fails, the other one will still initiate the trip sequence.

All involved personnel must approve and document the limits and control ranges of the instrumentation. These limits and control ranges must be verified and locked during commissioning. Only authorised personnel should be able to change the limits to ensure safe operation of the pumps.

It is recommended to control an automated dewatering system from a centralised system. All the required data for the systems involved must be displayed or be available. This allows the operator or system to make an informed control decision from an overview of the entire system. It is possible to achieve noticeable electricity cost savings if a ToU tariff structure is used for electricity.

Real-time pump efficiency can be determined from the head developed and temperature rise across the pump. This can assist in calculating the efficiencies of pumps sharing a common column with only one flow meter.

5.3. Research opportunities

The improved control schedule of the dewatering system results in increased switching of the pump. This increases the maintenance cost of the pumps. It is also suspected that the increased switching will increase the rate at which the pump efficiencies deteriorate. The real-time efficiency calculation allows for the opportunity to examine the effect the switching of pumps has on the pump efficiencies.

The pumps were scheduled to run the most efficient pumps during the peak and standard periods first. The least efficient pumps would start first during the off-peak periods. This can realise an additional electricity cost saving. The additional electricity cost saving from prioritising the pumps according to their efficiencies can be verified.

Bibliography

[1] S. Walker, “The pump-makers' perpective,” *Engineering & Mining Journal,* vol. 214, no. 11, pp. 50-54, November 2013.

[2] W. Schoeman, “The integrated effect of DSM on mine chilled water systems,” M.Eng dissertation, North-West University, Potchefstroom, 2014.

[3] X. Zhang, L. Gao, D. Barrett and Y. Chen, “Evaluating water management practice for sustainable mining,” *Water,* vol. 6, no. 2, pp. 414-433, February 2014.

[4] S. Thein, “Demand side management on an intricate multi-shaft pumping system from a single point of control,” M.Eng dissertation, North-West University, Potchefstroom, 2007.

[5] R. W. Gaikwad, “Review and research needs of active treatment of acid mine drainage by ion exchange,” *Electronic Journal of Environmental, Agricultural and Food Chemistry,* vol. 9, no. 8, pp. 1343-1350, 2010.

[6] K. Farhadi, A. Bousbia-salah and F. D'Auria, “A model for the analysis of pump start-up transients in Tehran Research Reactor,” *Progress in Nuclear Energy,* vol. 49, no. 7, pp. 499-510, September 2007.

[7] D. Stephenson, “Distribution of water in deep gold mines,” *International Journal of Mine Water,* vol. 2, no. 2, pp. 21-30, 1983.

[8] D. A. J. Ross-Watt, “Presidential address: mining engineering - a discipline for the future,” *Journal of the South African Institute of Mining and Metallurgy,* vol. 95, no. 6, pp. 241-268, 1995.

[9] A. Prinsloo, “Energy cost optimisation of a complex mine pumping system,” M.Eng dissertation, North-West University, Potchefstroom, 2004.

[10] R. W. Wilson and A. Pieters, “Design and construction of a surface air cooling and refrigeration installation at a South African mine,” in *12th US/North American mine ventilation symposium*, Reno, 2008.

[11] D. J. Stanton, “Development and testing of an underground remote refrigeration plant,” M.Eng dissertation, North-West University, Potchefstroom, 2003.

[12] J. Van der Walt and A. Whillier, “Considerations in the design of integrated systems for distributing refrigeration in deep mines,” *Journal of the South African Institute of Mining and Metallurgy,* vol. 94, no. 3, pp. 109-124, 1994.

[13] M. Biffi and D. J. Stanton, “Cooling power for a new age,” in *Third International Conference "Platinum in Transformation"*, Rustenburg, 2008.

[14] A. Botha, “Optimising the demand of a mine water reticulation system to reduce electricity consumption,” M.Eng dissertation, North-West University, Potchefstroom, 2010.

[15] J. N. de la Vergne, “Explosives and drilling,” in *The Hard Rock Miner's Handbook*, North Bay, McIntosh Engineering, 2003, pp. 209-214.

[16] J. Vosloo, L. Liebenberg and D. Velleman, “Energy savings for a deep-mine water reticulation system,” *Applied Energy,* vol. 92, pp. 328-335, April 2012.

[17] G. Van den Berg and R. Cooke, “Hydraulic hoisting technology for platinum mines,” *Journal of the South African Institute of Mining and Metallurgy,* vol. 105, no. 5, pp. 323-332, 2010.

[18] J. N. de la Vergne, “Mine dewatering,” in *The Hard Rock Miner's Handbook*, North Bay, McIntosh Engineering, 2003, pp. 187-200.

[19] C. Cilliers, “Cost savings on mine dewatering pumps by reducing preparation- and comback loads,” M.Eng dissertation, North-West University, Potchefstroom, 2014.

[20] J. Hall, “Process pump control,” *Chemical Engineering,* vol. 117, no. 12, pp. 30-33, November 2010.

[21] B. Jafarzadeh, A. Hajari, M. M. Alishahi and M. H. Akbari, “The flow simulation of a low-specific-speed high-speed centrifugal pump,” *Applied Mathematical Modelling,* vol. 35, no. 1, pp. 242-249, 2011.

[22] E. Brito, “Making pump maintenance mandatory,” *Chemical Engineering,* vol. 118, no. 10, pp. 48-53, October 2011.

[23] S. Perju and L. V. Hasegan, “Reducing energy consumption by upgrading pumping stations in water distribution systems,” *Environmentral Engineering & Management Journal,* vol. 12, no. 4, pp. 735-740, April 2013.

[24] J. C. Vosloo, J. Van Rensburg and A. Botha, “Optimising the demand of a mine water reticulation system to reduce electricy consumption,” in *Industrial and Commercial Use of Energy (ICUE) conference*, Cape Town, 2010.

[25] H. J. Van Antwerpen and G. P. Greyvenstein, “Use of turbines for simultaneous pressure regulation and recovery in secondary cooling water systems in deep mines,” *Energy Conversion and Management,* vol. 46, no. 4, pp. 563-575, 2005.

[26] P. Fraser and D. Le Roux, “Three-chamber pump system for DSM,” *Energize,* vol. 19, no. 9, pp. 51-54, 2007.

[27] W. Rautenbach, D. L. Krueger and E. H. Matthews, “Reducing the electricity cost of a three-pipe water pumping system - a case study using software,” *Journal of Energy in Southern Africa,* vol. 16, no. 4, pp. 41-47, 2005.

[28] S. Yadav, “Some aspects of performance improvement of Pelton wheel turbine with reengineered blade and auxiliary,” *International Journal of Science and Engineering Research,* vol. 2, no. 9, pp. 2-5, 2011.

[29] Eskom, “Tariff & Charges Booklet,” Eskom, Johannesburg, 2014/15.

[30] B. Barán, C. Von Lücken and A. Sotelo, “Multi-Objective pump scheduling optimisation using evolutionary strategies,” *Advances in Engineering Software,* vol. 36, no. 1, pp. 39-47, 2005.

[31] Y. Tang, G. Zheng and S. Zhang, “Optimal control approaches of pumping station to achieve efficiency and load shifting,” *International Journal of Electrical Power & Energy Systems,* vol. 55, pp. 572-580, 2014.

[32] X. Zhuan and X. Xia, “Optimal operation scheduling of a pumping station with multiple pumps,” *Applied Energy,* vol. 104, pp. 250-257, 2013.

[33] J. LePree, “Pump it up,” *Chemical Engineering,* vol. 118, no. 2, pp. 25-28, June 2011.

[34] R. Pelzer, R. P. Richter, M. Kleingeld and J. Van Rensburg, “Performance comparison between manual and automated DSM pumping projects,” in *Industrial and Commercial Use of Energy (ICUE) conference*, Cape Town, 2009.

[35] I. Kougias and N. Theodossiou, “Multi-objective pump scheduling optimization using harmony search algorithm (HSM) and polyphonic HSA,” *Water Resources Management,* vol. 27, no. 5, pp. 1249-1261, 2013.

[36] J. C. Vosloo, “A new minimum cost model for water reticulation systems on deep mines,” Ph.D thesis, North-West University, Potchefstroom, 2008.

[37] A. Almasi, “Renovation and system upgrades,” *World Pumps,* vol. 2013, no. 1, pp. 16-18, January 2013.

[38] R. Beebe, “Optimize time for overhaul of your pumps using condition monitoring,” *World Pumps,* vol. 2004, no. 452, pp. 24-28, May 2004.

[39] E. Hoop, “Control valves: an evolution in design,” *Chemical Engineering,* pp. 48-51, August 2012.

[40] A. Almasi, “Power plant condition monitoring,” *Power Engineering,* vol. 115, no. 8, pp. 60-63, August 2011.

[41] A. Almasi, “CPI Machinery: commissioning, startup and piping,” *Chemical Engineering,* vol. 119, no. 13, pp. 42-50, December 2012.

[42] A. Almasi, “Condition monitoring for rotating machinery,” *Chemical Engineering,* vol. 119, no. 3, pp. 55-60, March 2012.

[43] S. K. Chatterjee, “Improve rotary equipment reliability with checklists,” *Chemical Engineering,* vol. 120, no. 9, pp. 52-57, September 2013.

[44] S. Shiels, “Optimizing centrifugal pump operation,” *World Pumps,* vol. 2001, no. 412, pp. 35-39, 2001.

[45] A. Almasi, “Practical notes on component failure,” *World Pumps,* vol. 2012, no. 10, pp. 40-43, October 2012.

[46] A. T. Sayers, “Hydraulic pumps,” in *Hyrdaulic and compressible flow turbomachines*, London, McGraw-Hill, 1990, pp. 31-87.

[47] I. Halkijevic, Z. Vukovic and D. Vouk, “Frequency pressure regulation in water supply systems,” *Water Science & Technology: Water Supply,* vol. 13, no. 4, pp. 896-905, 2013.

[48] W. Chaiworapuek, J.-Y. Champagne, M. El Haj em and C. Kittichaikan, “An Investigation of the Water Flow Past the Butterfly Valve,” *AIP Conference Proceedings,* vol. 1225, no. 1, pp. 249-262, June 2010.

[49] B. R. Munson, D. F. Young, T. H. Okiishi and W. W. Heubsch, “Viscous flow in pipe,” in *Fundamentals of fluid mechanics*, John Wiley & Sons, 2010, pp. 383-460.

[50] J. Tonkin, “Reducing costs in parallel pumping,” *World Pumps,* vol. 2012, no. 5, pp. 32-37, May 2012.

[51] S. D. Kyparissis and D. P. Margaris, “Experimental investigation and passive flow control of a cavitating centrifugal pump,” *International Journal of Rotating Machinery,* vol. 2012, pp. 1-8, 2012.

[52] R. Beebe and S. Jankins, “Condition monitoring methods for pumps,” *Chemical Engineering,* vol. 119, no. 9, pp. 34-39, September 2012.

[53] G. Rohlfing, “Condition monitoring of multiphase pumps,” *World Pumps,* vol. 2010, no. 4, pp. 34-39, April 2010.

[54] M. Yates, “Pump performance monitoring complements condition monitoring,” *World Pumps,* vol. 2002, no. 428, pp. 36-38, May 2002.

[55] E. W. Wallace, M. White and G. Parks, “Commissioning and start-ups of new units (pumps),” in *The 25th International Pump Users Symposium*, Houston, 2009.

[56] R. Beebe, “Pump monitoring: unusual incidents,” *World Pumps,* vol. 2010, no. 4, pp. 24-28, April 2010.

[57] A. Budris, “Power precaustions,” *WaterWorld,* vol. 29, no. 8, pp. 10-13, August 2013.

[58] S. Elaoud and E. Hadj-Taïeb, “Influence of pump starting times on transient flows in pipes,” *Nuclear Engineering and Design,* vol. 241, no. 9, pp. 3624-3631, September 2011.

[59] R. Birajdar, R. Patil and K. Khanzode, “Vibration and noise in centrifugal pumps - Sources and diagnosis methods,” in *3rd International Conference on Integrity, Reliability and Failure*, Porto, 2009.

[60] S. K. Chatterjee, “Get the most out of vibration analysis,” *Chemical Engineering,* vol. 118, no. 1, pp. 36-42, January 2011.

[61] A. Almasi, “Practical vibrational monitoring to identify-damaged, cracked and worn components in power plants,” *Power Engineering,* vol. 116, no. 4, pp. 20-26, April 2012.

[62] A. Almasi, “How vibrations can affect condition,” *World Pumps,* vol. 2013, no. 2, pp. 26-27, February 2013.

[63] N. R. Sakthivel, V. Sugumaran and S. Babudevasenapati, “Vibration based fault diagnosis of monoblock centrifugal pump using decision tree,” *Expert Systems with Applications,* vol. 37, no. 6, pp. 4040-4049, June 2010.

[64] M. A. Abu-Zeid and S. M. Abdel-Rahman, “Bearing problems' effects on the dynamic performance of pumping stations,” *Alexandria Engineering Journal,* vol. 52, no. 3, pp. 241-248, 2013.

[65] A. Almasi, “Thermal analysis for temp apps,” *World Pumps,* vol. 2013, no. 5, pp. 30-33, May 2013.

[66] R. Koch, “Remedy to black oil problems in centrifugal pumps with ball bearings,” *Tribology & Lubrication Technology,* vol. 60, no. 6, pp. 51-55, June 2004.

[67] R. Arifulin, I. Kashtanov and N. Antonov, “Shut-off device for well-head equipment,” *Chemical & Petroleum Engineering,* vol. 48, no. 1/2, pp. 35-39, January 2012.

[68] B.-S. Yang, W.-W. Hwang, M.-H. Ko and S.-J. Lee, “Cavitation detection of butterfly valve using support vector machines,” *Journal of Sound and Vibration,* vol. 287, no. 1, pp. 25-43, 2005.

[69] P. Naseradinmousavi and C. Nataraj, “Nonlinear mathematical modeling of butterfly valves driven by solenoid actuators,” *Applied Mathematical Modeling,* vol. 35, no. 5, pp. 2324-2335, 2011.

[70] Fisher Controls International, “Valve and actuator types,” in *Control Valve Handbook*, Marshalltown, Emerson Process Management, 2005, pp. 41-66.

[71] R. Beebe, “Alternative measures,” *Mechanical Engineering,* vol. 133, no. 8, pp. 42-43, August 2011.

[72] M.-J. Chern, P.-H. Hsu, Y.-J. Cheng, P.-Y. Tseng and C.-M. Hu, “Numerical study on cavitation occurrence in globe valve,” *Journal of Energy Engineering,* vol. 139, no. 1, pp. 25-34, March 2013.

[73] B. Nesbitt, “Valve selection for process systems,” *World Pumps,* vol. 425, no. 2, pp. 42-46, 2002.

[74] T. Bishop, M. Chapeaux, L. Jaffer, K. Nair and S. Patel, “Ease control valve selection,” *Chemical Engineering Progress,* vol. 98, no. 11, pp. 52-56, 2002.

[75] V. Ivanov, A. Olienikov, D. Denisevich and B. Pektimirov, “Emergency shut-off valve for pipelines,” *Chemical & Petroleum Engineering,* vol. 49, no. 5/6, pp. 400-402, September 2013.

[76] Q. Zuo, S. Qiu, W. Lu, W. Tian, G. Su and Z. Xiao, “Water hammer characteristics of integral pressurized water reactor primary loop,” *Nuclear Engineering and Design,* vol. 261, pp. 165-173, August 2013.

[77] W. J. Rahmeyer, H. L. Miller and S. V. Sherikar, “Cavitation testing results for a tortuous path control valve,” *ASME - Publications - FED,* vol. 210, pp. 63-68, 1995.

[78] J. Wu, S. Sun and D. Wang, “The new design of globe valve virtual assembly design,” *Advanced Materials Research,* no. 926-930, pp. 1623-1626, 2014.

[79] C. C. Tsai, C. Y. Chang and C. H. Tseng, “Optimal design of metal seated ball valve mechanism,” *Structural and Multidisciplinary Optimization,* vol. 26, no. 3-4, pp. 246-255, 2004.

[80] X. G. Song, L. Wang, S. H. Baek and Y. C. Park, “Multidisciplinary optimization of a butterfly valve,” *ISA Transactions,* vol. 48, no. 3, pp. 370-377, 2009.

[81] X. Song, L. Wang and Y. Park, “Fluid and structural analysis of large butterfly valve,” *AIP Conference Proceedings,* vol. 1052, no. 1, pp. 311-314, July 2008.

[82] J. R. Valdés, J. M. Rodríguez, R. Monge, J. C. Peña and T. Pütz, “Numerical simulation and experimental validation of the cavitating flow throug a ball check valve,” *Energy Conversion and Management,* vol. 78, pp. 776-786, February 2014.

[83] M. Chudina, “Noise as an indicator of cavitation in a centrifugal pump,” *Acoustical Physics,* vol. 49, no. 4, pp. 463-474, July 2003.

[84] M. M. Stopa, F. B. Cardoso and C. B. Martinez, “Incipient detection of cavitation phenomenon in centrifugal pumps,” *IEEE Transactions on Industry Applicatoins,* vol. 50, no. 1, pp. 120-126, January 2014.

[85] D. Wu, L. Wang, Z. Bao, Z. Hao and Z. Li, “Experimental study on hydrodynamic performance of a cavitating centrifugal pump during transient operation,” *Journal of Mechanical Science and Technology,* vol. 24, no. 2, pp. 575-582, February 2010.

[86] A. S. Shapiro, S. S. Panaiotti and A. A. Artem'ev, “Calculation of suction capacity of centrifugal pumps,” *Chemical & Petroleum Engineering,* vol. 43, no. 9/10, pp. 554-562, September 2007.

[87] A. Whillier, “Pump efficiency determination in chemical plant from temperature measurements,” *Industrial & Engineering Chemistry Process Design & Development,* vol. 7, pp. 194-196, April 1968.

[88] Thermodynamics Research Center, NIST Boulder Laboratories and M. Frenkel, “Thermodynamics Source Database,” in *NIST Chemistry WebBook, NIST Standard Reference Database Number 69*, Eds. P.J. Linstrom and W.G. Mallard.

[89] WIKA Alexander Wiegand SE & Co. KG, “WIKA operating instruction resistance thermometers, thermocouples,” WIKA, Klingenberg, 2013.

Appendix A: Original graphs from literature study

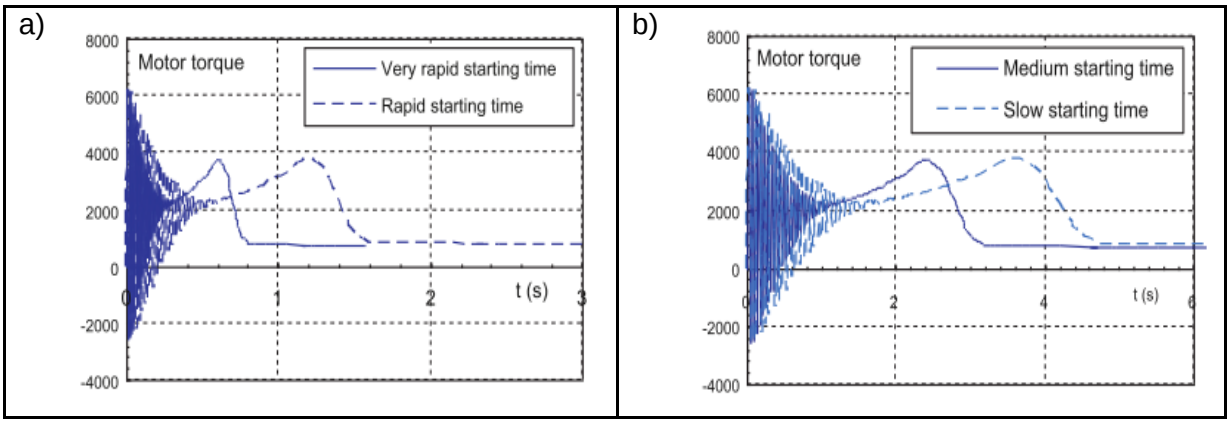

Figure A-1: Pump starting torque graphs: a) Very rapid and rapid; and b) Medium and slow. Combined in Figure 11 [58]

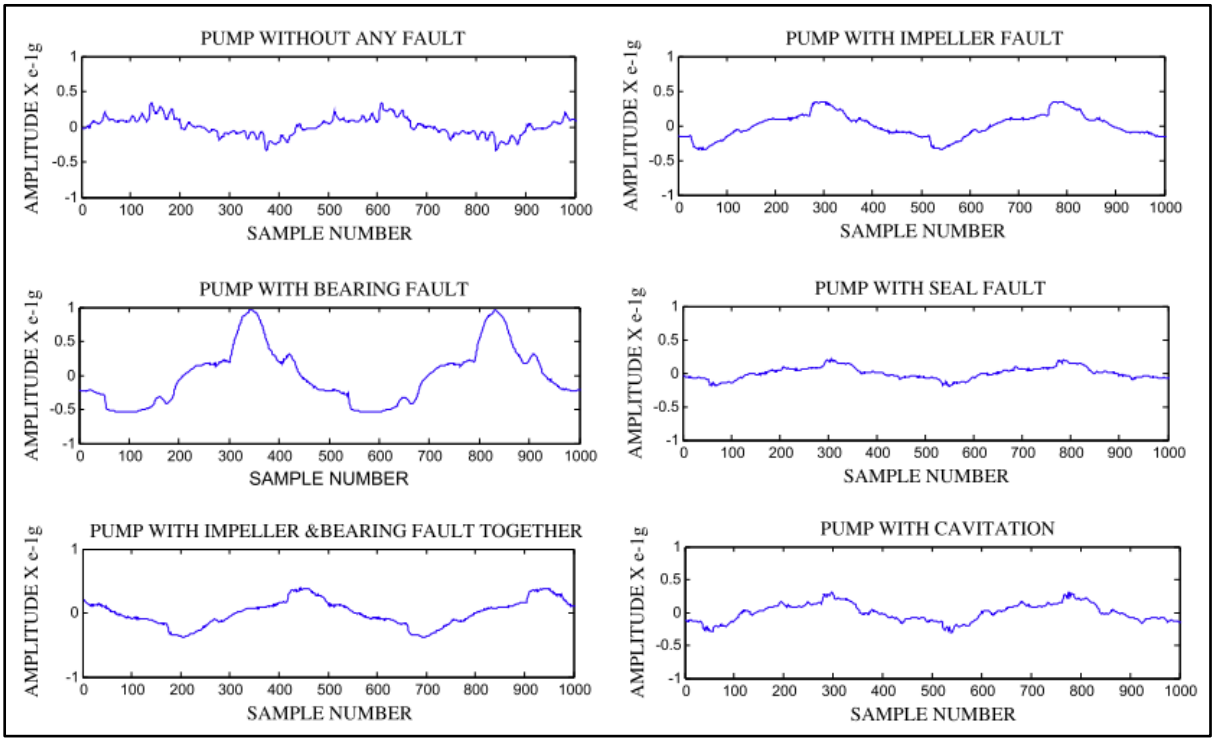

Figure A-2: Vibration graphs in Figure 12 [63]

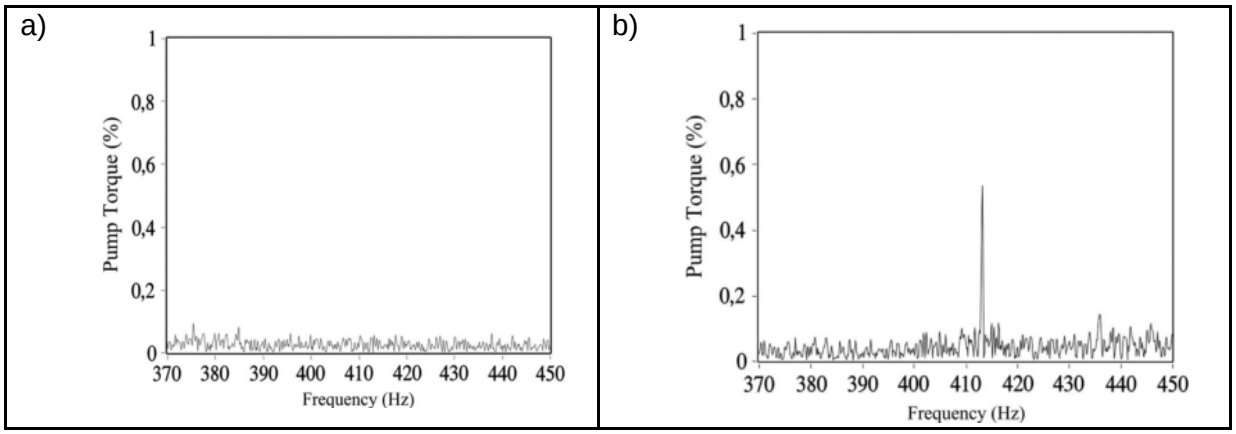

Figure A-3: Pump torque graphs: a) normal operating condition; and b) cavitation present. Combined in Figure 20 [84]

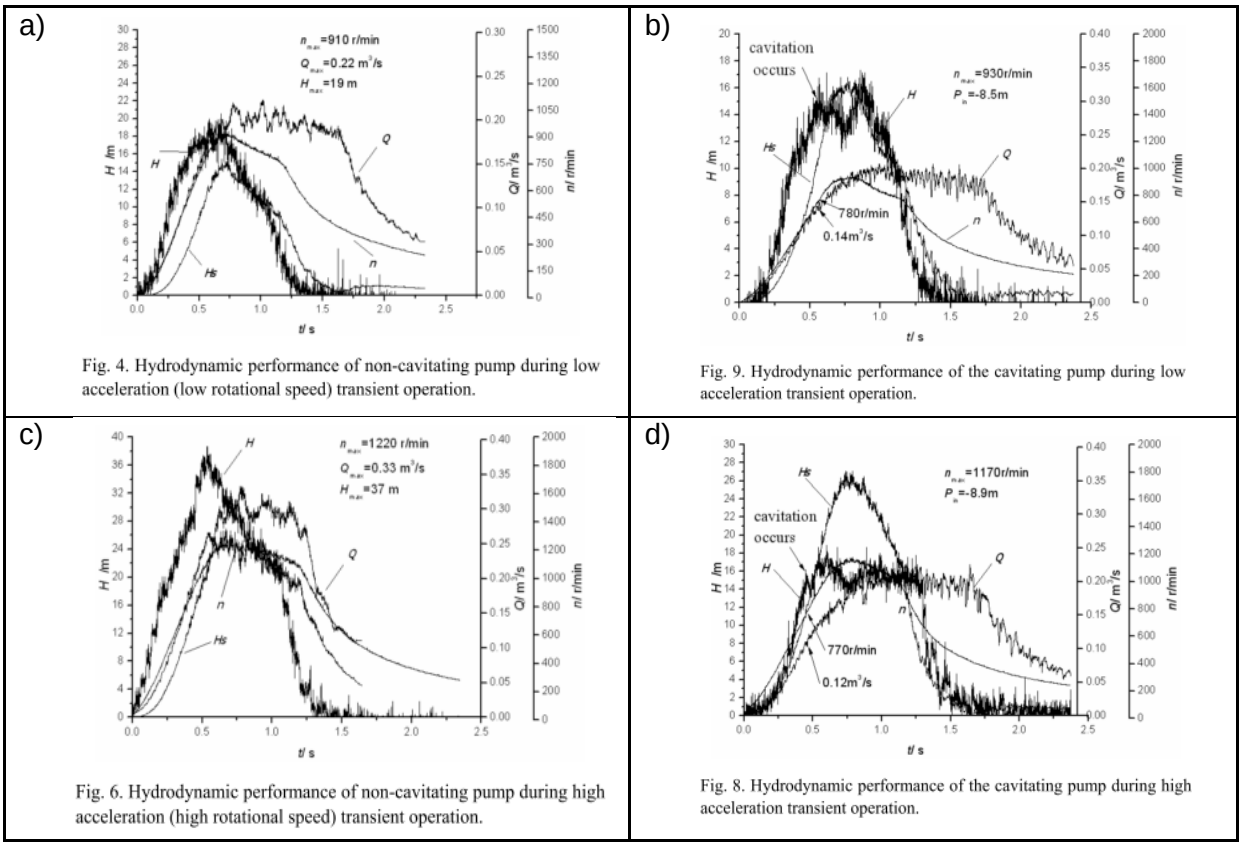

Figure A-4: Pump hydrodynamic performance: a) Low rotation speed without cavitation; b) low rotational speed with cavitation, high rotation speed without cavitation; and d) high rotational speed with cavitation. Simplified in Figure 21 [85]

Appendix B: Installed instrumentation photos

Figure B-1: Emergency switch

Figure B-2: Suction pressure switch

Figure B-3: Power meter

Figure B-4: Pump impeller displacement switch

Figure B-5: Motor cooling water flow switch

Figure B-6: Instrumentation junction box

Figure B-7: Pump and motor

Figure B-8: Motor internal temperature junction box

Figure B-9: Motor shaft displacement sensor

Figure B-10: Motor NDE temperature sensor

Figure B-11: Discharge pressure sensor

Figure B-12: Suction temperature probe

Figure B-13: Motor DE temperature probe and vibration sensor

Figure B-14: Discharge temperature probe

Figure B-15: Suction flow switch

Figure B-16: Discharge NRV and actuated gate valve

Figure B-17: Inlet valve position proxies

Figure B-18: Balance disc flow temperature probe

Figure B-19: Balance disc flow box

Figure B-20: Pump balance disc flow

Figure B-21: Motor and pump coupling

Figure B-22: Pump NDE temperature probe

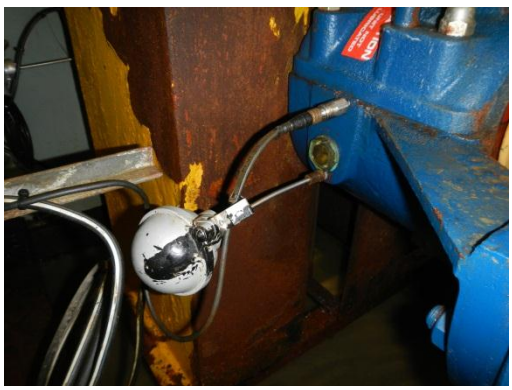

Figure B-23: Pump DE temperature probe and vibration sensor

Appendix C: Optimised control

C.1. Level-22

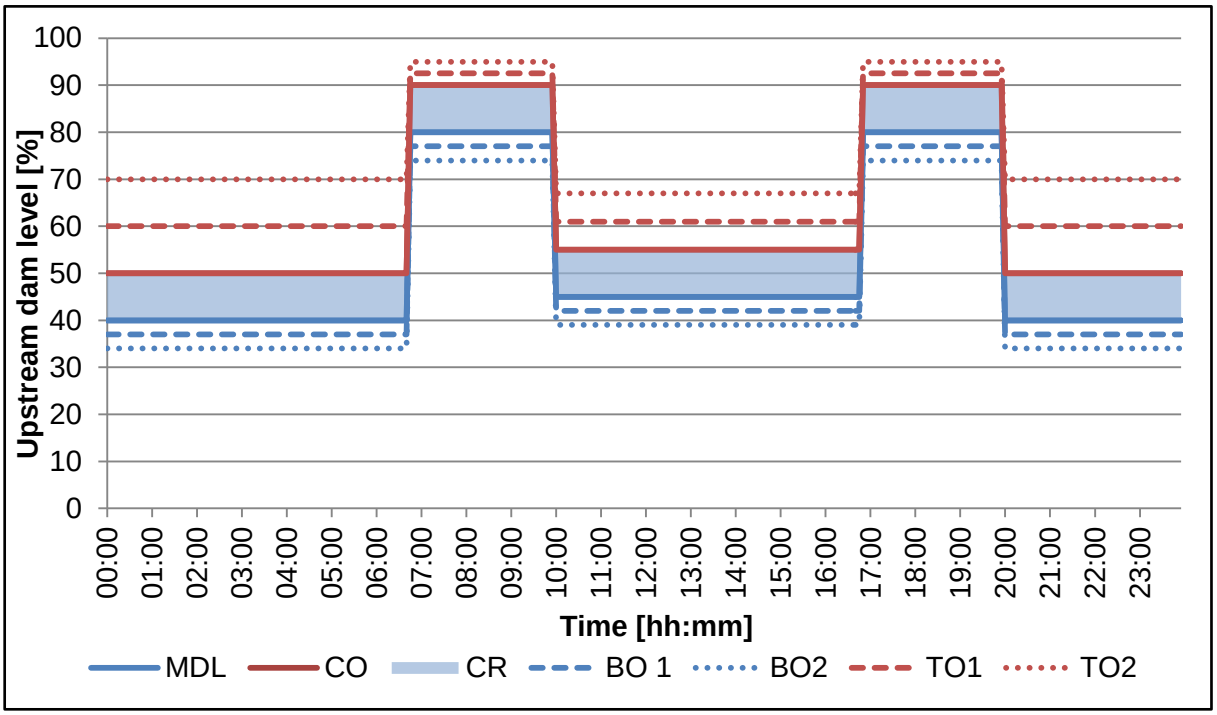

Figure C-1: Level-22 optimised control schedule

Table C-1: Level-22 maximum number of pumps

Pumps available	Level-22 Dam St1	IPCM Dam St1	IPCM Dam St2	Max nr of pumps
4	>90	N/A	N/A	3
	<90	>90	>98	1
			<98	2
		<90	N/A	3
3	>90	N/A	N/A	2
	<90	>90	>98	0
			<98	1
		<90	N/A	2
2	>90	N/A	N/A	2
	<90	>90	>98	0
			<98	1
		<90	N/A	2
1	>90	N/A	N/A	1
	<90	>90	>98	0
			<98	0
		<90	N/A	1
0	N/A	N/A	N/A	0

C.2. IPC Sub optimised control schedule

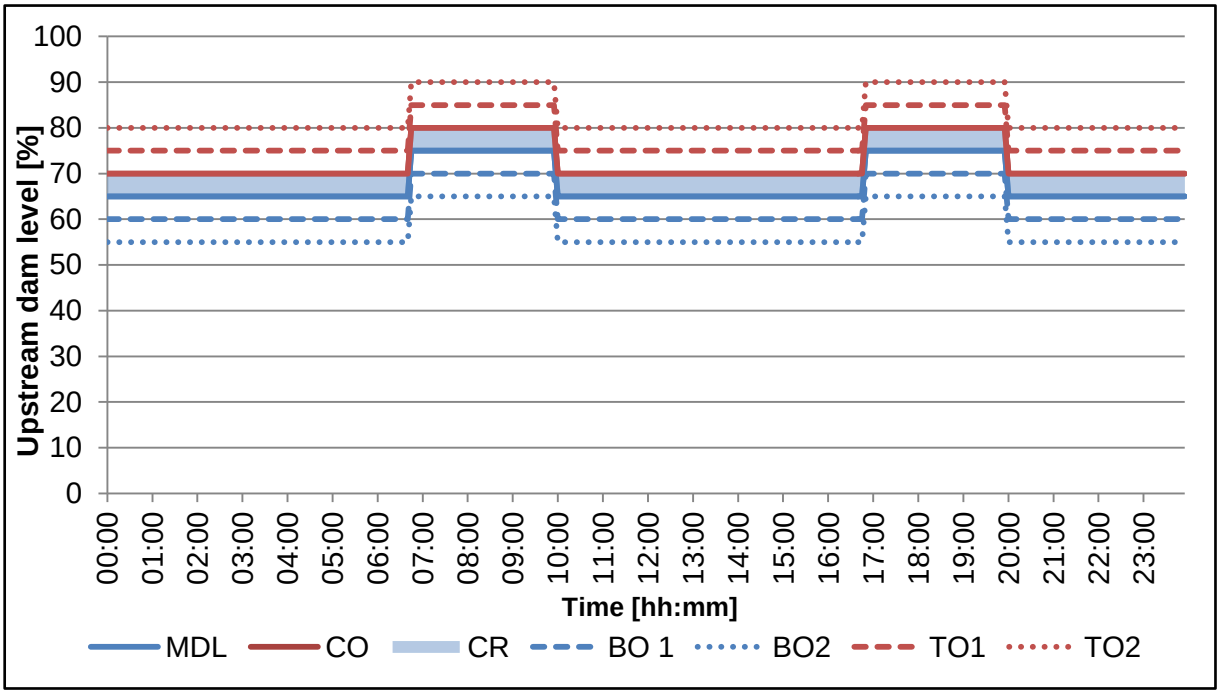

Figure C-2: IPCS optimised control schedule

Table C-2: IPCS maximum number of pumps

Pumps available	IPCS Dam St2	Level-22 Dam St1	Level-22 Dam St2	Max nr of pumps
4	>90	N/A	N/A	3
	<90	>85	>90	1
			<90	2
		<85	N/A	3
3	>90	N/A	N/A	2
	<90	>85	>90	0
			<90	1
		<85	N/A	2
2	>90	N/A	N/A	2
	<90	>85	>90	0
			<90	1
		<85	N/A	2
1	>90	N/A	N/A	1
	<90	>85	>90	0
			<90	0
		<85	N/A	1
0	N/A	N/A	N/A	0

C.3. Level-46 optimised control schedule

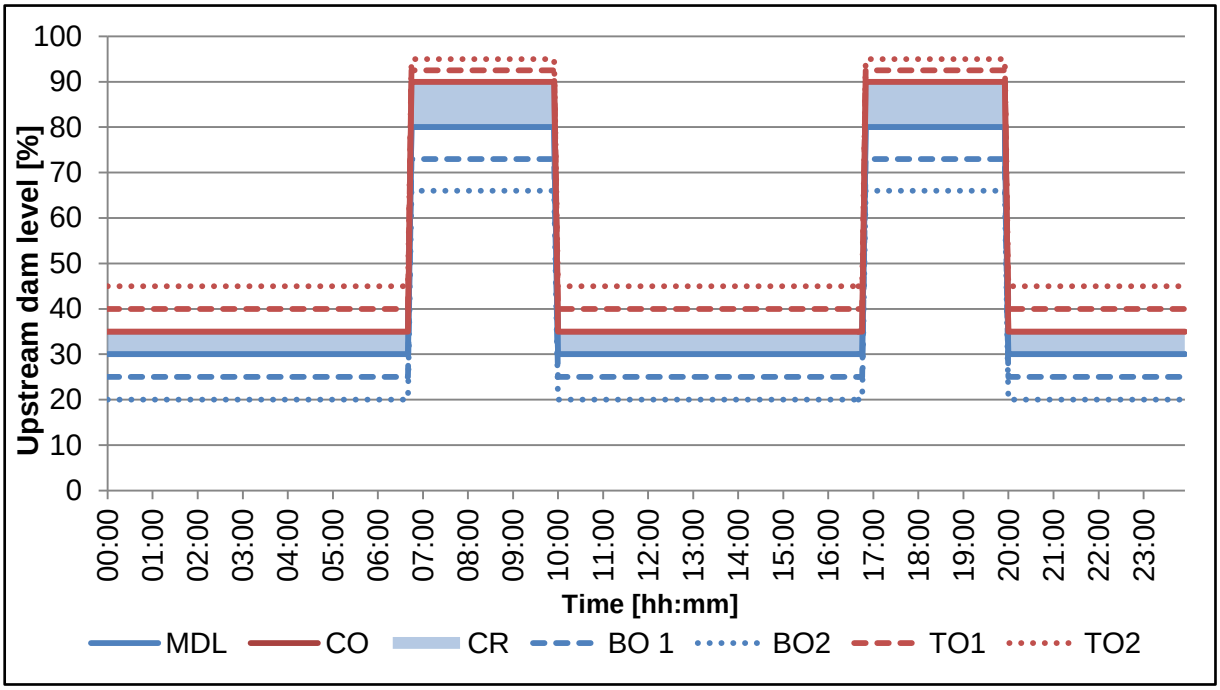

Figure C-3: Level-46 optimised control schedule

Table C-3: Level-46 maximum number of pumps

Pumps available	Level-46 Dam St2	IPCS Dam St1	IPCS Dam St2	Max nr of pumps
4	>90	N/A	N/A	3
	<90	>97	>99	1
			<99	2
		<97	N/A	3
3	>90	N/A	N/A	2
	<90	>97	>99	0
			<99	1
		<97	N/A	2
2	>90	N/A	N/A	2
	<90	>97	>99	0
			<99	1
		<97	N/A	2
1	>90	N/A	N/A	1
	<90	>97	>99	0
			<99	0
		<97	N/A	1
0	N/A	N/A	N/A	0

Appendix D: Water thermodynamic tables

Table D-1: Specific volume [dm^3/kg]

Temperature [°C]	Pressure [kPa]				
	100	**200**	**300**	**400**	**500**
20.0	1.0018	1.0018	1.0017	1.0017	1.0016
20.5	1.0019	1.0019	1.0018	1.0018	1.0017
21.0	1.002	1.002	1.0019	1.0019	1.0018
21.5	1.0021	1.0021	1.002	1.002	1.0019
22.0	1.0022	1.0022	1.0021	1.0021	1.002
22.5	1.0023	1.0023	1.0023	1.0022	1.0022
23.0	1.0025	1.0024	1.0024	1.0023	1.0023
23.5	1.0026	1.0025	1.0025	1.0024	1.0024
24.0	1.0027	1.0027	1.0026	1.0026	1.0025
24.5	1.0028	1.0028	1.0027	1.0027	1.0027
25.0	1.003	1.0029	1.0029	1.0028	1.0028
25.5	1.0031	1.003	1.003	1.003	1.0029
26.0	1.0032	1.0032	1.0031	1.0031	1.003
26.5	1.0034	1.0033	1.0033	1.0032	1.0032
27.0	1.0035	1.0035	1.0034	1.0034	1.0033
27.5	1.0036	1.0036	1.0035	1.0035	1.0035
28.0	1.0038	1.0037	1.0037	1.0036	1.0036
28.5	1.0039	1.0039	1.0038	1.0038	1.0037
29.0	1.0041	1.004	1.004	1.0039	1.0039
29.5	1.0042	1.0042	1.0041	1.0041	1.004
30.0	1.0044	1.0043	1.0043	1.0042	1.0042
30.5	1.0045	1.0045	1.0044	1.0044	1.0043
31.0	1.0047	1.0046	1.0046	1.0045	1.0045
31.5	1.0048	1.0048	1.0047	1.0047	1.0047
32.0	1.005	1.005	1.0049	1.0049	1.0048
32.5	1.0052	1.0051	1.0051	1.005	1.005
33.0	1.0053	1.0053	1.0052	1.0052	1.0051
33.5	1.0055	1.0054	1.0054	1.0054	1.0053
34.0	1.0057	1.0056	1.0056	1.0055	1.0055
34.5	1.0058	1.0058	1.0057	1.0057	1.0057
35.0	1.006	1.006	1.0059	1.0059	1.0058
35.5	1.0062	1.0061	1.0061	1.006	1.006
36.0	1.0064	1.0063	1.0063	1.0062	1.0062
36.5	1.0065	1.0065	1.0064	1.0064	1.0064
37.0	1.0067	1.0067	1.0066	1.0066	1.0065
37.5	1.0069	1.0069	1.0068	1.0068	1.0067
38.0	1.0071	1.007	1.007	1.007	1.0069
38.5	1.0073	1.0072	1.0072	1.0071	1.0071
39.0	1.0075	1.0074	1.0074	1.0073	1.0073
39.5	1.0077	1.0076	1.0076	1.0075	1.0075
40.0	1.0078	1.0078	1.0078	1.0077	1.0077

Table D-2: Specific heat [J/kg.K^{-1}]

Temperature [°C]	Pressure [kPa]				
	100	**200**	**300**	**400**	**500**
20.0	4184.1	4183.7	4183.4	4183.1	4182.8
20.5	4183.7	4183.4	4183.1	4182.8	4182.5
21.0	4183.4	4183.1	4182.8	4182.5	4182.2
21.5	4183.1	4182.8	4182.5	4182.2	4181.9
22.0	4182.8	4182.5	4182.2	4181.9	4181.6
22.5	4182.5	4182.2	4181.9	4181.6	4181.3
23.0	4182.2	4181.9	4181.6	4181.3	4181.1
23.5	4182	4181.7	4181.4	4181.1	4180.8
24.0	4181.8	4181.5	4181.2	4180.9	4180.6
24.5	4181.5	4181.2	4180.9	4180.7	4180.4
25.0	4181.3	4181	4180.7	4180.5	4180.2
25.5	4181.1	4180.8	4180.5	4180.3	4180
26.0	4180.9	4180.6	4180.4	4180.1	4179.8
26.5	4180.8	4180.5	4180.2	4179.9	4179.6
27.0	4180.6	4180.3	4180	4179.7	4179.5
27.5	4180.4	4180.2	4179.9	4179.6	4179.3
28.0	4180.3	4180	4179.7	4179.5	4179.2
28.5	4180.2	4179.9	4179.6	4179.3	4179.1
29.0	4180	4179.8	4179.5	4179.2	4178.9
29.5	4179.9	4179.7	4179.4	4179.1	4178.8
30.0	4179.8	4179.6	4179.3	4179	4178.7
30.5	4179.7	4179.5	4179.2	4178.9	4178.6
31.0	4179.6	4179.4	4179.1	4178.8	4178.6
31.5	4179.6	4179.3	4179	4178.8	4178.5
32.0	4179.5	4179.2	4179	4178.7	4178.4
32.5	4179.4	4179.2	4178.9	4178.6	4178.4
33.0	4179.4	4179.1	4178.9	4178.6	4178.3
33.5	4179.3	4179.1	4178.8	4178.6	4178.3
34.0	4179.3	4179.1	4178.8	4178.5	4178.3
34.5	4179.3	4179	4178.8	4178.5	4178.2
35.0	4179.3	4179	4178.7	4178.5	4178.2
35.5	4179.2	4179	4178.7	4178.5	4178.2
36.0	4179.2	4179	4178.7	4178.5	4178.2
36.5	4179.2	4179	4178.7	4178.5	4178.2
37.0	4179.2	4179	4178.7	4178.5	4178.2
37.5	4179.3	4179	4178.8	4178.5	4178.3
38.0	4179.3	4179	4178.8	4178.5	4178.3
38.5	4179.3	4179.1	4178.8	4178.6	4178.3
39.0	4179.3	4179.1	4178.8	4178.6	4178.3
39.5	4179.4	4179.1	4178.9	4178.6	4178.4
40.0	4179.4	4179.2	4178.9	4178.7	4178.4

Table D-3: Joule-Thompson coefficient [K/MPa]

Temperature [°C]	Pressure [kPa]				
	100	**200**	**300**	**400**	**500**
20.0	-0.22492	-0.22491	-0.22491	-0.2249	-0.2249
20.5	-0.22456	-0.22456	-0.22456	-0.22455	-0.22455
21.0	-0.22421	-0.22421	-0.2242	-0.2242	-0.2242
21.5	-0.22386	-0.22386	-0.22385	-0.22385	-0.22385
22.0	-0.22351	-0.22351	-0.22351	-0.2235	-0.2235
22.5	-0.22317	-0.22316	-0.22316	-0.22316	-0.22315
23.0	-0.22282	-0.22282	-0.22282	-0.22281	-0.22281
23.5	-0.22248	-0.22248	-0.22248	-0.22247	-0.22247
24.0	-0.22214	-0.22214	-0.22214	-0.22213	-0.22213
24.5	-0.2218	-0.2218	-0.2218	-0.2218	-0.22179
25.0	-0.22147	-0.22146	-0.22146	-0.22146	-0.22146
25.5	-0.22113	-0.22113	-0.22113	-0.22112	-0.22112
26.0	-0.2208	-0.2208	-0.22079	-0.22079	-0.22079
26.5	-0.22047	-0.22047	-0.22046	-0.22046	-0.22046
27.0	-0.22014	-0.22014	-0.22013	-0.22013	-0.22013
27.5	-0.21981	-0.21981	-0.21981	-0.2198	-0.2198
28.0	-0.21948	-0.21948	-0.21948	-0.21948	-0.21948
28.5	-0.21916	-0.21916	-0.21915	-0.21915	-0.21915
29.0	-0.21883	-0.21883	-0.21883	-0.21883	-0.21883
29.5	-0.21851	-0.21851	-0.21851	-0.21851	-0.21851
30.0	-0.21819	-0.21819	-0.21819	-0.21819	-0.21819
30.5	-0.21787	-0.21787	-0.21787	-0.21787	-0.21787
31.0	-0.21755	-0.21755	-0.21755	-0.21755	-0.21755
31.5	-0.21724	-0.21724	-0.21723	-0.21723	-0.21723
32.0	-0.21692	-0.21692	-0.21692	-0.21692	-0.21692
32.5	-0.21661	-0.21661	-0.21661	-0.21661	-0.2166
33.0	-0.2163	-0.21629	-0.21629	-0.21629	-0.21629
33.5	-0.21598	-0.21598	-0.21598	-0.21598	-0.21598
34.0	-0.21567	-0.21567	-0.21567	-0.21567	-0.21567
34.5	-0.21536	-0.21536	-0.21536	-0.21536	-0.21536
35.0	-0.21506	-0.21506	-0.21506	-0.21506	-0.21506
35.5	-0.21475	-0.21475	-0.21475	-0.21475	-0.21475
36.0	-0.21444	-0.21444	-0.21444	-0.21444	-0.21444
36.5	-0.21414	-0.21414	-0.21414	-0.21414	-0.21414
37.0	-0.21384	-0.21384	-0.21384	-0.21384	-0.21384
37.5	-0.21353	-0.21353	-0.21353	-0.21353	-0.21353
38.0	-0.21323	-0.21323	-0.21323	-0.21323	-0.21323
38.5	-0.21293	-0.21293	-0.21293	-0.21293	-0.21293
39.0	-0.21263	-0.21263	-0.21263	-0.21263	-0.21263
39.5	-0.21233	-0.21233	-0.21233	-0.21234	-0.21234
40.0	-0.21204	-0.21204	-0.21204	-0.21204	-0.21204